Urban Heat Islands: Potential effect of organic and structured urban configurations on temperature variations in Dubai, UAE

الجزر الحرارية الحضرية: التأثيرات المحتملة للتكوينات العمرانية الناشئة عن تطور طبيعي والتكوينات العمرانية المنظمة على تغيرات درجات الحرارة في دبي، الامارات العربية المتحدة

By
Dana Taleb
Student ID: 80113

Dissertation submitted in partial fulfillment of
MSc. in Sustainable Design of the Built Environment

Faculty of Engineering and IT

Dissertation Supervisor
Professor Bassam Abu-Hijleh

May 2011

DISSERTATION RELEASE FORM

Student Name	Student ID	Programme	Date
Dana Taleb	80113	MSDBE	May 3, 2011

Title
Urban Heat Islands: Potential effect of organic and structured urban configurations on temperature variations in Dubai, UAE

I warrant that the content of this dissertation is the direct result of my own work and that any use made in it of published or unpublished copyright material falls within the limits permitted by international copyright conventions.

I understand that one copy of my dissertation will be deposited in the University Library for permanent retention.

I hereby agree that the material mentioned above for which I am author and copyright holder may be copied and distributed by The British University in Dubai for the purposes of research, private study or education and that The British University in Dubai may recover from purchasers the costs incurred in such copying and distribution, where appropriate.

I understand that The British University in Dubai may make that copy available in digital format if appropriate.

I understand that I may apply to the University to retain the right to withhold or to restrict access to my dissertation for a period which shall not normally exceed four calendar years from the congregation at which the degree is conferred, the length of the period to be specified in the application, together with the precise reasons for making that application.

Signature

ABSTRACT

Urban heat islands are phenomena that occur coupled with rapid urban developments. The study was carried out to show the effect of organic and structured urban configurations on temperature variations throughout the year, especially in summer. The study carried out investigated a larger area of the city rather than merely building-to-building relationships. It went beyond the confinement of street and building geometries and investigated how a number of these geometries put together in one context contributed to temperature variations.

A computer simulation software was used to simulate three different urban configurations, namely the Bastakiyah, Orthogonal, and Volume Ortho configurations in Dubai, UAE. The simulations were carried out for summer, winter, and autumn with initial input temperature value of 305.15K and varying initial wind speeds.

Assessment of the results showed that the Bastakiyah configuration recorded lower temperatures in summer than both the Orthogonal and Volume Ortho configurations. The Orthogonal configuration did not respond as an intermediate configuration between the organic and highly structured. The Volume Ortho configuration, though recorded the highest wind values, did not result in lowered temperature values. It was shown that different configurations manipulated the behavior of the wind within the configuration. The sky-view factor and standard deviation were plausible explanations in the absence of obvious trends in some cases, and showed how urban configurations impacted temperature variations.

It was concluded that, given this specific site location and the alignment of prevailing winds parallel to the roads, the Bastakiyah configuration showed better potential of the three in terms of temperature performance.

الملخص

ترتبط ظاهرة الجزر الحرارية الحضرية بالتطور العمراني السريع. ويركز هذا البحث على التأثير الناتج عن التكوينات العمرانية المنظمة والتكوينات العمرانية الناشئة عن التطور الطبيعي لاحتياجات سكانها على تغيرات درجات الحرارة خلال السنة، وخاصة في فصل الصيف. واستهدف البحث أجزاء كاملة من المدينة، بدلاً من دراسة التأثيرات التي تنظر إلى العلاقة بين مبنى وآخر. وتجاوز البحث محدودية النظر في مكونات هندسة الشوارع والمدن، ليركز على دراسة ما يحصل عند جمع عدد من هذه المكونات في محيط واحد وتأثير ذلك على درجات الحرارة.

وقد تم استخدام برنامج كمبيوتر لمحاكاة عدة سيناريوهات وتركيبات عمرانية، لتشمل التنظيم الطبيعي المتمثل في "حي البستكية"، والتنظيم المتعامد، وتنظيم الكثافات المتعامدة، وجميعها في دبي، الإمارات العربية المتحدة. وقد تم تطبيق هذه السيناريوهات خلال فصول الصيف والشتاء والخريف واعتبار قيمة أولية للحرارة تساوي 305,15 كلفن وسرعات متباينة للرياح.

لقد أظهرت الدراسة بأن تكوين "حي البستكية" سجل أقل الدرجات في فصل الصيف، هذا ولم يمثل التكوين المتعامد تنظيماً متوسطاً بين التكوين الطبيعي والتكوين عالي التنظيم . وبينما سجل تكوين الكثافات المتعامدة أعلى سرعات للرياح، لم ينتج عن ذلك درجات حرارة أقل. وقد أظهر البحث بأن التكوينات المختلفة غيرت من سلوك الرياح ضمن هذه التكوينات العمرانية. وحسب الدراسة، وفي غياب ميول واضح يفسر السلوك الحراري، قدم كل من معيار الانحراف و عامل رؤية عرض السماء تفسيرات معقولة لتلك السلوك وأظهرت كيف أثرت هذه التكوينات العمرانية على تباينات الحرارة.

وقد استخلصت الدراسة بأن التكوين العمراني لحي البستكية أظهر أفضل احتمالية في الأداء الحراري من التكوينات الأخرى وفقاً لموقعه الجغرافي الحالي ومحاذات الطرق فيه لمسالك الرياح السائدة.

ACKNOWLEDGEMENT

I would like to extend my deepest thanks and appreciation to my professor and advisor Professor Bassam Abu-Hijleh. He has supported and encouraged me to work up to my potential and was a continuous source of knowledge and inspiration.

I would also like to thank the British University in Dubai for making all this possible.

And last but certainly not least, tremendous gratitude goes out to my mother, my muse and endless unconditional source of love and support.

TABLE OF CONTENTS

LIST OF FIGURES

LIST OF TABLES

CHAPTER ONE
INTRODUCTION

1.0 A Matter of Sustainability

The triple bottom line concept is at the forefront of research regarding sustainability. Sustainability, in its basic form, is the ability to achieve current needs without compromising resources for future generations to meet their own needs (EPA, 2009). The triple components that define sustainability are those of environmental, economic, and social magnitudes. At the root of urban expansion and sustainability is what is defined as sustainable urban development. Although many regulations have been set towards what defines sustainable urbanism, none have compared the different urban typologies. At present, there is a trend for most of the urban configurations to head towards an ordered layout. The structured approach is perceived as the requirement for a better and sustainable life style. It helps regulate the conditions and limitations of how and what is to be constructed. This is not to argue that sustainable development is not required in all its facets be it transportation, waste management, water management, building regulations, and land use zoning, to name a few. It is to argue whether or not it is a must for such developments to take a certain configuration or a preference of one over the other. The image that people have when asked about sustainable urban development is that of square building plots, an abundance of vegetation, water bodies, structured roads and offset right-of-ways. It is almost never seen represented in dense compact irregular building plots, meandering and winding roads, and overshadowing of open spaces. Both scenarios have their advantages and disadvantages. Not all climatic conditions allow for large water bodies and vegetated areas to be planned. Not all economies support such infrastructure. And not all have the availability of land for expansive planning. There is a need for structured planning, however, not when it means that all communities look the same and are almost identical in their formation. Structured planning can also be achieved for a more “evolutionary” type of urban configurations, namely the organic form. But this does not mean it cannot support the components of the triple bottom line: the environmental, economic, and social, using the same type of regulations and policies used for structured forms. Even though the organic form seems to promote a denser configuration, there are cities planned on a grid-configuration and still have a high-density issue. It can then be argued that the urban configuration of the city is not a measure of its sustainability. The dynamics of the city and the factors in play are far too complex to deduce that one urban configuration is better than another based on its layout.

1.1 The Phenomenon

One of the major dilemmas facing mankind today is the increase of microclimate temperature. The Urban Heat Island (UHI) is the phenomenon tightly associated with the development of cities and urban expansion. This topic was and still is the focus of researchers in the fields of architecture, urban design, engineering and climatology, to name a few. This is true because of its vast impacts and implications on the environment and ultimately human comfort and health. Furthermore, urban heat islands have indirect implications related to cost savings and expenditure.

The urban heat island phenomenon, in its basic definition, is the increase in temperature of urban areas in comparison to its rural surroundings. Wanphen and Nagano (2009) report that “temperature difference between urban and rural areas can be as high as 5-15ºC”. These “islands” are pockets or areas within an urban context that are characterized by increased temperature creating a slightly warmer micro-climate. Other definition of UHI also relevant to this research paper is one stated by Kolokotroni (2006) indicating that the urban heat island phenomenon is caused by micro-climatic variations due to “man-made” intervention and modification to urban surfaces. Many factors contribute to this phenomenon, and most are imposed through human intervention into the natural environment. Landsberg (1981) describes it as “a reflection of the totality of microclimatic changes brought about by man-made alterations of the urban surface”. Another definition of the UHI is by Akbari (2005) who defines it as areas that “tend to have higher air temperatures than their rural surroundings as a result of gradual surface modifications that include replacing the natural vegetation with buildings and roads”. Synnefa et al. (2007b) defined the urban heat island effect as the increased ambient temperature of an urban area caused by warmer surfaces.

This variation in temperature started to be noted as the population moved from rural areas and created urban centers higher in density and activity levels. According to Kolokotsa (2009), “approximately 50-60% of the world population lives in cities or towns” with urbanization increasing from 160 million people to 3 billion in the last 100 years. This figure is expected to increase to 5 billion by the year 2025 (Kolokotsa, 2009). With this shift, the nature of the land, surface types, land uses, and urban configurations changed to meet the demands and needs of the population.

In order to further the understanding of the urban heat island dynamics and consequently the observation of such a phenomenon, it is necessary to recognize that there are different types of urban heat islands (Oke, 1995). The three types of urban heat islands are:

- *Surface heat islands*: As the name indicates, it is related more than the other two types to temperature variations due to urban surfaces and its impact on the overall temperature.
- *Canopy layer heat island*: identifies temperature variation in a layer closest to the surface of the urban context and is defined to be below the mean height of roof-levels.
- *Boundary layer heat island*: identifies temperature variations in an area above the canopy layer and could reach 1km high in the day or a few meters at night.

Figure 1.1 shows the different components of the urban atmosphere through which the different types of urban heat islands are defined (Voogt, 2004).

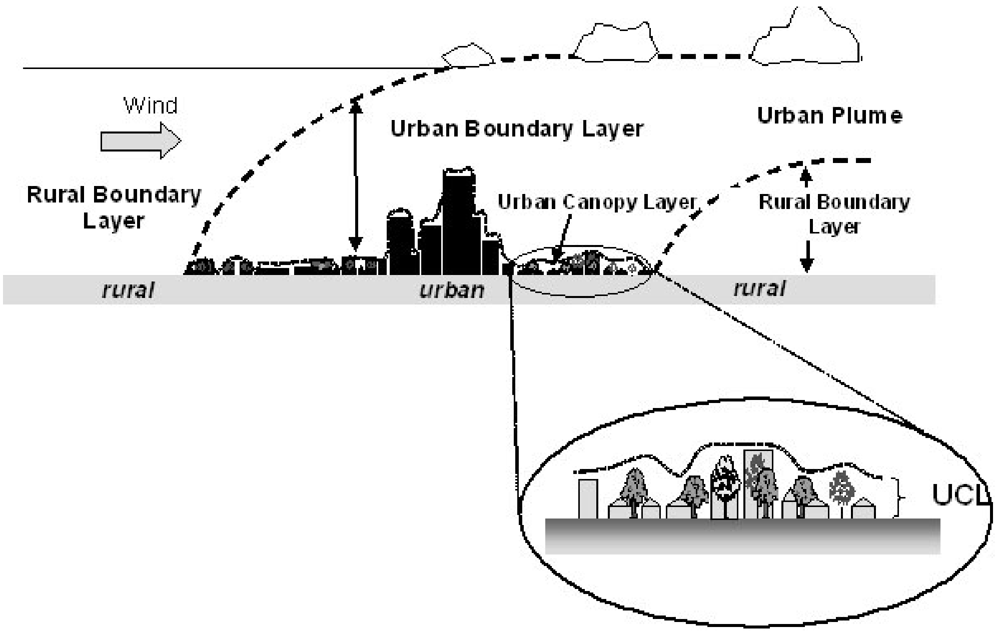

Figure 1.1 Different components of the urban atmosphere (Voogt, 2004)

The Environmental Protection Agency (EPA) (2009) has defined the Canopy urban heat island and the Boundary urban heat island as atmospheric urban heat islands as opposed to surface urban heat island as the other type.

Che-Ani (2009) has referenced Givoni (1998) in identifying the factors affecting the occurrence and intensity of the UHI. Those are divided into two broad categories:

1. Meteorological factors which may include wind speed and direction, humidity, and cloud cover.
2. Urban parameters such as density, built-up areas, aspect ratio, sky-view factor, building material, and urban structures.

In the following section, each of the factors will be investigated briefly through the literature review. The main focus of the paper, however, will be on the urban parameters factors. (Appendix A)

One of the main reasons to further research in the field of urban heat island phenomenon is its adverse negative impact on the environment and quality of life. As urban heat islands in all its forms contribute to the increase of temperature of the micro-climate, it influences several aspects of the environment. According to EPA (2009), some of the impacts include diminishing human comfort, the increase in air pollution, increase in energy consumption, and decrease in water quality. These negative impacts are all interconnected and have a ripple effect on each other. Starting from the most vital component of an urban area, human beings get affected easily with changes in the micro-climate. With this increase in temperature, the basic response will be the need for cooler indoor spaces and consequently higher electrical demands. This increase of demand on the electrical grid during the day increases “1.5 to 2 percent for every 1^{o}F (0.6^{o}C) increase in summertime temperature” (EPA, 2009).

Akbari (2005) reported that in the United States, increases of temperature due to UHI is responsible for increasing energy demands on the electrical grid of 5-10 percent to overcome this increase in temperature through the use of air conditioners as cooling measures.

1.2 Urban Context

At present, cities no longer undergo a natural evolution process. It is now more of an imposed reaction to needs that neglect those of humans and are more oriented to economical reasons. Material selection in any case is impacting the urban heat island phenomenon regardless of countless efforts to promote certain materials that mitigate this problem. Developers will not abide by those if it does not suit their financial demands and requirements or the marketing image they seek. Furthermore, other mitigating measures are not taken into account in the planning process such as allowing for ample wind circulation between buildings, considering building profiles and their impact on urban canyons, or even considering a simple site related approach such as building orientations. Taking Dubai as an example of multiple urban forms (liner in the newer parts of Dubai, and more organic in the older parts of Dubai), it is a good testing field to simulate the various magnitudes of urban heat islands depending on the urban form or configuration. If cities are going to be planned the way they are now, then it might serve a better purpose to include in the criteria of planning a preventative measure to urban heat island effects through the choice of a suitable urban form for the city- or at least part of a city.

In this research paper, city form will be referred to as urban form mainly because it investigates a portion of the city, a neighborhood rather than an entire city structure. It is also important to note that most of the literature reviewed for this research used the term urban form interchangeably to refer to building forms, such as courtyard houses or pavilions.

Urban form in this paper refers to a cluster of buildings organized in a certain configuration. There will be two urban forms highlighted in this paper and researched, namely the centralized organic urban form and the grid-iron urban form.

According to Moughtin (2005) there are three main types of city forms: the centralized, the linear, and the grid form. Although each can represent a metaphoric function, each also has criteria identifying the need for a city to be organized and configured in a certain manner.

In general, urban forms and city configurations are affected by some factors that include social structures, industry, density, and the distribution of the various functions within the city.

A brief description of the three main urban configurations is presented in order to identify the main features of each to enhance comparisons and recommendations at the end of the research.

1.2.1 Linear Form

Moughtin (2005) has described the linear form as one that provides “infinite growth” and occurs in unplanned development of cities (Fig 1.2 a). In Dubai, Sheikh Zayed road is the perfect example of the linear urban form. It was a quick solution to expanding the city and stretching out from the old city center. It was meant to be a “spine” to drive people and businesses to expand their city in a specific direction (Fig. 1.2 b).

Not only has this type of urban form allowed for expansion along the spine, its location also allowed for development to happen along the sides of the spine. Businesses and commercial functions are located at the spine and residential and entertainment expand on the sides.

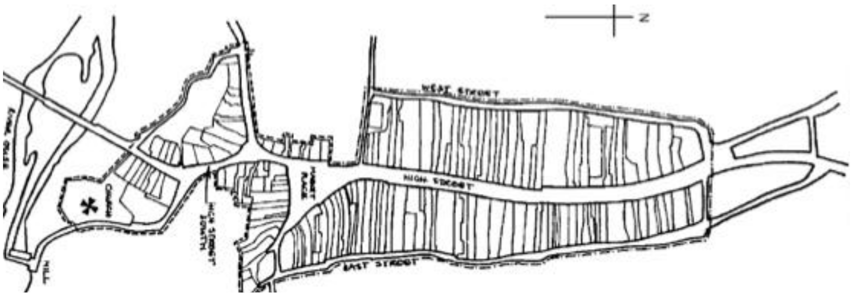

Figure 1.2 (a) Linear configuration (Moughtin, 2005)

Figure 1.2 (b) Sheikh Zayed Road as an example of the linear configuration (Google Earth)

1.2.2 Grid Form

The grid form is considered to be the most structured approach to urban form. According to Moughtin (2005), there are five main forms for the grid configuration:

1. a hierarchy of boxes as a nesting grid
2. the grid iron form, which is orthogonally structured (Fig. 1.3 a)
3. directional
4. triangular
5. informal pathways in the form of lacework

The grid form is commonly valid where the city has a planned approach and certain criteria is set in terms of land use, distances to certain nodes or functions, or transportation needs. With this urban form a major grid of roads is established and land is then subdivided to the various land uses required. It is easier with this form to subdivide plots and distribute land use zones based on the needs of the population. As the concern with sustainable development grew, the grid configuration became more popular as a city planning approach because it was structured enough to monitor and implement the requirements of a sustainable development. Infrastructure is easier to lay out, roads are easier to plan, and land use planning is more manageable when the city is planned in parcels with known parameters. The highly structured configuration made such planning feasible with cost effective implementation schemes. The Jumairah district in Dubai is a good example of such configuration as shown in Figure 1.3 b. The zoning of the area is based on dividing the land into parcels with equal setbacks, and specific dimension for each of the parcels including building heights. Roads within the area are highly ordered and orthogonal.

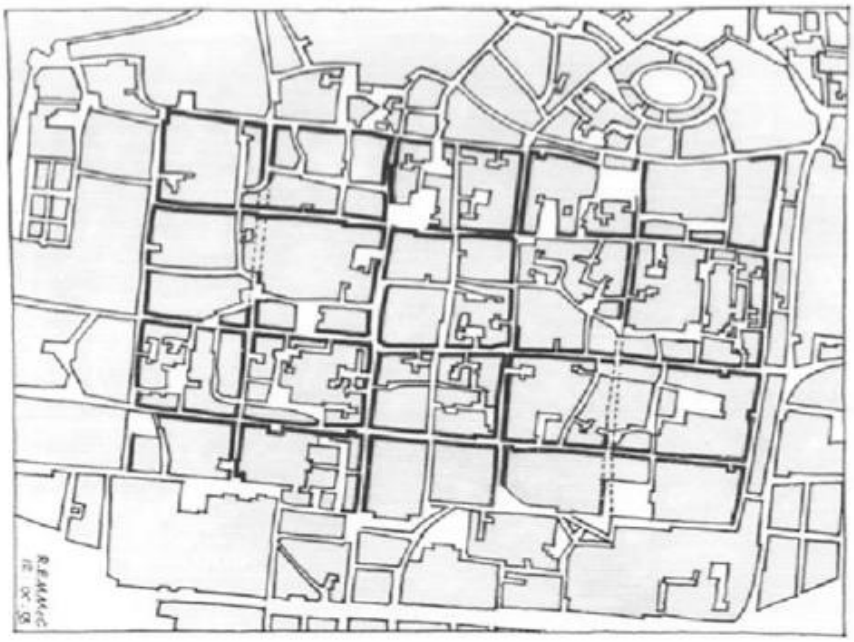

Figure 1.3 (a) Grid iron configuration (Moughtin, 2005)

Figure 1.3 (b) Grid iron configuration in the Jumairah district, Dubai (Google Earth)

1.2.3 Centralized Form

The traditional approach to this urban form is introverted, “inward-looking city”. It is usually bound by a city wall and gateways to enter the city. It is most common in Islamic districts or cities. This urban form supports the concept of privacy in all its components, roads, building form, and building types. The center of the city is a public open space containing the market place, the mosque, and the palace (Fig.1.4 a). This urban form is also called the organic configuration. Most of the cities following this type of configuration are a result of direct interaction of its people with its growth. It is a direct translation of their needs. Therefore the spatial quality and composition is a result of the people’s interaction with their surroundings. Needs for privacy and segregations from public areas shape the roads of this organic city. Roads are wider around public areas and become narrower towards the houses and private areas. The roads are also meandering and offset to increase visual privacy. Many of these roads become alley-ways and could end as vistas or cul-de-sac. These types of cities are usually compact and dense and for those reasons “may be the inspiration of ‘green planners’ who advocate a compact city of dense three and four storey developments limited in extent” (Moughtin, 2005).

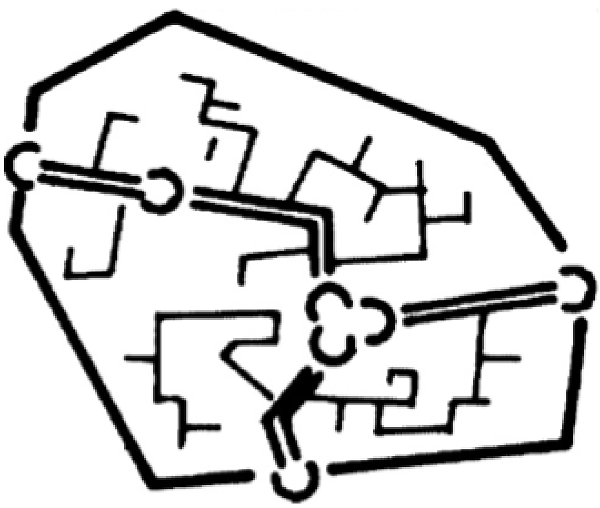

Figure 1.4 (a) Centralized configuration (Moughtin, 2005)

A good example of the organic urban configuration is shown in Fig 1.4 b of an area in Nigeria (Moughtin, 2005) and another of the Bastakiyah area in Dubai in Fig 1.4 c.

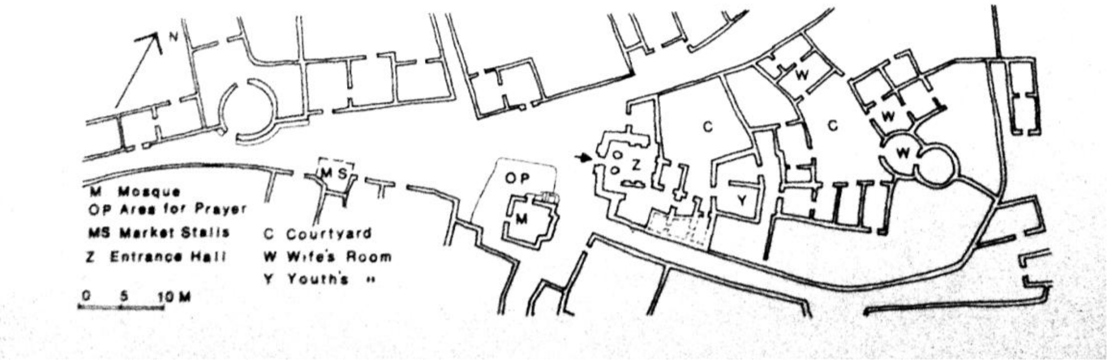

Figure 1.4 (b) Organic configuration in Nigeria (Moughtin, 2005)

Figure 1.4 (c) Organic configuration in Bastakiyah, Dubai (Google Earth)

1.3 Research Outline

This research paper is divided into the following chapters:

Chapter one is an introduction and overview of the concept of Urban Heat Islands, including its definitions and types. The chapter also highlights the importance of understanding such a phenomenon and mitigating its effect on the environment and human comfort.

Chapter two will be a comprehensive discussion on the various factors impacting and causing Urban Heat Islands through reviewing scientific papers.

Chapter three is the methodology section which includes a literature review of papers based on their methodologies. The different types of methodologies will be compared with regards to their advantages and limitations. The chapter will also describe the selected methodology for this dissertation and research parameters. Software selection and site selection are also discussed in this section.

Chapter four will include information on computer model set-up and validation process. The chapter will describe the baseline computer model and the verification process through which decisions regarding the set up of the model were made.

Chapter five will provide a comprehensive results discussion. The findings will be discussed and a comparison will be set up to identify the advantages and disadvantages of each of the scenarios.

Chapter six will provide a comprehensive conclusion based on the findings and the identified factors contributing to these findings will be highlighted. Further studies and future research recommendations will be suggested.

CHAPTER TWO

LITERATURE REVIEW

2.0 Background

This chapter will highlight the main scientific papers that have addressed the Urban Heat Island phenomenon. In this section the reviewed papers will be presented depending on some of the major factors that affect urban heat islands.

2.1 Urban Geometry

Shashua-Bar et al. (2004) have investigated the effect of urban geometry on the Urban Canopy layer (UCL) microclimate. The urban geometry in their research is defined by building dimensions and spacing between buildings. The forms selected for the study were generic representation of the cities under study, illustrated in the Figure 2.1 (a)-(d) below.

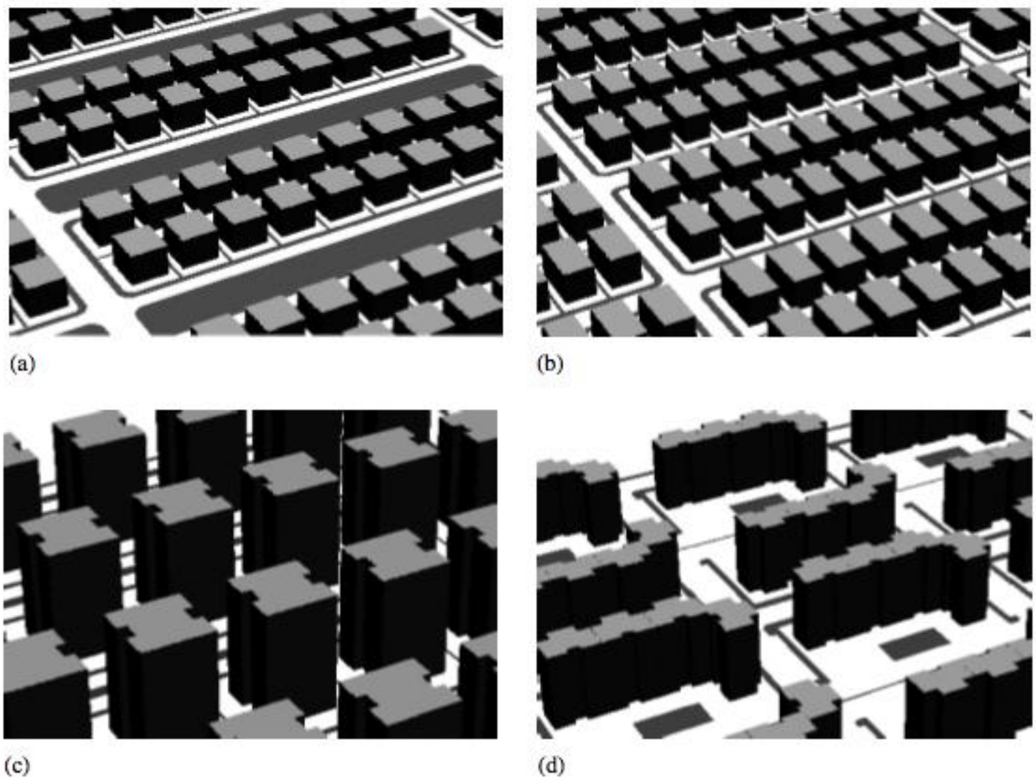

Figure 2.1 Diagram to illustrate the different investigated aspect ratios **(a)** H/W= 0.25, **(b)** H/W=0.5, **(c)** H/W=1.0, **(d)** H/W= 2.0 (Shashua-Bar et al., 2004)

The urban geometry was defined by “geometric ratios”: spacing ratio representing the spacing between adjacent buildings, building depth ratio representing the depth of the building in relation to its frontal length, and aspect ratio representing the height to width ratio of the UCL (height of the building to the width of the adjacent open space or street). The study has investigated, through simulation models using Green CTTC, 4 aspect ratios (H:W 0.25, 0.5, 1.0 and 2.0). For each of the four different aspect ratios there are 3 depth ratios represented (D:L2 of 0.67, 1.0, and 1.34) and each line on the graph plots 5 spacing ratio simulations (L1:L2 of 0.33, 0.5, 0.66, 0.83, and 1.0). Shashua-Bar et al. (2004) concluded from the linear relationship that the wider the spacing between buildings the higher the temperature of the UCL, the higher depth ratio of the building the lower the UCL temperature, and the higher the aspect ratio the cooler the UCL is. Figure 2.2 shows the relationship between the different geometry ratios and temperature variations.

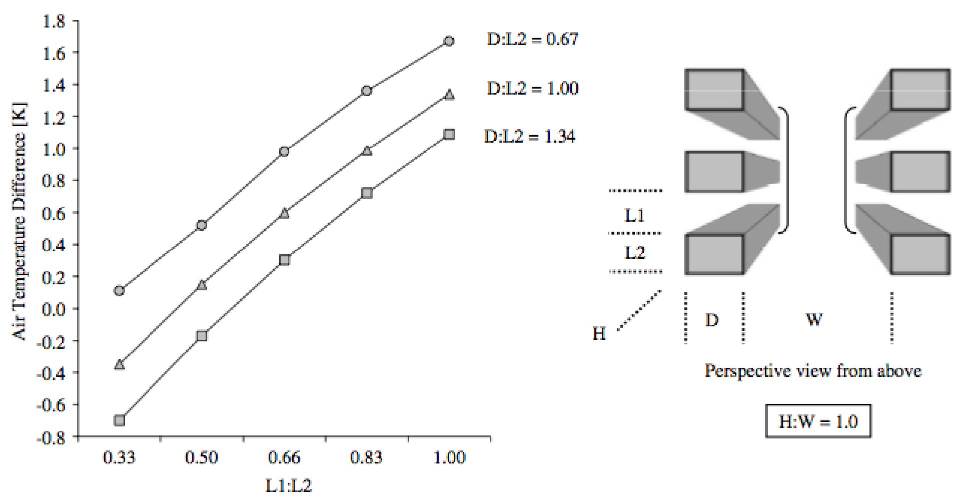

Figure 2.2 A graph illustrating the impact of geometry on air temperature for aspect ratio of 1.0 (Shashua-Bar et al., 2004)

The research indicated that the difference in temperature record 4.7K higher than the baseline measurements, used from a meteorological reference, in areas with shallow open spaces and wider spacing. On the other hand, in areas that have deep open areas and narrow spacing have recorded 2.1K below the baseline measurements. Shashua-Bar et al. (2004) concluded that a higher aspect ratio has a strong cooling effect, whereas higher spacing ratio has a warming effect. The depth ratio, however, indicated the least impact on the overall UCL temperature variation.

This research has a major advantage in quantifying what defines an urban geometry, including adjacency relationships between urban structures to each other as well as their relationship to open spaces in terms of measurable dimensions. It helps give indications as to what the behavior might be by altering any of the ratios discussed in the paper. However the limitation of this research is that it is structured around a generic orthogonal layout. Should any of the blocks be offset it becomes increasingly difficult to calculate the ratios accurately and derive temperature variations on that basis.

Thapar and Yannas (2008) researched how urban form may affect the microclimate of different areas in Dubai, UAE. The Deira and Bastakiyah area represented the older areas of Dubai and Dubai Marina represented the newer districts of the city. The research was conducted for the hottest period of the year (July 2007). The work included both on site measurements and observations and later supported with further investigation and validation through software simulation. The factors that are investigated in the research are those directly related in affecting human comfort levels, such as shaded areas, the presence of vegetation, and proximity to water bodies.

Measurements were taken from inland drier areas where there is no effect of water bodies and vegetation and considered as the baseline.
In the older areas of Dubai, measurements were taken from inside the courtyard of a house as well as a nearby street. The courtyard of 1.8:1

aspect ratio recorded a temperature 1-3K lower than the nearby street of 2:1 aspect ratio, and 4-6K lower than the baseline measurement. Measurements taken in Deira have suggested the effect of nearby water masses and the cooling effect of evaporation in lowering and stabilizing the temperature. This was despite the fact that the areas close to the water edge where the measurements were taken are not shaded. Areas that are shaded also recorded lower temperatures than those recorded in the un-shaded exposed parallel street. The nearby street, even though narrow, was exposed to the sun for part of the day thus recording higher temperatures.

The thermal comfort survey revealed that higher temperatures and higher humidity levels were more tolerable and acceptable by pedestrians when there was higher wind circulation.

In comparison to the older areas of Dubai, Dubai Marina and the Greens community were selected to highlight the impact of large water bodies and extensive vegetation respectively. Both have recorded lower temperature by 7K before sunset compared to the baseline measurement.

The researchers also used Envi-met to assess the impact of a variety of built forms on the ambient temperature. In all three scenarios, the volume was fixed and modeled as single high-rise tower, a four block mid-rise block, and a dense courtyard block. The courtyard block recorded cooler temperatures with the courtyard itself being the coolest spot shown in Figure 2.3. Simulation results of vegetation and water bodies were able to confirm the same results taken from field measurements even though measurements recorded from the simulations were lower than those taken from the field. The researchers concluded that the built form (ventilated, shaded, and transitional), vegetation, water bodies, and adaptive activity zones will all influence the microclimate by lowering temperatures. The built form, however, was not addressed in terms of the urban configuration. Even though the characteristics of the Bastakiyah area were highlighted to have winding roads and high density where wind circulation will be minimal, the results from the ENVI-met simulation illustrated that the courtyard scenario did in fact record the lowest temperature levels. This may have been due to the shading effects of the configuration and despite the low wind circulation around the courtyard block.

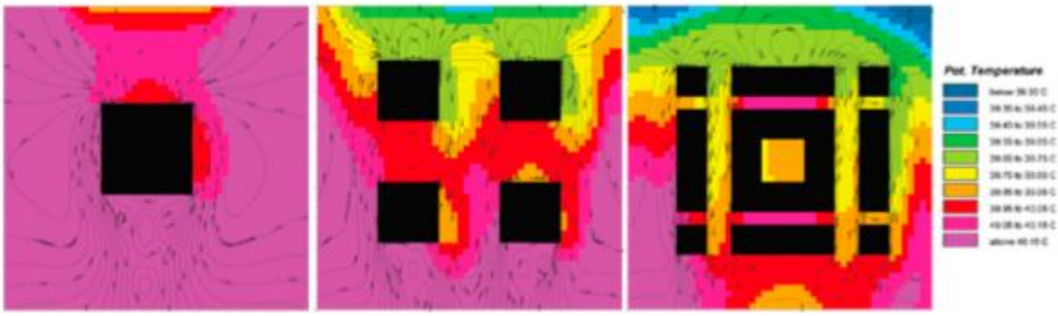

(a) (b) (c)

Figure 2.3 ENVI-met simulation results for **(a)** single high rise building, **(b)** four block mid-rise buildings, **(c)** dense courtyard block (Thapar and Yannas, 2008)

Along the lines of the investigation by Thapar and Yannas (2008), Ahmed (2003) investigated the thermal variations and thermal comfort ranges in tropical urban environments. The investigation included different outdoor spatial categories. The spatial categories are illustrated in Figure 2.4. Some of the spaces are entirely exposed to the environment, one is close to a large water body, and some partially enclosed within buildings and one represents only an overhang shading device with all the sides exposed. Through comfort surveys, the main findings were that higher relative humidity levels are more acceptable by people when there is substantially more airflow. However, the increase in airflow does not necessarily increase the acceptance of higher temperature levels.

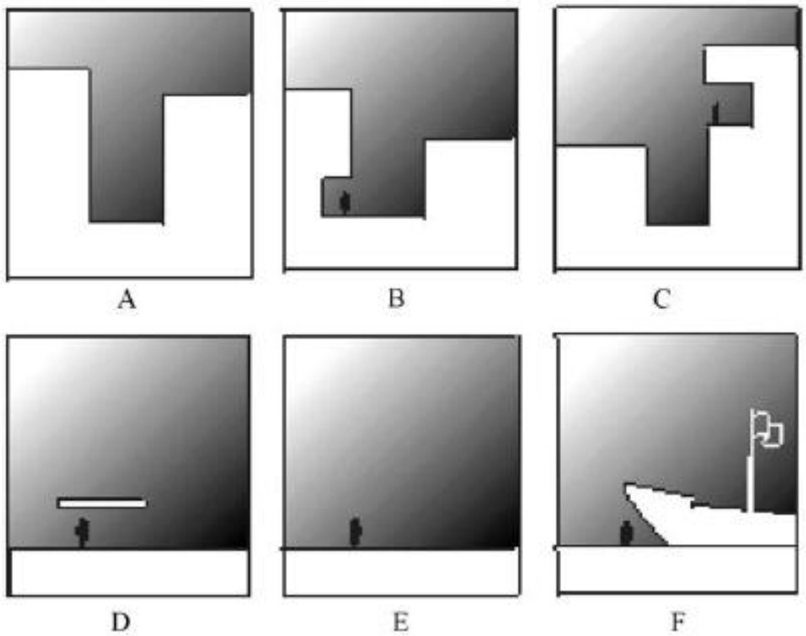

Figure 2.4 Spatial configuration investigated ranging from completely exposed spaces to spaces next to large water body (Ahmed, 2003)

Unger (2004) also investigated the relationship between urban geometry represented in sky view factors (SVF) and temperature variations in large scale areas, representing large portions of the city. The conclusion was that there is a strong correlation between intra-urban temperature and SVF. The major difference with this paper is that the researcher focused on studying a large portion of the city instead of singling out pairs of elements for comparison. He advocated for measurements and investigations to be done on larger areas to properly understand the interaction between urban geometry and temperature variations on a city scale. It was also indicated that comparisons between areal readings and readings of paired elements should take place in connection with the tested variables.

Other researches, such as the one carried out by Montavez et al. (2000), studied urban heat islands in terms of their relation to recorded meteorological station readings. They also concluded a correlation between urban geometry represented in terms of aspect ratio and temperature variations. In Granada, Spain, where the research took place, they found that UHI readings were more intense in winter and the maximum difference was evident in the early hours of the day when the daily minimum temperature was recorded. They suggested that in order to get accurate rural temperature readings to be compared to urban temperatures, the meteorological stations should be located in areas where it is ensured they are not affected by the UHI.

Ratti et al. (2003), investigated the effect of urban form on the environmental performance. The built form was represented in a series of urban arrays from selected archetypical building forms. They have reassessed a research that was done in the 60's but in environmental terms using computer analysis. This research examines an array of courtyards that represent the older type of architectural form in comparison to pavilions which represent tower buildings dominating modern architecture. Orthogonal patterns have been developed from pavilions and courts both representing the same site coverage, building height, and total floor space. By adding an additional component to the pattern, namely the street, more patterns were generated. The original research concluded that courtyards perform better than pavilions in terms of land use performance.

Even though earlier research had indicated that courtyard houses as an architectural form are ideal in responding to environmental and climatic factors in hot-arid climates, they were mainly based on "observations and common sense". Ratti et al. (2003) addressed the same concept through computer imaging but with more environmental factors than the original research. The major variables addressed included: surface to volume ratio, shadow densities, daylight accessibility, and sky-sky view factors. These variables address, from an environmental perspective "solar radiation, thermal comfort, and urban temperatures" (Ratti et al., 2003). The other aspect of this research which differs from the original one is that it addresses more realistic and specific versions of the urban types. The investigation starts with the simple courtyard type followed by combinations that resemble urban transformation.

The three urban forms include one array of courtyard houses, and two of pavilion arrays. One is comprised of pavilions replacing each courtyard house but maintaining the same height and volume. The second pavilion array replaces four courtyard plots with one maintaining the same building volume as well by altering the height of the buildings. The different configurations are illustrated in Figure 2.5 below.

Figure 2.5 Axonometric of the investigated urban forms (left to right: 3 floor courtyards, three floor micro pavilion, six floor pavilion) (Ratti et al., 2003)

The conclusions of this research have highlighted that the performance of surface to volume ratio represented in the thermal mass has a positive effect on thermal performance. Furthermore, the shadow density was highest and the daylight distribution was lowest in the courtyard type due to its narrower streets. Therefore the courtyard configuration is the best for pedestrians in terms of protection from the sun and thermal comfort. It is worthy to note that the results of the daylight distribution are an average of the interior of the courtyard in addition to the streets outside the houses. If the value is taken only from the courtyards, the daylight reading is about 9% higher inside the courts than it is in the streets. This gives rise to the advantage of making use of the daylight within the courtyards (Ratti, et al., 2003).

As for the sky view factor, it was indicated in this research that it directly relates to the urban heat islands effect. Ratti et al. (2003) noted, based on a formula introduced by Oke in 1981 correlating the temperature difference between rural and urban areas with the sky view factors, that the courtyard type recorded higher temperatures than the pavilion types. At first glance, this suggested that urban configurations might need to be less dense and compact. However, Ratti et al. (2003) questioned and highlighted that in hot-arid climates consideration must be taken with regard to temperature variations between night and day. Further, and more importantly, Ratti et al. (2003) also highlighted that thermal comfort is also affected by radiated temperature. Therefore having a lower sky view factor resulted in better thermal comfort in the narrow streets and open spaces during the day. Figure 2.6 illustrates the sky view factor ranges in the three investigated urban forms.

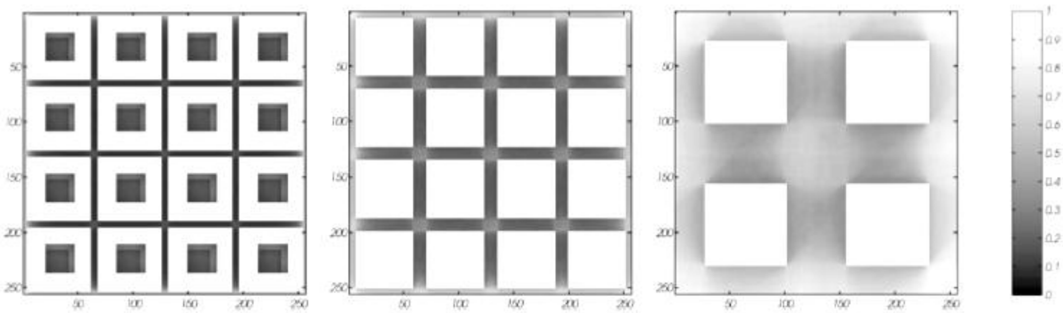

Figure 2.6 Sky view factors from street level for the three urban configurations (Ratti et al., 2003)

This research indicated that in many aspects the courtyard house has a better environmental performance than that of pavilion types. Now that this has been established in terms of an organized orthogonal distribution of courts and pavilions, this gives further rise to the question addressed in this dissertation. What happens with the microclimate when the distribution is not orthogonal?

As stated by Ratti et al. (2003) reiterating Oke (1988), there are “infinite combinations of different climatic contexts, urban geometries, climate variables, and design objectives. Obviously there is no single solution, i.e. no universally optimum geometry". Ratti et al. (2003) however highlighted that there are associated building forms with certain climatic types, "such as the courtyard type and the hot-arid climate".

Golany (1996) investigated the relationship between thermal performance and urban morphology. He classified climate to 6 major types identifying that each climatic profile requires a special urban design solution. He set a few guidelines to assist urban designers to respond to the various climatic properties. Those considerations are divided into two major approaches, one relates to site selection on a city scale, and the other relates to urban configuration. The first of the urban forms is the compact form known to be "concentrated and firmly unified" with the land uses joined in "tight physical relationships" linking them to each other and the structures around them. He concluded from historical practices that this urban form is characteristic of hot-dry/ cold-dry regions as a response to environmental needs. The second of the forms discussed was the dispersed form, and the third is the clustered form. When linked to climatic responses, Golany (1996) stated that the configuration of a city can assist wind circulation and affects wind velocity which in turn impacts temperature variations. He points out that city morphology directly affects the movement of the wind within it depending on its design, shape and orientation of the roads within it. He made clear distinction regarding roof lines in a city and its effect on wind movement. Flat roof skyline known to be found in indigenous architecture allows for "strong wind movement" with little obstruction. Pitched roofs found in hot-humid cities will slow down the wind and the modern city with its varying building heights has the effect of breaking down the strength of the wind and in some cases diverting it. Those distinctions are summarized in (Table 1.1).

Table 2.1 Summary of different climate types and urban design responses (Golany, 1996)

Table 1. Main climatic regions, their profile, major problems, basic urban design responses and urban form

Main climates, example (1)	Basic Profiles (2)	Major problems (Issues) (3)	Basic urban design response (4)	Prefered urban form (5)
Hot-humid (equatorial zone)	Hot diurnally and seasonally with minor temperature range Heavy rain More comfort at high elevation	Excessive heat High humidity	Ventilation: open ends and dispersed form Widely open streets to support wind movement Extensive shadow Dispersion of high rise buildings to support ventilation Combined variation of building heights Wide, yet shadowed open spaces Shadowing, planned tree zones	Dispersed form with open ends to support ventilation
Cold-humid, temperature (northern U.S.A. and southern Canada	Snowy Windy, blizzad conditions Very cold nights	Low temperature Winter and summer high precipitation Windy	Heating (passive and active): Mixture of open and enclosure forms Protected edges at winter windward side (with structures or trees) Uniformed building heights Medium dispersed open space Circumfernetial and intersecting tree strips	Mixed of open and controlled enclosure forms
Hot-dry (middle east and north Africa)	Intense solar radiation Large temperaure amplitude between day and night Dusty storms Torrential rain Low cloudy days Intense dehydration High salinization Evaporation exceeding precipitation	Excessive dryness combined with high day temperature Dusty and stormy	Compact forms Shadowing Eevaporative cooling Protected urban edges from hot winds Windward location near a body of water Narrow winding neighborhood roads and alleys Mix of building height to shadow the city Small, dispersed, and protected public open spaces Circumferential and intersecting tree zones Use of Geo-space city concept	Compact form
Cold-dry (inland plateau)	Stressful and uncomfortable Strong dry cold wind	Excessive low temperature associated with dryness Stressful wind	Compact and aggregate forms, clustered forms Protected urban edges Narrow winding neighborhood roads and alleys Uniformed city height Small, dispersed, and protected public open spaces Circumferential and intersecting tree zones Use of Geo-space city concept	Compact and aggregates form, clustered forms

Golany (1996) also noted the basic rules in terms of urban thermal performance. He identified some rules regarding urban thermal performance through land use patterns, design patterns, and public open spaces, to name a few. The most significant of all those related to this dissertation is the orientation of the streets, especially the peripheral ones. Golany (1996) stated that when those streets are aligned with the direction of prevailing winds, it allows for the wind to penetrate deep within the city. Those winds might be damaging in winter because it further drops the temperature. On the other hand, streets that are offset from each other help in reducing strong and sandy winds by reducing its velocity. Those street orientations are illustrated in (Figure 2.7 and 2.8). Another important feature discussed by Golany (1996) and relevant to this research is the shape of the streets and their width. Narrow and winding alleyways are considered to be a good protection from strong winds and have the tendency to receive less solar exposure through protective overshadowed spaces in between.

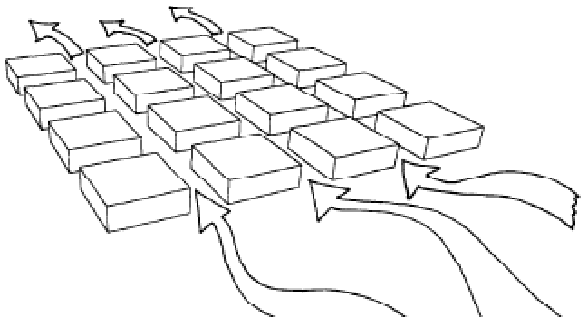

Figure 2.7 Grid layout allows for wind penetration deep within the layout (Golany, 1996)

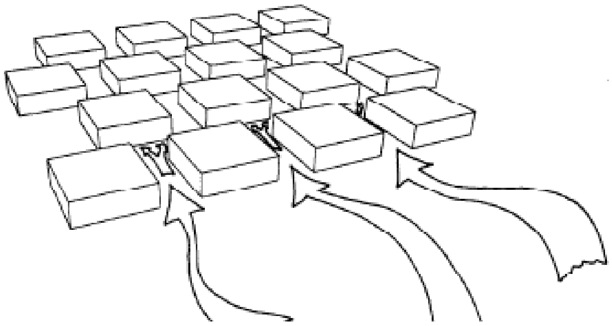

Figure 2.8 Staggered and offset street layout breaks down the wind velocity (Golany, 1996)

Ratti et al. (2003) quotes Fathy who stated in 1986 on the impact of climate on the built form: “By simple analysis it becomes quite understandable how much a pattern came to be universally adopted by the Arabs. It is only natural for anybody experiencing the severe climate of the desert to seek shade by narrowing and properly orienting the street, to avoid the hot desert winds by making the streets winding, with closed vistas”.

2.2 Building Form

According to Okeil (2010), some research papers have addressed the effect of building form on energy consumption. It relates to solar exposure of building surfaces and the resultant increase and decrease in temperature of indoor and outdoor spaces. Research that relates the built form with climatic changes can be categorized to those that investigate human thermal comfort and passive design strategies. Others correlate building design and solar access as a measure for passive heating and daylight access. A third category studies a large scale urbanization impact on climatic conditions.

In Okeil’s research (2010), a comparison was drawn between three types of building forms and configurations. The first was the linear building form. The building dimensions create elongated footprints. The orientation of these buildings to the sun would determine the solar exposure and overlaying shadows onto the surrounding open spaces and adjacent buildings. The next formation is typical of a residential block with a more square shape and outdoor areas. These structures also require a grid-iron urban configuration in order to function as required. There is more solar exposure in these structures than in the first form. The third formation is what Okeil (2010) refers to as the Residential Solar Block (RSB). These structures were created in order to gather the functional advantages of the block urban form and energy efficiency benefits of the linear form. Figure 2.9 shows the three different urban forms studied by Okeil (2010).

Figure 2.9 The three building forms investigated (left to right: linear block, typical square residential block, RSB form with accessible green roofs) (Okeil, 2010)

Results from the CITY SHADOWS program conclude that the Residential Solar Block received higher solar radiation in winter than the other two building forms. This was mainly due to its orientation and the building form extracted from solar profiles during December. During the summer, the RSB receives more solar radiation than the linear form and less than the block form. However, in September and March, the RSB and the other building forms receive more or less the same amount of solar radiation. Using Envi-met the airflow was also investigated and yielded observations of increased airflow at the higher levels of the structure and enough airflow at ground level to avoid wind stagnation. Figure 2.10 illustrates ENVI-met results for air flow from different directions at different heights of the RSB building form.

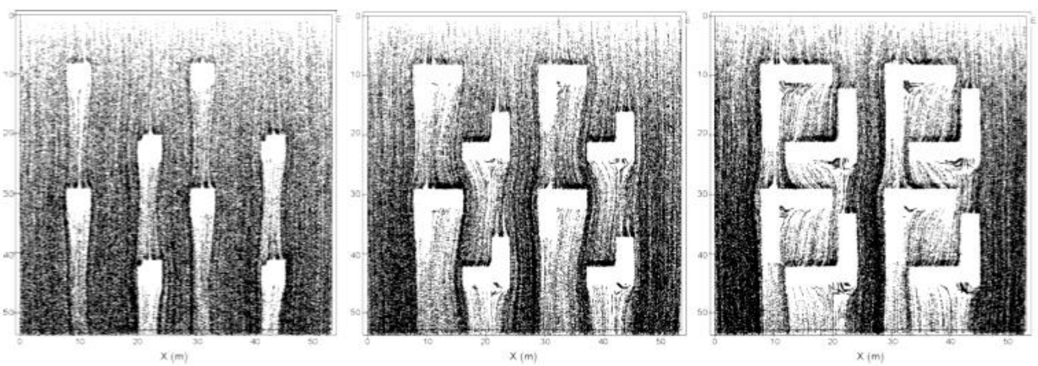

Figure 2.10 ENVI-met air flow results from different directions at different heights of the RSB form (Okeil, 2010)

Overall, this research highlighted the benefits of creating a structure which encompasses the advantages of linear building forms and block building forms. The structure maximizes the opportunity to tackle issues of material selection, green roofs, the design of open spaces based on the solar exposure of the structure. The limitation of the design, however, lies in the fact that it requires that the structures are designed in this particular way on a grid layout. The monotony that the researcher wanted to avoid might be an issue with a city planned using these structures. Furthermore, it is questionable if these structures would behave in the same manner from an airflow point of view if they are offset from a grid layout.

Panao et al. (2008) linked in mid-latitude climates between energy efficiency to building geometries with changing variables such as height (through number of floors), building length ratio, grid azimuth (the anti-clockwise rotation from the south axis) and aspect ratio. Panao et al. (2008) tested the different configurations depending on different "local radiation conditions as a function of latitude" (Panao et al., 2008). They studied terraces, pavilions, and slabs as possible urban forms shown in Figure 2.11 a, b, and c. Through a variety of studies which altered the number of floors of the structures, the grid azimuth, and the base length, they concluded that for lower latitudes, all of those urban forms are possible. Furthermore, they concluded that for the higher latitudes, pavilions perform better, and for latitude of 45º terraces are preferred. With regards to the spacing between the blocks, slabs and terraces with spacing oriented north-south should be maximized by altering the aspect ratio (mainly decreasing the aspect ratio as the latitude increases). Other findings showed that for all latitudes tested the base length should be kept at a minimum. Additionally, Panao et al. (2008) concluded that of all the different configurations tested, pavilions are best used for lower latitudes (35º) and higher latitudes (50º). It is optimal for lower latitudes because of the minimal roof area and therefore solar incidence on the roof is reduced in the summer season. It is ideal for the higher latitudes because vertical solar incidence is increased in the winter. For the pavilions, the north-south oriented aspect ratio is independent of the latitude, unlike with the slabs and terraces forms. It was shown that for all latitudes the aspect ratio in the order of 0.7 for pavilions ensures mutual shading between the buildings in winter. By altering the space between buildings, shading may be minimized. They have also concluded that pavilions demonstrate inter-reflections between the buildings resulting in increasing diffused irradiation (Panao el al., 2008).

(a)

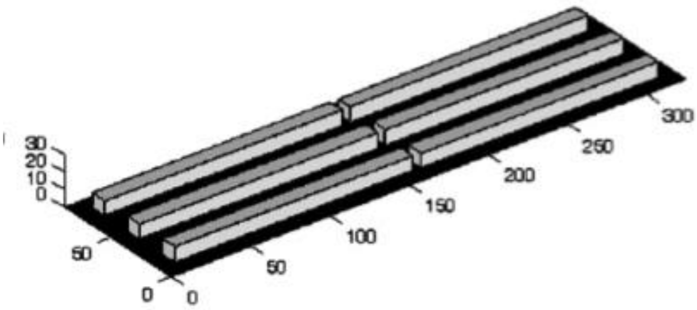

(b)

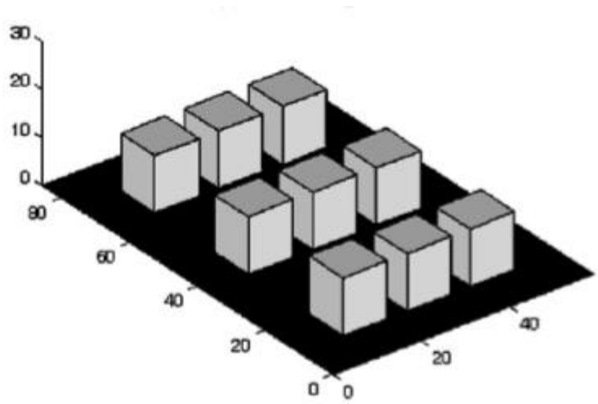

(c)

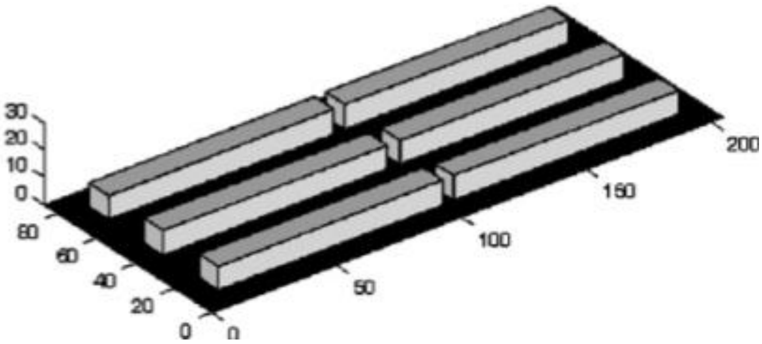

Figure 2.11 Urban forms (a) terraces, (b) pavilions, (c) slabs as defined by Panao et al. (2008)

2.3 Street Geometry

One of the main factors affecting temperature variation in urban contexts and related to urban parameters is the aspect ratio – the building height to street width ratio. Ali-Toudert and Mayer (2006) investigated this factor in addition to the orientation of the urban canyons in Ghardaia, Algeria. Using Envi-met as simulation software, the micro-climatic variations and the physiological equivalent temperature (PET) distributions were measured. The aspect ratios simulated were at values of 0.5, 1, 2, and 4 and oriented towards the east-west, north-south, northeast-southwest, and northwest-southeast. The wind direction in the simulations was assumed to be perpendicular to the street orientation. Figure 2.12 shows the different aspect ratios simulated and their orientations.

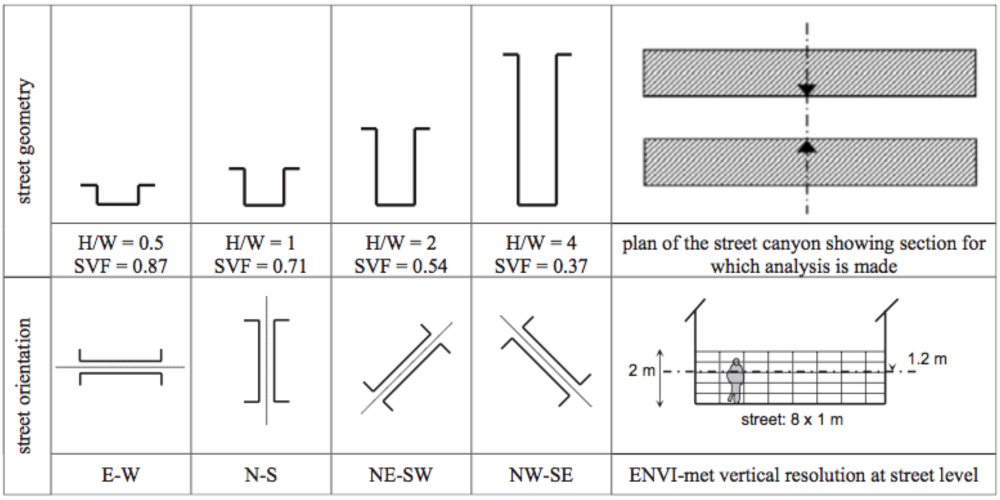

Figure 2.12 Illustrations of the simulated scenarios (Ali-Toudert and Mayer, 2006)

Conclusions based on these parameters showed that “both aspect ratio and solar orientation were found to have considerable influence on the street thermal environment…” (Ali-Toudert and Mayer, 2006). The results showed that lower aspect ratios are more thermally “stressful” due to the higher exposure to the sun. However, overlapping the orientation factor, streets oriented towards the east-west axis are also high in temperature even if the aspect ratio is equal to 4. This is mainly due to the lack of shadows casting from the buildings onto the streets. A better thermal environment was achieved in the north-south orientation. An even better comfort condition was evident in the oblique orientations of northeast-southwest and northwest-southeast as the shading influence was much higher. Another important factor briefly mentioned in the research was the direction of the wind and its influence in reducing the physiologically equivalent temperature (PET) value. Some simulations, not presented in the paper, show a decrease in PET of up to 12K when the wind direction was parallel to the street orientation compared to the perpendicular wind direction of the same aspect ratio scenario.

Emmanuel and Johansson (2006) investigated the effect of urban morphology and approximation to sea breeze on the microclimate of a hot-humid city in Sri-Lanka. Urban morphology was defined by aspect ratio. The investigated locations were located in Colombo with areas varied in aspect ratio, ground cover, and distance from the sea. The main findings were that the daytime temperature decreased significantly as the aspect ratio increased, giving rise to the significant impact this urban factor has on daytime temperature. Another finding was that the closer and more open the site was to the sea, cooler temperatures were recorded. As the aspect ratio increased, the wind speed decreased. Also, the temperature difference recorded between shaded and exposed urban areas was 20K.

Another research which also supports the effect of aspect ratio was conducted by Hamdi and Schayes (2008). They demonstrated that a lower aspect ratio, i.e. a wider street canyon in relation to the height of the building will show an increase in UHI effect. Whereas, a higher aspect ratio (narrower street canyon in relation to the height of the building) will have a higher shadowing effect and thus reducing the effect of UHI. The results of two aspect ratios and the reduction in temperature they result in are shown in Figure 2.13.

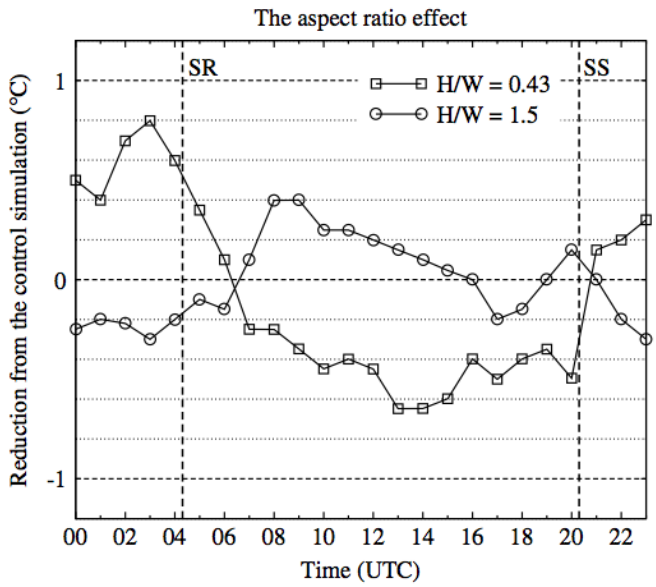

Figure 2.13 Graph showing the difference in behavior of two aspect ratios with respect to their temperature reduction values from a control simulation (Hamdi and Schayes, 2008).

Hamdi and Schayes (2008) also demonstrated in Figure 2.14, and based on earlier studies by Oke et al. in 1991 and Yamashita et al. in 1986, that there is also a linear relationship between the sky view factor and the reduction of nocturnal UHI.

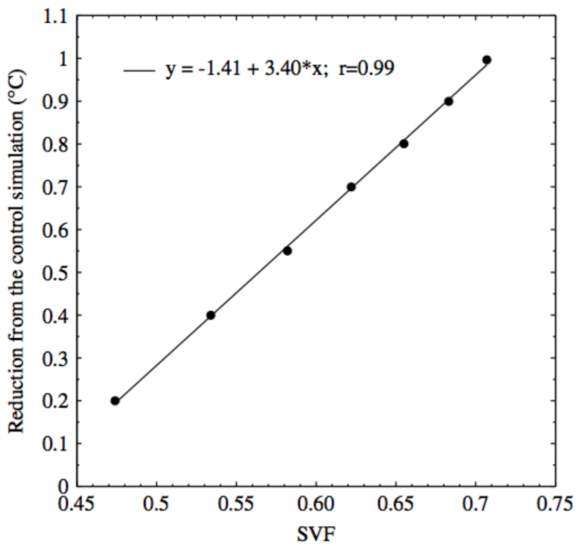

Figure 2.14 Graph shows the linear relationship between sky view factor and reduction in nocturnal urban heat island (Hamdi and Schayes, 2008).

This earlier research carried out by Yamashita et al. (1986) indicated a very strong correlation between the sky view factor and the urban heat island phenomenon. After investigating the temperatures of five cities and documenting them it was found that it was difficult to accurately correlate city size (through population density) and variations in these cities' temperature. The research showed that the UHI phenomenon does exist in each of the cities. Therefore, a correlation was made between temperature variations and the sky view factor in each of the cities. The graph in Figure 2.15 shows that there is a relationship between the minimum sky view factor values and heat-island intensities. The lower the sky view factor the higher the UHI intensity is. This relationship is also more pronounced for the daytime values than those of the nighttime.

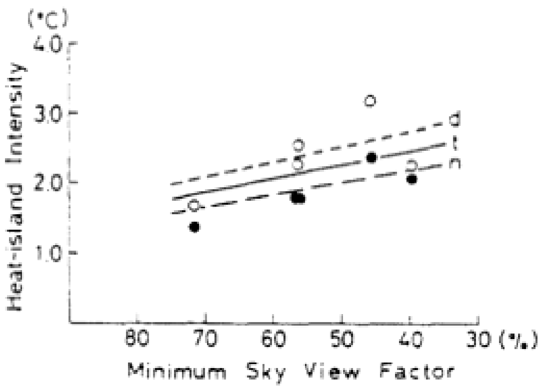

Figure 2.15 Graphs showing the relationship between minimum sky view factor and heat island intensity (Yamashita et al., 1986)

Other research regarding city size and its effect on urban heat islands was reported by Seaman et al. (1988) who found that an increase of the city size by a factor of 3 increased the urban heat island intensity by only 0.1°C. Hamdi and Schayes (2009) reported Atkinson's finding in his paper dated 2003 relating city size and the urban heat island intensity. It was reported that Atkinson (2003) varied the horizontal dimension of the urban areas from 6 to 20km and found that the sensitivity of the urban heat island intensity to the city size is in the order of only 0.2°C. Oke (1973) related the size of the city to the "magnitude of urban heat island it produces”. Oke (1973) incorporated the wind speed, population, and urban heat island intensity in one model. He found that in cloudless days the intensity of heat islands is related to inverse of the regional wind speed and the logarithm to the population. This was applicable to cities in the United States and to European cities through a modified model.

A more recent research carried out by Bourbia and Boucheriba (2010) in which they investigated street design and its impact on urban microclimate in semi-arid climate. The site selected is characterized by multiple variety of urban geometry defined by the sky view factor and aspect ratio. The results support previously documented findings. The areas which were more exposed and open recorded higher daytime temperature. The higher the SVF, approaching 1, the higher the temperature was. However, the relationship between aspect ratio and temperature values was inversed. The higher the aspect ratio the lower temperature. Bourbia and Boucheriba (2010) suggested that the SVF should be incorporated in urban geometry design as it plays a role in mitigating the effect of urban heat island.

Eliasson (1996) studied the urban nocturnal temperature in relation to street geometry and land use. The most prominent finding in his research was that there is very little variation between open spaces and urban canyons within the city center. It suggested that the lack of connection between urban geometry and air temperature readings in the city center during the night should result in not overestimating the importance of geometry. The research suggested that the major difference in temperature was reported between urban areas with different land uses. Eliasson (1996) demonstrated that the difference in air temperature between a large park southwest of the city and the city center of an average of 4°C was similar to the average temperature between urban and rural readings which was in the order of 3.5°-6°C. Another finding of this research was the distinction between surface and air temperature variations. Figure 2.16 shows readings of air and surface temperature moving from the city center towards rural areas.

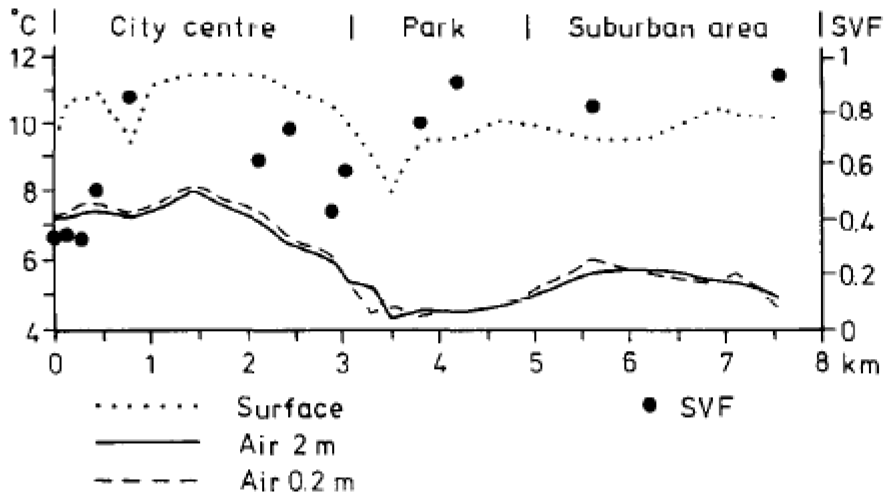

Figure 2.16 Graph showing air and surface temperature with regards to SVF and distance from city center (Eliasson, 1996)

Along the same lines of land use and city density, Stone and Rodgers (2001) showed that denser areas of the city produce less radiant heat and therefore contribute less to the urban heat island phenomenon. More expansive residential areas emit more radiant heat energy “per parcel than one of urban densification”. This was supported with another argument regarding land use, where the above theory does not apply. Large forested areas, for example, will not produce massive radiant heat and therefore will not play a role in the formation of urban heat islands. The formation of surface heat island is related to the nature of the exposed surfaces.

Mills in 1997 used the sky view factor in investigating the effect of a cluster of buildings on a single structure. Radiative effects in the daytime have been measured as a function of direct solar exposure. The cooling of the structures was measured as a function of the sky-view factor. This was mainly based on defining the sky view factor as “the proportion of radiation emitted by one surface which is incident upon another” (Mills, 1997). The computer model was set up to simulate a cluster of 9 buildings with equal distances from each other as illustrated in Figure 2.17.

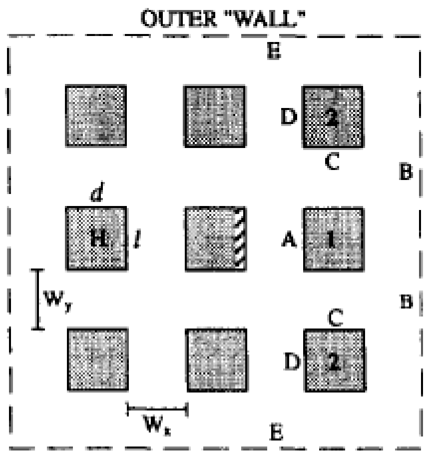

Figure 2.17 A sketch defining the parameters of the simulated model (H= height of the structure, W= spacing between structures, d= depth of the structure, l= length of the structure (Mills, 1997)

The simulation was run at different latitudes at different times of the year. The structures did not include any fenestrations, and the simulation did not take into account surface albedo and surface reflectivity. The entire research discussed heat gain and heat loss in terms of solar exposure and sky-view factor which in turn dictate the shape of the buildings in the configuration. For example, a high solar exposure and a low sky view factor renders itself in tall structures with small spacing. The research made conclusions to indicate some design strategies related to the season, orientation of the building, proportion of the buildings, and spacing. It ultimately showed that there is a relationship between a cluster of buildings and single structures and that there is mutual impact regarding thermal stresses. The drawback of this paper, however, lies in the fact that it addressed these criteria based on equal spacing between the blocks. No simulation was done considering un-equal spacing.

A research carried out by Sakakibara and Sato (2008), investigated the UHI intensity and urban geometry defined by the SVF. The measurements were taken in different seasons after sunset. The findings they concluded show that there is little correlation between the SVF and UHI intensity. The large variation in temperature in the order of 2-9C° for a sky view factor of 0.8 was not possible to be explained in their research. They have therefore concluded that there are other factors, asides from the SVF, which affect UHI intensity. Two explanations were provided. One related the intensity of the UHI to the UHI occurrence particularly during sunset. They attributed the value of UHI intensity at night to the UHI intensity at sunset in addition to the urban-rural cooling differences. The other explanation attributed the presence and development of UHI intensity to wind speed and cloud cover factors rather than the SVF. This was due to experimental results that showed that the larger the SVF, the smaller effect it had on the UHI intensity. They also concluded that nocturnal UHI intensity was due to “mechanical mixing” in the atmosphere because some of the results of their investigation showed that the high UHI intensity was not always associated with low wind speed values.

The only research conducted that particularly compared an old city fabric to a new one was a research carried out by Johansson (2006). He chose a part of Fez city which represented the medieval city to represent the old fabric, and a contemporary city fabric from the French colonization times representing the new fabric. In his study, he aimed at linking between urban geometry and its effects on the “microclimate and thermal comfort at street level in a hot dry climate”. The urban geometry, as with the previous reviewed literature, was represented using the aspect ratio and sky view factor. The area chosen from the old fabric represents a deep canyon (high aspect ratio) and the location selected from the new fabric is a shallow canyon (low aspect ratio), illustrated in Figure 2.18 a and b.

(a)

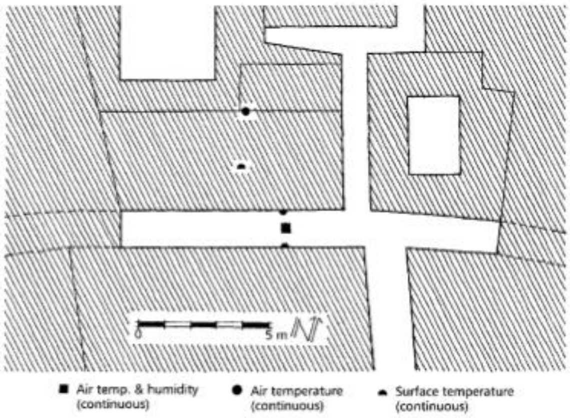

(b)

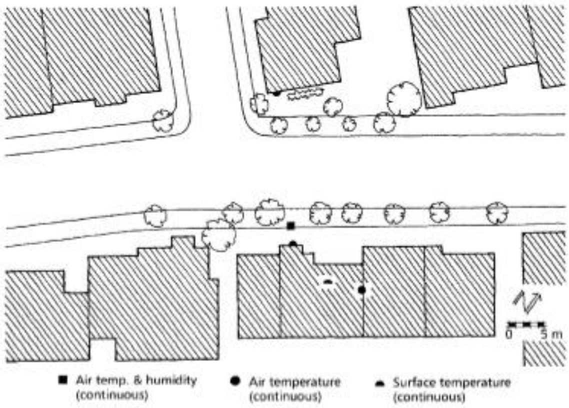

Figure 2.18 Illustration showing the location of measurements in **(a)** deep canyon in the old city fabric and in **(b)** shallow canyon in a modern city fabric (Johansson, 2006)

The field measurements conducted gave conclusions in line with previous findings. During the day, the high aspect ratio gave cooler readings than the lower aspect ratio canyon. This is mainly due to the geometric proportion of the deep canyon which allows for shadows and shade to continue throughout the entire day. Johansson (2006) also indicated that the warmer air at the roof top is unable to reach the lower parts of the canyon. At night however, the higher aspect ratio showed higher readings than that of the shallow canyons. This is mainly due to the low sky view factor. Although the compact urban form gives protection from the sun and reduces solar exposure resulting in lower temperatures during the summer, it is disadvantageous during the winter.

2.4 Material Albedo and Vegetation

Among the factors contributing to the urban heat island effect is surface properties. Solar reflectance, infrared emmitance, and surface albedo are some of the characteristics that have been investigated by researchers in this field. Some of the research addressed the surface application, such as roofs, facades, and open spaces. Some others have investigated the material property itself such as its color, permeability, and absorption in a variety of materials such as grass, tiles, glass, and coatings.

In Wong's research (2005), field measurements showed that there was a significant decrease in temperature in areas with larger green areas within the city. Bretz, et al. (1998) and Synnefa, et al. (2007a) indicated that the use of solar reflective materials and cool coatings respectively have the effect of mitigating the urban heat island effect. This consequently reduces the need for high cooling loads in the summer rendering it more economically feasible to invest in such measure on the long run. Yilmaz (2008) conducted a research to compare temperature variations between asphalt concrete, soil, and grass surfaces. These researchers, to name only a few, have introduced mitigation measures that are either implemented to change existing structures of open spaces, or are to be considered throughout the design process itself.

Takebayashi and Moriyama (2009) investigated the effect of converting back artificial surfaces to a more natural one. For this purpose, the site was a public parking lot with each car space defined in terms of different surface materials. Some of the materials also considered were environmentally friendly, such as recycled materials, plants, and different soils. They have concluded that there is a reduction of air temperature by 0.1C° for a grass-covered parking surface in comparison to asphalt.

2.5 Wind Speed and Cloud Cover

In the presence of complex interrelated factors contributing to the urban heat island phenomenon, Morris and Simmonds (2001) investigated the association between urban heat island intensity and wind speed and cloud cover. Their main findings were that calm winds and clear skies result in increased means of urban heat island values. Through regression analysis, it was found that increase in both wind speed and cloud cover resulted in reducing UHI values. In summer, when the results were most pronounced, it was found that an increase of wind speed by 1m/s the UHI variation was -0.139°C, i.e. a reduction in the value of UHI. Furthermore, an increase of 1 octa of cloud cover the UI variation was -0.122°C, i.e. a reduction in UHI as well.

Figuerola and Mazzeo (1998) carried out a research to investigate how urban heat islands are affected by factors such as cloud cover, wind speed and direction, the day of the week, and different seasons. They reported that in winter the temperature difference between a day with little sky coverage with weak wind speed was 1C° higher than a day with windy and cloudy conditions. Also, the maximum temperature difference occurred when the direction of the wind was from the rural areas towards the urban.

2.6 Research Limitations

After a thorough look at the literature available in the field of urban heat islands and the effects of building and urban forms, some limitations may be identified. Some of these limitations include the lack of investigation related to urban configurations on a city scale. Many of the investigations provide strong evidence and findings limited to building-to-building relationships. Urban form is defined on the basis of certain ratios that relate buildings or spaces and their immediate surrounding elements, for example, building to building, street to building, or building to street to vegetation relationships. The overall urban configuration factor behavior is reduced to those points where measurements can be taken. There is almost none, asides from those that include cross terrain or cross country measurements that investigate the urban configuration of a city as a whole. As Golany (1996) states "…, to the best of our knowledge, there is very little, if any, literature about urban design scale (neighborhood and city) as it relates to climatic considerations." It is envisaged that there is significance to study the impact of a group or cluster of roads and buildings on the overall neighborhood and consequently the micro-climate. Most of the research available will choose one point in a street that is considered to be representative of the behavior of areas with similar properties. Though this has provided much insight and set some guideline as to how variations of aspect ratios and sky view factors affect the micro-climate, it provided very little on how a number of these aspect ratios and sky view factors put together in one form or another affects temperature and wind variations. Those clusters of buildings and streets and the interrelationship between them and how they affect the micro-climate due to these relationships may shed light on the difference in the behavior in terms of temperature and wind between the different urban configurations defined in this paper. Each building and street creating a block interacts with the next block or unit next to it, creating an enlarged area with interlocking and coinciding effects. Those coinciding relationships, though difficult to define, do in turn affect the urban canopy layer.

Another main finding from the literature review is that many researchers concentrate the research to address UHI through outdoor thermal comfort. These efforts have been recognized to be of utmost importance in defining the measure for good climatic responsive design. With this in mind, this research focuses on the mere temperature measurements in absolute terms regardless if they fall within the thermal comfort zone or not. It is accepted that those then in turn may be used in order to define whether or not the urban configuration serves well in terms of outdoor thermal comfort.

The lack of investigations and published data in this part of the world, namely the gulf region, also imposes an additional challenge in data gathering and sufficient literature for comparison.

This research aspires to bridge this gap in micro-climatic research related to urban design and give insight on how different urban configurations may impact temperature and wind variations.

2.7 Aim and Objectives

The aim of this research is to investigate the effect and impact of the various urban forms on the urban heat island phenomenon in Dubai, UAE. It aims to answer whether or not different urban configurations within a certain city behave differently in terms of temperature and wind variations throughout the year. In the UAE, Dubai is the selected location for the study and the three main configurations investigated will be the centralized form from an old district in Dubai, Bastakiyah. The other forms include a more orthogonal version of the old fabric and another as a grid-iron form of the same buildings and in the same location. This research focuses on avoiding rather than mitigating the urban heat island phenomenon. Studying in advance the growth of the city and which urban form is best suited for its climatic conditions will reduce, on the longer run, problems arising from urban heat islands.
The aim of this research will be answered through the following set of objectives:

1. Define the variables affecting the urban heat islands and selecting the ones closely related to this research.
2. Simulate, through a computer software, temperature and wind variations of three different urban configurations.

3. Analyze simulation results through visual and numerical readings to define the most dominant factor in the varying behaviors of the different simulated urban configurations, if any.
4. Define and justify the better performing configuration of the three simulated alternatives.

CHAPTER THREE

METHODOLOGY

3.0 Methodology

The previous chapter looked at the various criteria that impact and contribute to the urban heat islands phenomenon. It is important to highlight that these factors contribute to the UHI effects in a complex manner. Each of the factors interacts with another that causes this complex phenomenon to take place. For example, as seen in the reviewed literature, building proportions impact wind circulation, and wind circulation in turn impacts heat transfer, so did the availability of overcast shadows.

Poreh (1995) had stipulated that the lack of knowledge in the field of UHI, despite the long history of investigations is attributed to the following:

1. the inherent complexity of the city-atmosphere system
2. lack of a conceptual theoretical framework for enquiry
3. high expense and enormous difficulties to perform observational research in cities

3.1 Methodology Literature Review

This section aims at presenting literature review of the different research methodologies relevant to the topic of urban heat islands. Advantages and limitations of each are also discussed.

3.1.1 Field Measurements

Some of the field measurements in the following methodology literature review include location specific measurements. These are ideal for measurements that are smaller in scale and relate directly to micro-climatic variations. They are also usually used to study the interaction between buildings and their direct environs and surroundings.

Emmanuel and Johansson (2006) and Johansson (2006) used field measurements to collect data from selected measurement sites. In both researches, they were specific in locating the probes and sensors for their measurements. The former was particular about the location of the probes from the building facades and how accurately they represent the height of a pedestrian. Other instantaneous measurements were taken for surface temperature and wind speed. Some of the instruments used were infrared thermometers and “directionally independent wind sensors” (Emmanuel and Johansson, 2006). The latter was particular about the location of the probes in relation to the nature of his investigation. The location of the probes related to the depth and height of the urban geometry to get the best representative results of the two different urban areas they investigated.

Other field measurements revealed from the literature review are ones taken in an urban-rural transect method. Measurements taken in this method intersect a large section of a city or cross-country in order to gather data across different and larger locations. Those were ideal to gather data of a meso-climatic nature. It is ideal to understand the relationship of factors such as land zoning, land cover, population density, and city scale on climatic variation. These measurements include mobile surveys with probes and data loggers mounted on automobiles and driven across the terrain.

Some researchers have used the method of observation and field measurements in order to investigate the relationship between city size as defined by its population and the urban heat island it consequently creates. In his investigation, Oke (1973) had used automobile traverses to gather data from several towns and cities across Quebec, Canada. The results gathered from the field measurements were compared to earlier published data. Yamashita et al. (1986) used the special instrumentation mounted on automobiles and through groups on foot to gather data. They mentioned that the limitation of such approach was the lack of man-power and specialized instruments to cover all the areas and had to limit the investigation to two cities at a time.

Eliasson (1996) utilized automobile traverses, mobile data loggers, and infrared thermography system to study the impact of different land uses on urban temperature variations. The investigation created a cross section through the city center outwards to a peripheral park reaching suburban areas.

Wong and Yu (2005) used this method to study the cooling impact of green areas on urban heat islands, as well as the severity of UHI at a macro-level in Singapore.

Morris et al. (2000) used the urban-rural transect method to study wind and cloud cover as factors affecting nocturnal urban heat islands across Melbourne, Australia. This method created a "network of monitoring stations in and around the city" from which data was gathered across a long period of time.

In each of the mentioned papers, the gathered data was compared to previously published and readily available weather data from meteorological stations.

Field measurements have also been used in the study of material behavior in situ, exposed to the natural environment without a proxy. Although this might be a good methodology to obtain "real" measurements, it has the limitation of lack of control over the conditions of the measurements. It becomes increasingly difficult to track the variable that contributed to the readings. With such investigation, the factors contributing to the readings should be defined beforehand in order to ensure some level of control and accurate reading of which is affecting the reading and whether or not there are other outer factors affecting the readings. Prado and Ferreira (2005), in their research of albedo materials used on roof surfaces in Brazil, have made a distinction between measurements obtained from a lab and those obtained from a natural setting. Lab measurements will express characteristics of the material itself; while in the field it will express the final product.

The limitation of this type of methodology is the need for specific instrumentation, monitoring devices and data loggers. The time factor is also a limitation, as they require a longer time to gather the required data. For example, in the case of vehicle mobile surveys, the traverses need to be synchronized for readings to be taken at the same time across the various locations of the city or country. Also, another limitation of field measurements is the inability to change climatic conditions at the time of measurements. Should there be a requirement for clear sky during the logging of data, for example, and weather conditions are not according to those requirements, the measurements would need to be postponed until the conditions are in accordance to the research criteria. The lack of previously published data in terms of temperature variations across the different parts of Dubai is also a limitation in the case of this research. Furthermore, even though field measurements give results from a natural setting without a ‘proxy’, independent variables become increasingly difficult to track especially in a subject matter such as urban heat islands where the dynamics contributing to it are already too complex to track. It becomes more difficult to isolate each cause of the obtained results.

3.1.2 Simulation

Simulation and computer modeling are ideal in replicating a certain condition or situation to be investigated. It allows for a high level of flexibility in controlling certain variables and changing others. It makes it easier for the researcher to test a variable and increasingly add other variables and monitor the behavior of the investigated scenario.

Simulations resolve some of the limitations of other methodologies such as restrictions due to climatic conditions, or long time frames for investigations, far geographic locations, or unattainable contexts. The size of the simulated scenario is also rarely a limitation. In the field of urban heat islands the covered areas and dimensions set for investigation are usually an important input that needs to be considered. On the flip side of these advantages, is the lack of a “natural” setting and the overestimation and error factors built into simulation software. Also, as stated by Arnfield (2003), numerical modeling and simulations lack the process of validation. Validation in most cases rely on the likelihood of the results rather than “direct comparison to process variables”.

This literature review revealed that some researchers rely on several simulation software, each to investigate a certain aspect of their research. Okeil (2010) used City Shadows, created by him, to simulate and calculate solar exposure of different urban forms. He then used ENVI-met to simulate wind circulation from different directions exposed to the studied form. Fahmy and Sharples (2009), also used ENVI-met to study the impact of a grid urban form and green structure and calculated the PMV for the assessment of thermal comfort. Ali-Toudert and Mayer (2006) used ENVI-met to calculate physiologically equivalent temperature (PET) values to assess thermal comfort depending on aspect ratio and orientation of street canyons. Thapar and Yannas (2008) used simulation software (ENVI-met) to support data collected from field measurements.

Mills (1997) used a computer model to assess the impact of a cluster of buildings on a single structure. It was intended for the model to determine the “best” configuration in a certain latitude responding to certain climatic conditions. Ratti et al. (2003) used the Digital Elevation Model (DEM) in addition to Matlab, an image processing software, to reassess work done by previous researchers. Shashua-Bar et al. (2004) used Green CTTC model, an extension of the CTTC model developed by Swaid and Hoffman in 1990. “The CTTC is an analytical model incorporating a cluster thermal time constant for predicting air temperature variations in the urban canopy layer (UCL)” (Elnahas, 1997).

3.1.3 Case Studies, Literature Review, Surveys, and Historical Data

The advantage of such approach is that it provides a breadth of knowledge for researchers to refer to as a source of collected, correlated, and compared data from the scientific community. They synthesize the findings of a certain topic and present them in a less detailed account than the original research, but still pertaining to the important findings respectively.

Golany (1996) and Arnfield (2003) used the method of historical data, literature review, and case studies to summarize the findings up to the time of their research. The method was used in order to define the progress in the field of urban heat islands, and where the scientific community stands with regards to the way forward. Arnfield (2003) drew similarities and comparisons between the findings in two decades related to urban climate research. He also summarized recommendations for future work in that field. Golany (1996) employed this methodology to summarize the relationship between urban morphology and characteristics and thermal performance. He included design recommendations on the basis of previously concluded observations regarding different climatic regions.

In the reviewed literature, surveys were mainly used in order to assess thermal comfort. Both Thapar and Yannas (2008) and Ahmed (2003), used thermal comfort surveys in order to assess the comfort levels of subjects passing by or sitting in the tested locations. Those were coupled with hand held devices that took instantaneous measurements of the conditions at the same location.

Che-Ani et al. (2009) used the case study method to study the city of Tehran and explore the factors causing urban heat islands. In general the paper aims at giving recommendations to mitigate this phenomenon and reduce its negative impacts through preventative action. They set up a series of all the factors contributing to urban heat islands and defined them in the context of the examined city and supported by previous data and literature reviews.

Using the literature review and case study methodologies, however, have their limitations. They give an indication of certain research parameters related to the researchers themselves and the theory in question. Even though literature reviews and case studies give a good indication to the type of knowledge that is available on a certain topic, it might be outdated. Literature review and case studies are important to give a basis for further investigation within the field of urban heat islands but should be substantiated with simulations and measurements directly related to the intended investigation. It would be insufficient to use only previous literature reviews and case studies to support the argument of this research.

3.1.4 Laboratory Measurements and Scaled Models

Laboratory measurements in most cases entail the use of scaled models. These models are inserted in labs with pre-specified conditions depending on the requirements of the research. As was the case with simulations, laboratory experiments have a higher level of control than field measurements. It is also a representation of a natural setting. Unlike with simulations, laboratories might have limitations in terms of the scale of the models that can be used in those facilities. Scaled models are therefore significantly smaller in scale than the real scenario. Laboratories are also expensive to set up and usually require expensive instruments and machines, such as wind tunnels for example. Physical models require that a scaled prototype stands in as representation of the “real” configuration. There are limitations to such approach regarding the dimensions representative of the real boundaries being tested. Some dimensions are difficult to obtain. Other limitations include those related to the “time-dependant” characteristic of the UHI. Some of the components contributing to the UHI are either ignored or reduced to one or two criteria to be studies to limit the complexities.

Poreh’s research (1995) is an example of one that used a scaled physical model. The intention and conclusion of the research was ascertained that it is possible to study UHI through the use of small scale models.

Sakakibara and Sato (2008) studied the impact of urban geometry on temperature readings. The scale model was placed in a “climate chamber” where the temperature was controlled and thermocouple probes were placed on the model to measure surface temperature. Different screening of the chamber walls was used to simulate night conditions. The model was then altered through several layers of material to resemble the different aspect ratios studied in the city. The findings were then compared to field measurements collected through mobile surveys.

3.2 Methodology Selection

In this research there are several limitations that need to be considered for the selection of a methodology most appropriate for the question at hand. Therefore the selected methodology is computer simulation. It covers the limitations of the research conditions and gives a good alternative to other methodologies such as the observational method, field measurements, and laboratory measurements. The most important limitation of this research is the size of the area under investigation. It covers a large area and there are several other scenarios derived from the original that also need to be studied. The simulation allows for flexibility to draft out several scenarios that do not exist on the site. The simulation method gives a higher level of control over both environmental and building related factors that may affect the results.

The other limitation is the time frame of this research. Time is limited and the investigation is intended to cover 3 seasons of the year: summer, winter, and autumn. In the observational and field measurements methods, it will only be possible to gather data on those exact days. The conditions of those days might also not be accurately representative of the season. Field measurements require certain kinds of instrumentation that are expensive and difficult to obtain. In addition, laboratories with wind tunnels and sun domes to simulate wind flow and sun exposure are not available. Another limitation in this research is the lack of published data regarding UHI in Dubai, UAE. According to Dubai Municipality, and at the time this research was conducted, there is no published data presenting the rural temperatures measured over a period of time.

3.3 Software Selection

The research is intended to measure micro-climatic variations in temperature at street level. Most of the software available is capable of simulating individual buildings and indoor spaces such as Integrated Environmental Solutions (IES) (www.iesve.com). The requirement for this research is software that is capable of simulating outdoor urban areas. Some of the software available that is capable of simulating urban contexts include ENVI-met, CityCAD, CITY SHADOWS, and Autodesk Ecotect Analysis. CityCAD (www.holisticcity.co.uk), although capable of modeling sustainability criteria, such as energy budgets, CO_2 emissions, shadow rendering, it lacks the ability to model temperature and wind variations. CITY SHADOWS is used to simulate solar exposure, and Ecotect is limited in its capabilities intended for this dissertation.

Therefore, the primary software selected for this research is ENVI-met (www.envi-met.de). It is a software developed by Michael Bruse. It has the ability to calculate the microclimatic dynamics of complex urban structures. The software can calculate wind flows, temperature variations, humidity, radiation fluxes, as well as PET values, to name a very few. The software is flexible enough to add vegetation, add soil profiles, change surface materials, and change geographical locations. Because it is based on the fundamentals of fluid dynamics and thermodynamics it has the ability to calculate, amongst other things, flow around and between buildings, and heat exchange processes between the various surfaces (Bruse, 2003). The software requires a variation of input details regarding the location of the site. Those are usually readily available such as relative humidity, wind speed and direction, and average temperature through meteorological references. ENVI-met is also a free software and easily obtained with no fee or time limitations.

Some of the researchers who used ENVI-met in their investigations included Thapar and Yannas (2008) to study the relationship between urban aspects and the microclimate in Dubai. Ali-Toudert and Mayer (2006) used it to investigate the effects of aspect ratio and street orientation on outdoor thermal comfort. Okeil (2010) used ENVI-met to measure the airflow around the RSB building form at various heights, whereas Fahmy and Sharples (2009) used it in their study of green structures as passive measures for thermal comfort.

The secondary software used is Autodesk Ecotect Analysis for the weather tool plug-in to obtain solar orientation stereograph, and other climatic data related to the site.

3.4 Site Selection

The areas selected for this investigation are all located in Dubai. Bastakiyah, an old district of Dubai, south of the Dubai Creek was selected for this study. Figure 3.1 shows the location of the Bastakiyah area in Dubai.

Figure 3.1 Location of the renovated Bastakiyah area in Dubai, UAE (Google Earth)

A small portion of this traditional area has been renovated and preserved on the old urban fabric, with narrow alleyways and a more organic natural configuration. It is significantly different from the newer areas of Dubai characterized by a more gird oriented configuration. The parameters of the site are used in all the simulated scenarios. The buildings in the area are all low rise ranging between a single story and double story structures. Many of the buildings have courtyards within them. The winding roads are narrow in the range of 2 to 3 m wide, some as narrow as 1m. There are some open space nodes within the neighborhood. There is very little vegetation and the roads are made of pavers, not asphalt (Figure 3.2 and 3.3). The parameters of the site and buildings that will be studied in the following chapters include climatic data such as initial temperature and wind speeds, relative humidity, etc. Building properties included material albedo of walls and roofs.

Figure 3.2 The old renovated area of the Bastakiyah in Dubai, UAE (Google Earth)

(a)

(b)

(c)

Figure 3.3 Images around the Bastakiyah area in Dubai (a) open spaces, (b) narrow winding roads, (c) alleyways (Google Image)

3.5 Dubai Weather Overview

Dubai is geographically located at 25° 15′ 0″ N, 55° 18′ 0″ E and covers an area of 4,114sq km after land reclamation from the sea. Dubai's landscape is predominantly sandy desert and the Dubai creek runs northeast-southwest through the city.

Due to the proximity of Dubai to the Tropic of Cancer line, it has a hot arid climate with hot and windy summers and cooler winters. Throughout the year, Dubai skies are sunny with a clear cloud cover and precipitation is minimal throughout the year. Wind direction in predominantly northwest throughout the year with a maximum speed of 5 m/s.

Details of the Climatic Data of Dubai are further explained based on extraction from Autodesk Ecotect Weather Data File:

Solar Position

The diagram shows the direction and solar position throughout the months of the year and time of day.

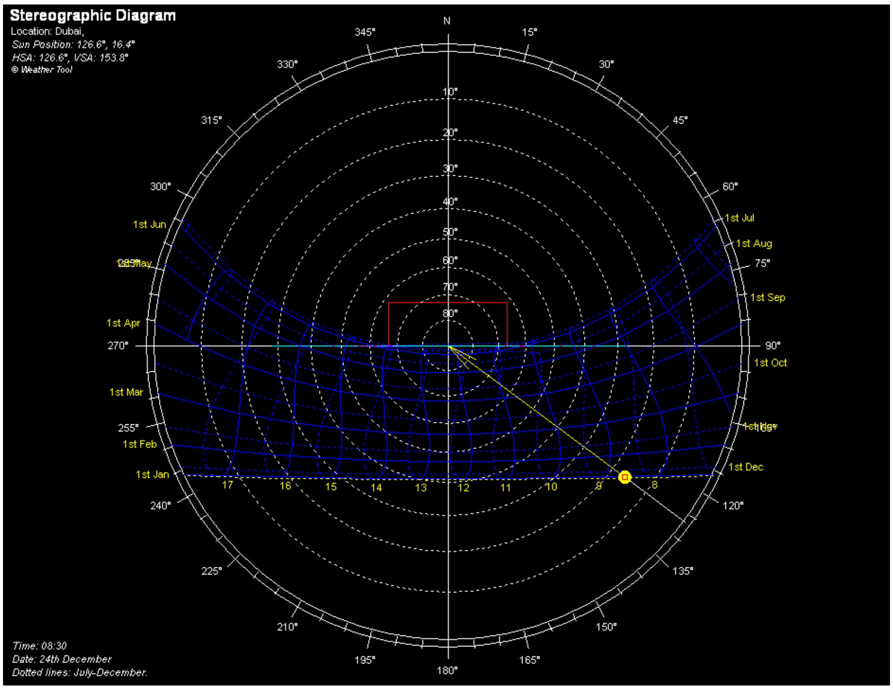

Figure 3.4 Stereograph for solar position in Dubai, UAE (Ecotect)

Wind Speed and Direction

Wind blows from all directions throughout the year with prevailing winds coming from the northwest direction. The highest frequency occurs at wind speeds of 2.7-5.5 m/s for more than 254 hours a year, which is equivalent to 6% of the year's wind.

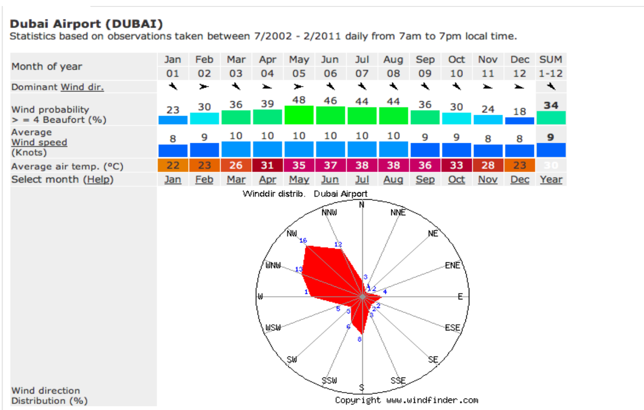

Dubai Airport (DUBAI)
Statistics based on observations taken between 7/2002 - 2/2011 daily from 7am to 7pm local time.

Month of year	Jan 01	Feb 02	Mar 03	Apr 04	May 05	Jun 06	Jul 07	Aug 08	Sep 09	Oct 10	Nov 11	Dec 12	SUM 1-12
Dominant Wind dir.													
Wind probability > = 4 Beaufort (%)	23	30	36	39	48	46	44	44	36	30	24	18	**34**
Average Wind speed (Knots)	8	9	10	10	10	10	10	10	9	9	8	8	**9**
Average air temp. (°C)	22	23	26	31	35	37	38	38	36	33	28	23	30
Select month (Help)	Jan	Feb	Mar	Apr	May	Jun	Jul	Aug	Sep	Oct	Nov	Dec	Year

Wind direction Distribution (%)

Figure 3.5 Wind direction and speed over a 9 year period in Dubai, UAE (www.windfinder.com)

Average Rainfall

Rainfall in Dubai is infrequent and is in the form of irregular bursts and thunderstorms between the months of December and March. The average number of days of rainfall during the year is 28 with a total of amount of rainfall of 88mm.

Climate data for Dubai [hide]													
Month	Jan	Feb	Mar	Apr	May	Jun	Jul	Aug	Sep	Oct	Nov	Dec	Year
Record high °C (°F)	31 (88)	31 (88)	41 (106)	41 (106)	45 (113)	45 (113)	47 (117)	48 (118)	43 (109)	40 (104)	41 (106)	31 (88)	48 (118)
Average high °C (°F)	24.0 (75.2)	25.4 (77.7)	28.2 (82.8)	32.9 (91.2)	37.6 (99.7)	39.5 (103.1)	40.8 (105.4)	41.3 (106.3)	38.9 (102)	35.4 (95.7)	30.5 (86.9)	26.2 (79.2)	33.4 (92.1)
Daily mean °C (°F)	19 (66)	20 (68)	22.5 (72.5)	26 (79)	30.5 (86.9)	33 (91)	34.5 (94.1)	35.5 (95.9)	32.5 (90.5)	29 (84)	24.5 (76.1)	21 (70)	27.5 (81.5)
Average low °C (°F)	14.3 (57.7)	15.4 (59.7)	17.6 (63.7)	20.8 (69.4)	24.6 (76.3)	27.2 (81)	29.9 (85.8)	30.2 (86.4)	27.5 (81.5)	23.9 (75)	19.9 (67.8)	16.3 (61.3)	22.3 (72.1)
Record low °C (°F)	8 (46)	7 (45)	11 (52)	8 (46)	17 (63)	22 (72)	25 (77)	25 (77)	22 (72)	16 (61)	13 (55)	10 (50)	7 (45)
Precipitation mm (inches)	15.6 (0.614)	25.0 (0.984)	21.0 (0.827)	7.0 (0.276)	0.4 (0.016)	0.0 (0)	0.8 (0.031)	0.0 (0)	0.0 (0)	1.2 (0.047)	2.7 (0.106)	14.9 (0.587)	88.6 (3.488)
Avg. precipitation days	5	7	6	3	0	0	1	0	0	0	1	5	28
Source #1: Dubai Meteorological Office[5]													
Source #2: Qwikcast [6]													

Figure 3.6 Rainfall throughout the year in Dubai, UAE (Wikipedia)

Temperature

The highest temperatures are recorded during the months of June, July, and August with the highest temperature recorded at 40°C. The lowest temperature is recorded during the months of December, January, and February at 15°C.

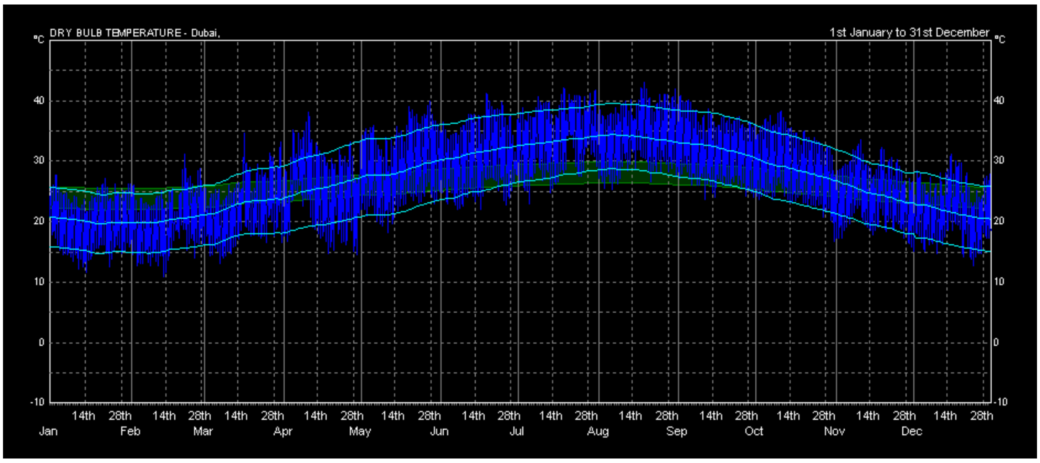

Figure 3.7 Dry-bulb temperature throughout the year in Dubai, UAE (Ecotect)

Relative Humidity

Humidity levels are consistent throughout the year ranging from 30% to 90% all year long. The average humidity is recorded at 30-50% for yearly wind speed of 8-13 m/s. In near coastal areas, humidity ranges from 50-60%.

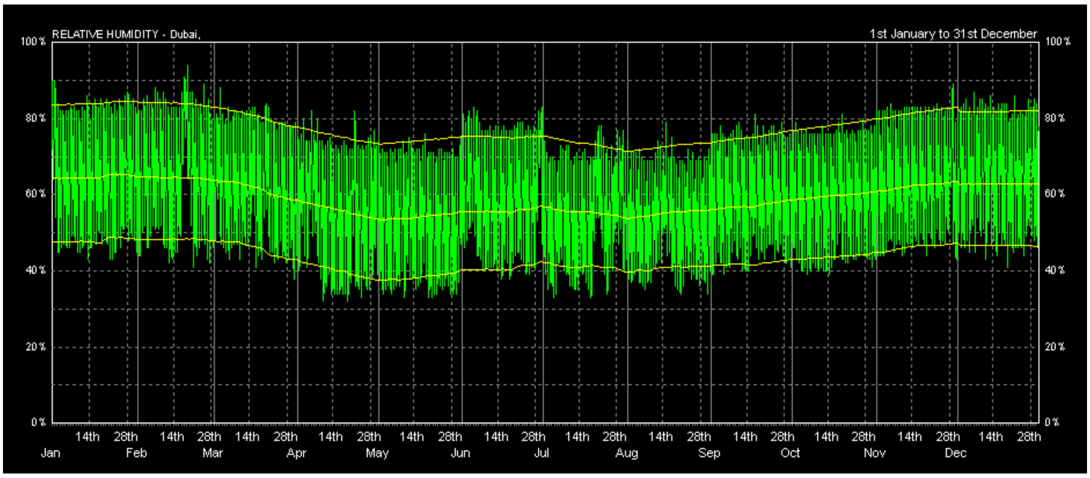

Figure 3.8 Relative humidity throughout the year in Dubai, UAE (Ecotect)

Solar Radiation

Solar radiation, which is the electromagnetic radiation emitted by the sun, is divided to direct and diffused solar radiation. The scattered, reflected, and absorbed sunlight due to the atmosphere and clouds is what is known as diffused solar radiation. Direct solar radiation is the solar radiation that reaches the earth without being affected by the elements.

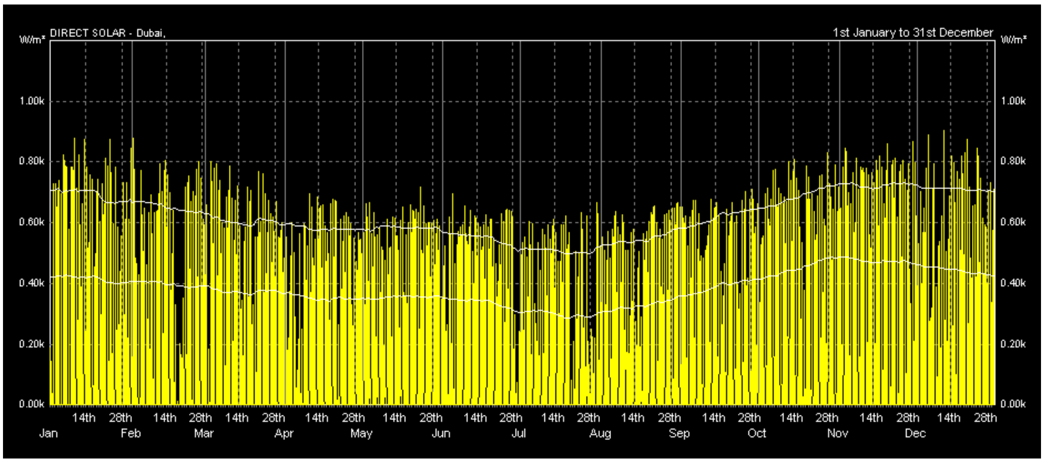

Figure 3.9 Direct solar radiation throughout the year in Dubai, UAE (Ecotect)

CHAPTER FOUR

COMPUTER MODEL SET-UP AND VALIDATION

4.0 Computer Model Set-up and Validation

4.1 Model Set-up

Before the beginning of simulation runs, a few verification runs were performed to ensure that ENVI-met registers the effect of open spaces and courtyards. All the verification simulations were run from 10:00 till 14:00. Figure 4.1 a and b representing each of the simulations are results obtained at 11:00.

Two sets of simulations were carried out. One model represented a high building with a courtyard (10m) and lower surrounding blocks (6m) shown in Figure 4.1a. The other model represents a low building with a courtyard (6m) and higher surrounding blocks (10m) shown in Figure 4.1b. In the figures, the simulation results show differences in temperature and wind flow. This verified that the software takes into account height variations in thermal and wind calculations.

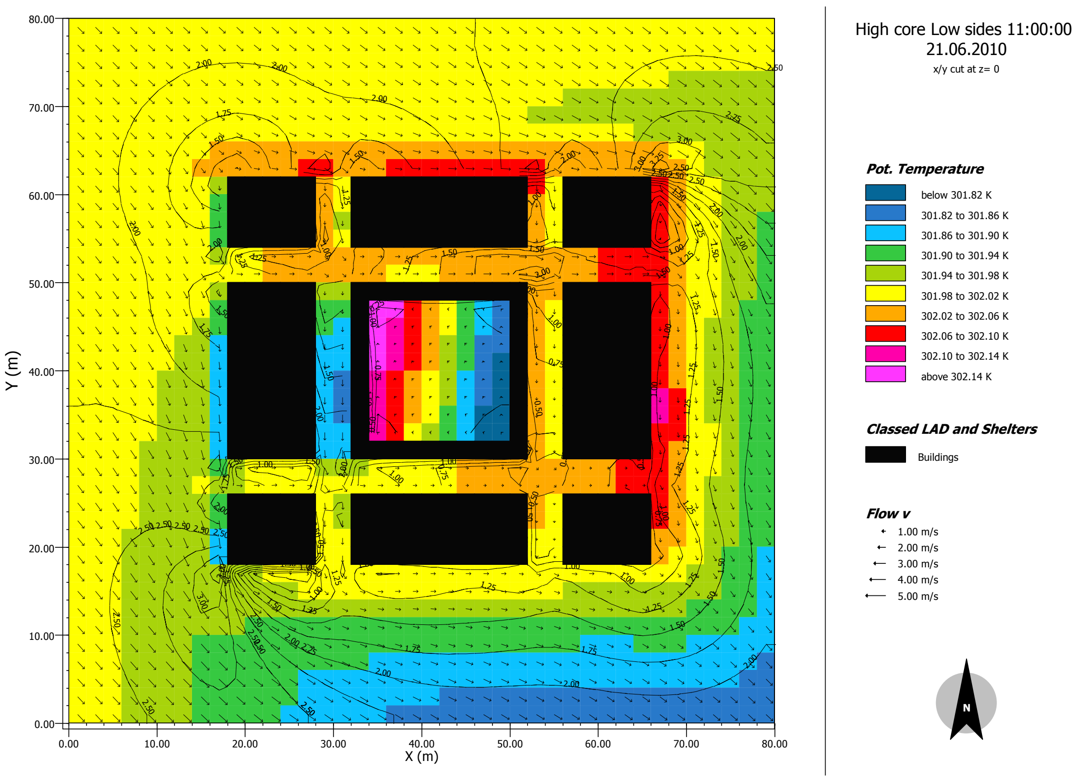

Figure 4.1 (a) Simulation results for a model with high courtyard block (10m) and low surrounding blocks (6m)

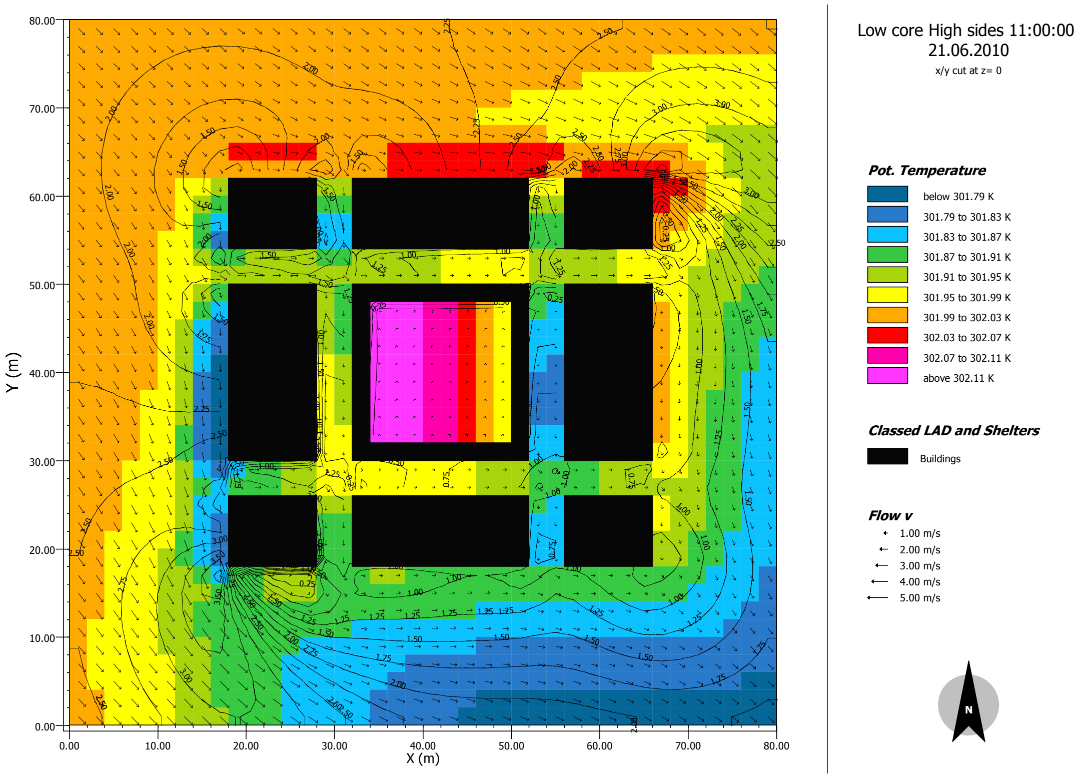

Figure 4.1 (b) Simulation results for a model with low courtyard block (6m) and high surrounding blocks (10m)

Another set of simulations were intended to verify that ENVI-met accurately depicts the behavior of thicker and thinner walls surrounding courtyards. Three sets of models were drawn with 8m solid building blocks and one void block with three varying thicknesses for the walls surrounding the courtyard in Figures 4.2 (a-c). The height of all the blocks is 8m. The results show that there are differences in the readings of temperature and wind corresponding to the thickness of the courtyards. This verified that the software accounted for different thicknesses and different enclosure sizes.

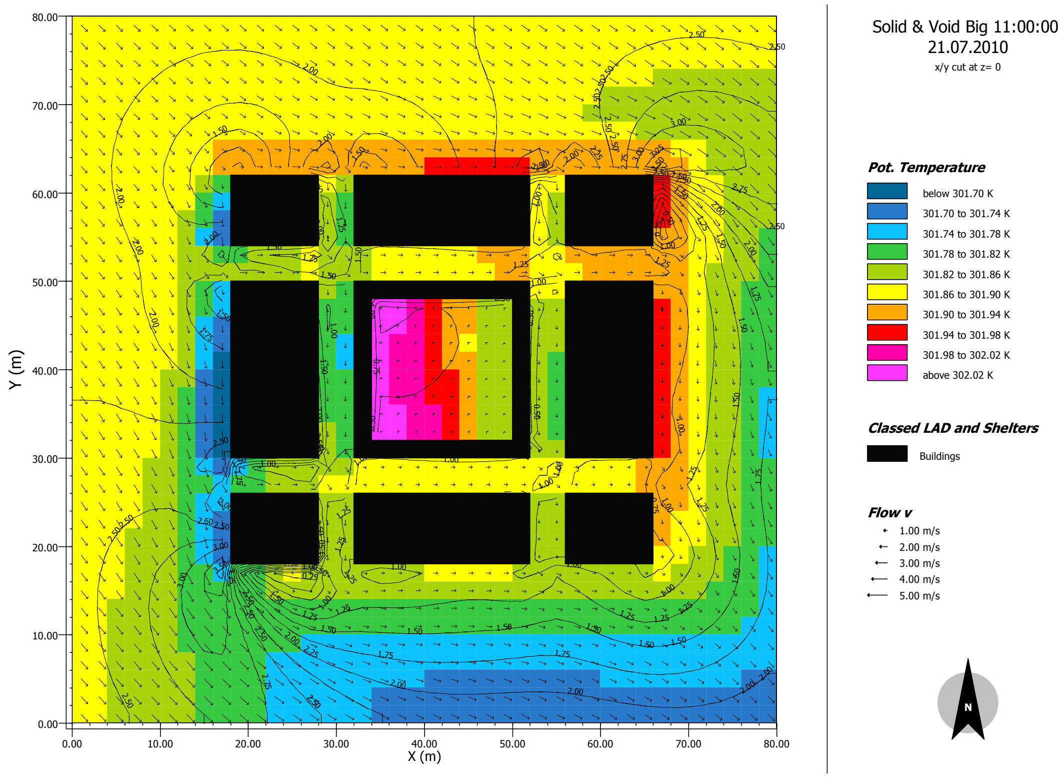

Figure 4.2 (a) Simulation results for thick courtyard wall

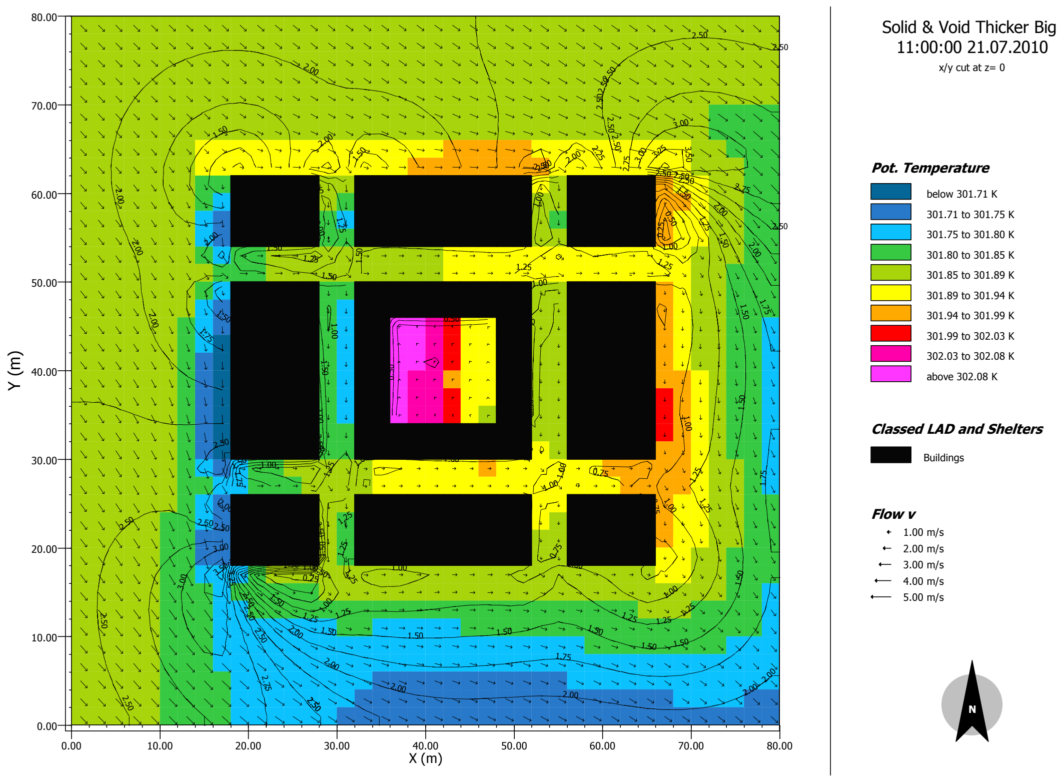

Figure 4.2 (b) Simulation results for thicker courtyard wall

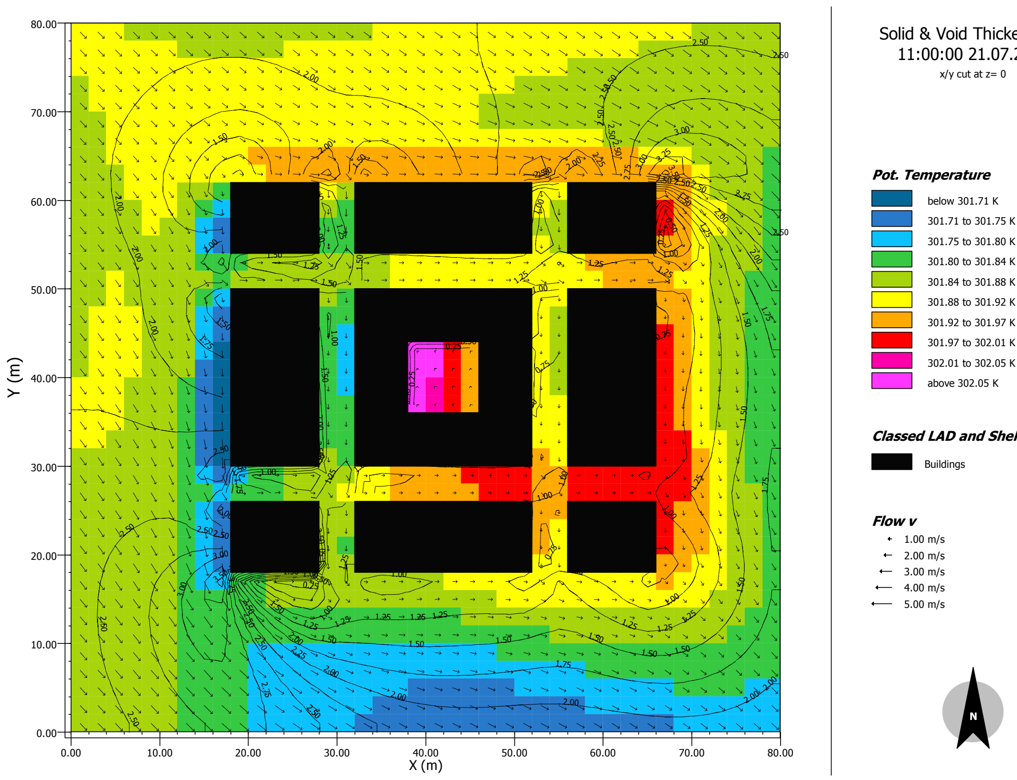

Figure 4.2 (c) Simulation results for thickest courtyard walls

The challenge of figuring out the appropriate grid size was overcome by setting up a group of simulations with varying grid sizes. The simulations were run to verify that the use of a finer grid in ENVI-met will result in more accurate numerical results. One model is drawn with each grid point representing 1m in reality making it a 1:1 scale shown in Figure 4.3 (a). The second model is a 1:2 scale model; each grid point representing 2m in reality shown in Figure 4.3 (b). The third model is a 1:4 scale model with every grid point representing 4m in reality shown in Figure 4.3 (c). All the simulated blocks are 8m high. It was found that the finer grid in the 1:1 scale model gave higher resolution in the numerical temperature readings. Grid independence was reached using the 1:1 scale.

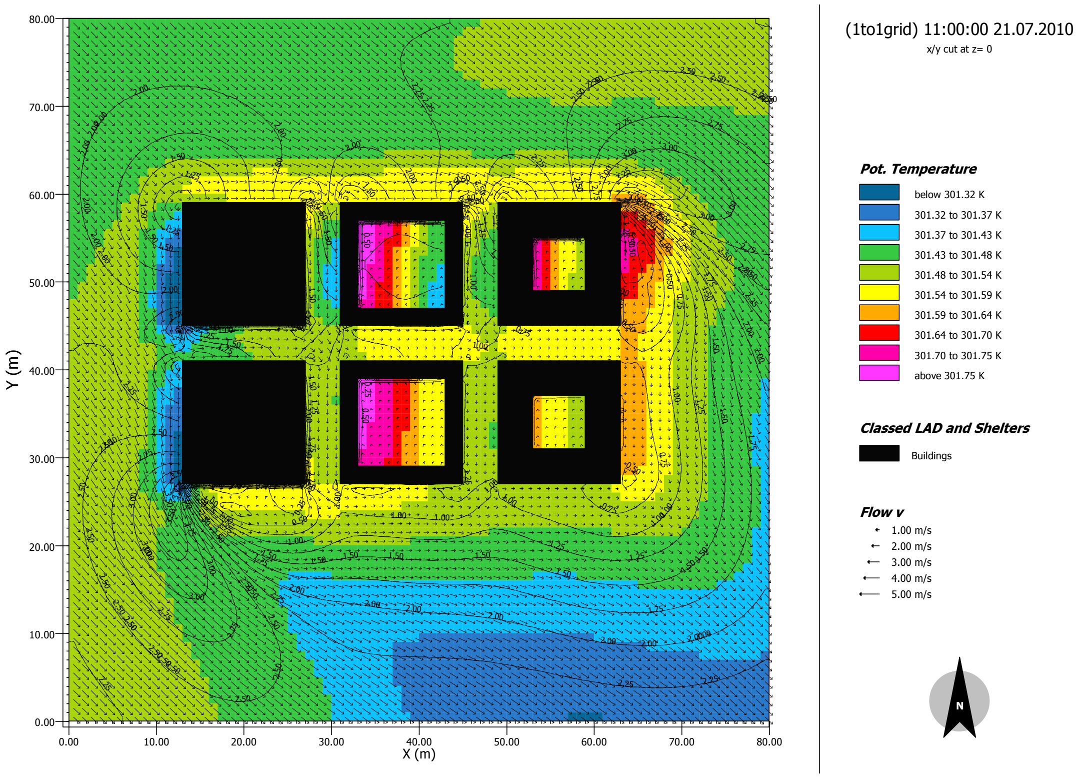

Figure 4.3 (a) Simulation results for 1:1 scale model

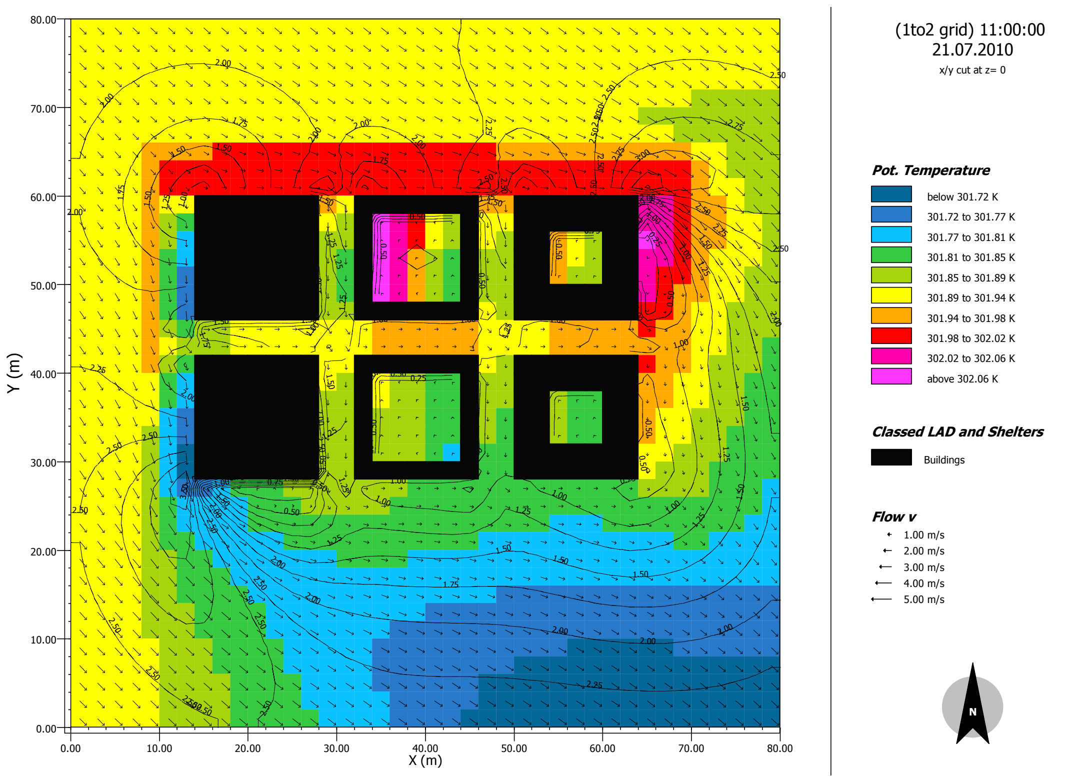

Figure 4.3 (b) Simulation results for 1:2 scale model

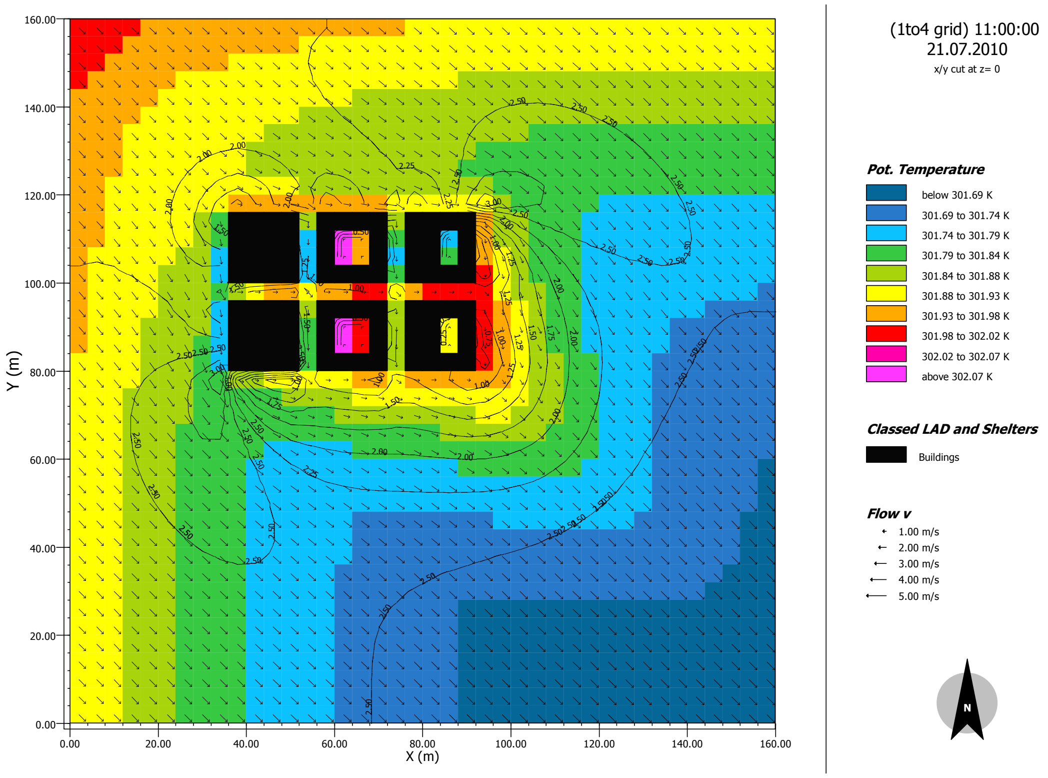

Figure 4.3 (c) Simulation results for 1:4 scale model

4.2 Simulation Methodology

Three different urban configurations will be simulated derived from two major types of urban forms. The centralized form is the starting original configuration from which two other layouts have been derived. The centralized form represents an old urban fabric in Dubai’s Bastakiyah area. It is a direct trace of an existing neighborhood. The second configuration is a derived formation which presents a more orthogonal representation of the current site. The third configuration is a purely orthogonal grid iron layout based on the same volume of the original buildings. The old fabric represents a dense and compact urban form. The only open spaces are either the ones within the structures as courtyards or open spaces surrounded by winding narrow streets in between the structures. The grid fabric is represented by highly structured layout with uniform building heights and street widths.

The number of variables that influence the occurrence and intensity of urban heat islands are many and interconnected. Each on its own has effect just as much as the interactions between these variable. In this research some of the variables have been set as constants and acknowledged as effective factors supported by literature reviews and earlier research results presented in the earlier chapter.

At the onset of the simulation process, it is important to define the fixed variables (control variables) in the research and the independent variables which will be tested as well as dependant variables which change by changing the independent variables.

Fixed variables, those that do not change throughout the simulations, are not necessarily factors that are fixed in all research done on the topic of urban heat islands. In this particular research, those fixed variables are vegetation, building and surface material, water bodies, and time of day. Those may be considered as the input that does not change in all the simulation scenarios, i.e. constants. These variables are there to ensure that the observations or the results from the simulation are in fact a result of the selected independent variables without the intrusion of other varying conditions or circumstances. Furthermore, climatic data such as wind speed and initial temperature are fixed variables but are season dependant.

The independent variables in the research are those that are being manipulated throughout the various scenarios to achieve the objective of the research. Specifically, one of those variables is related to the urban form and configuration. Each scenario will have an independent variable which is the time of year. Each scenario will be simulated in summer (June 21st), winter (December 21st), and Autumn (September 21st) and results will be recorded from 06:00 till 18:00.

The observed outcomes of the simulations which change upon changing the independent variables are the dependant variables. In this research it is expected that the dependant variable is temperature variations, the key outcome and objective of this research.

Due to the many factors contributing to the UHI phenomenon and the difficulty to track the interactions causing it to occur, the model was set-up resembling an experiment described by Poreh (1994) in his research. The research identified what was called a simple heat island. In this experiment, it was decided to simulate the “flow and temperature field” of an area surrounded by “inactive rural areas”. Inactive was defined as an area with “zero sensible heat flux”. Consequently, for the purposes of this research, heat transfer from surrounding surfaces has been eliminated by not including any surrounding buildings to the area under investigation.

The various factors of urban heat islands have been reduced in importance and hierarchy by setting up some as constants in all scenarios. The water and vegetation factors are eliminated by excluding them from the simulated models. This is to ensure that the factor of urban configuration is strictly the influencing factor of microclimate temperature variations.

The computer model parameters were set up according to site specific data, such as climatic information and building and surface materials. Below is a tabulation of the different parameters required as software input for the simulation:

Site Specific

City Location: Dubai, UAE. Lat: 25.25° Long: 55.33° (as identified by the software)

Simulation day: June 21st, Dec 21st, Sept 21st

Simulation duration: 16 hours 04:00 – 20:00

Model resolution: 1:1

Climate type: hot arid

Building Specific

Wall Albedo: 0.2 (reflects 20% of incoming radiation)

Roof Albedo: 0.3 (reflects 30% of incoming radiation)

U value of walls: 1.94 $W/m^2.K$

U value of roof: 6.0 $W/m^2.K$

Climatic data (fixed variables but season dependant):

Wind direction and speed: 325º at 3.6 m/s

Relative Humidity: 50%

Initial Temperature: 305.15K

Cloud Cover: Clear sky

4.3 Model setup

After runs of verifying simulations explained in the previous section, the grid scale was selected to be a 1:1 scale. This scale was found to be the most suitable in order to approach as close as possible more accurate readings of temperature and wind variation values. Furthermore, the alleyways and roads are fairly narrow in reality and needed to be represented in more that only one or two grid points. Although a finer grid was technically possible, it was difficult to draw the entire model within the allocated drawing space defined by the software with grid points representing smaller units in reality. The z-axis which represents the height of the buildings was also set up to a 1:1 scale, each grid point vertically represents one meter high.

The start-up model is representative of the original configuration on site and covers an area of approximately 50,625 sqm. The heights of the buildings are represented by 3.5m high volumes and 7m high volumes, for single and two storey buildings respectively. Figure 4.4 shows the

Bastakiyah building heights drawing from which the model was traced into ENVI-met (Olroyd-Robinson, 2006).

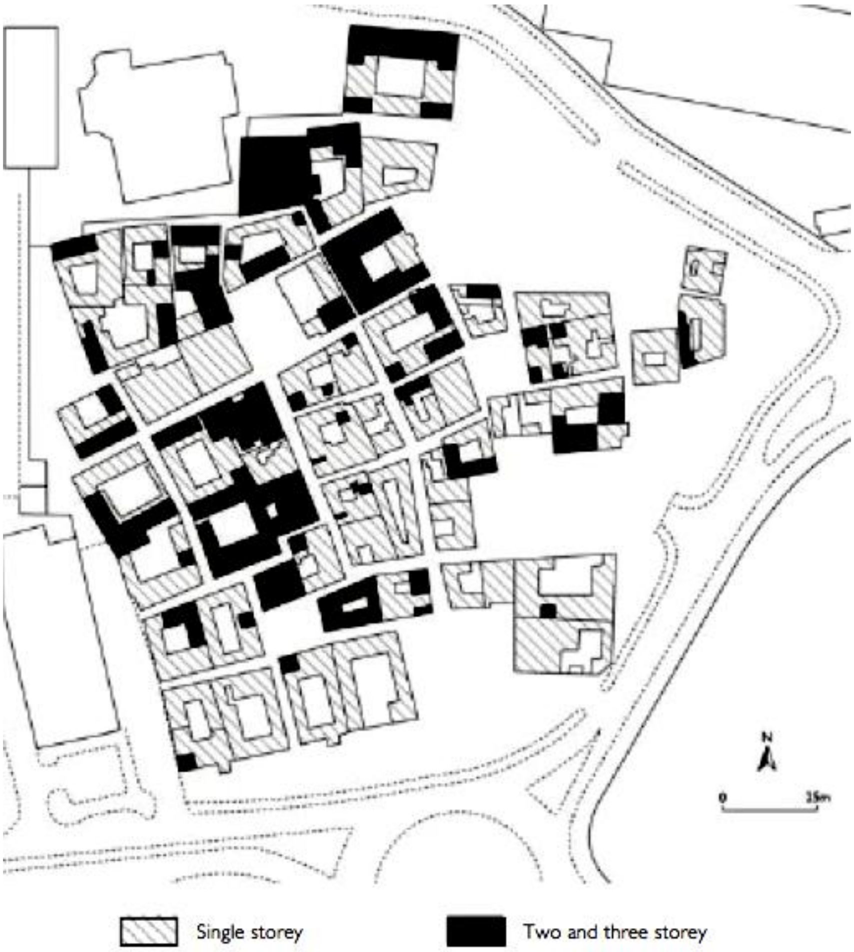

Figure 4.4 Plan showing the building heights of the selected site – Bastakiyah (Olroyd-Robinson, 2006).

Due to the difficulty of drawing in several rotated grids and tilted facades on the software itself, the drawing from which the model was traced was rotated to a degree where most of the lines and streets are oriented parallel and perpendicular to the edge of the drawing grid. This limited the need to stagger grid points unnecessarily to represent diagonal edges and streets. Once the drawing was traced, the north orientation was corrected in order to accurately represent the orientation of the configuration on site. The north arrow in the ENVI-met model is corrected by 30° east of the north.

The first of the software models produced representing the centralized organic original configuration of Bastakiyah is shown in the Figure 4.5 below. This configuration will be referred to as the Bastakiyah configuration from here on.

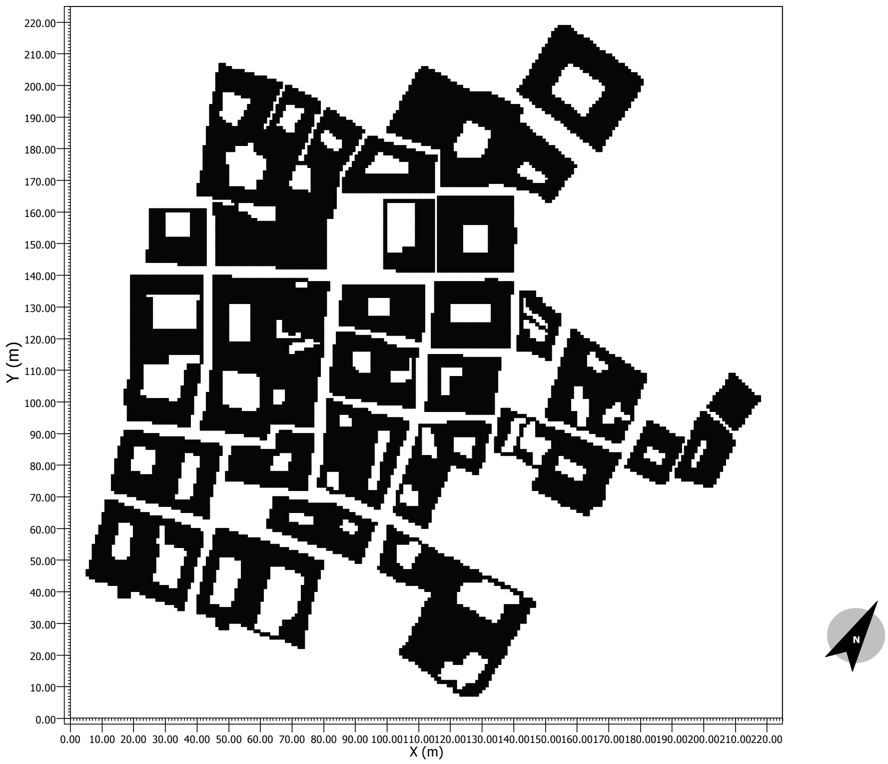

Figure 4.5 Original Bastakiyah configuration modeled in ENVI-met

The second of the models produced on ENVI-met was modeled to represent a more orthogonal version of the original Bastakiyah layout. This alternative was meant to keep the staggered road and alleyway layouts. Those alleyways were maintained as the same widths in the original configuration but more consistent throughout the entire formation than they are in the original layout. The buildings are less irregular and have orthogonal plans. In addition, courtyards and open areas have been retained within and around the buildings resembling the original layout. The volume of the buildings was kept as is by representing the buildings depending on their respective heights, i.e. 3.5 and 7 meters high. Figure

4.6 shows the second produced plan on ENVI-met referred to as the Orthogonal configuration from here on.

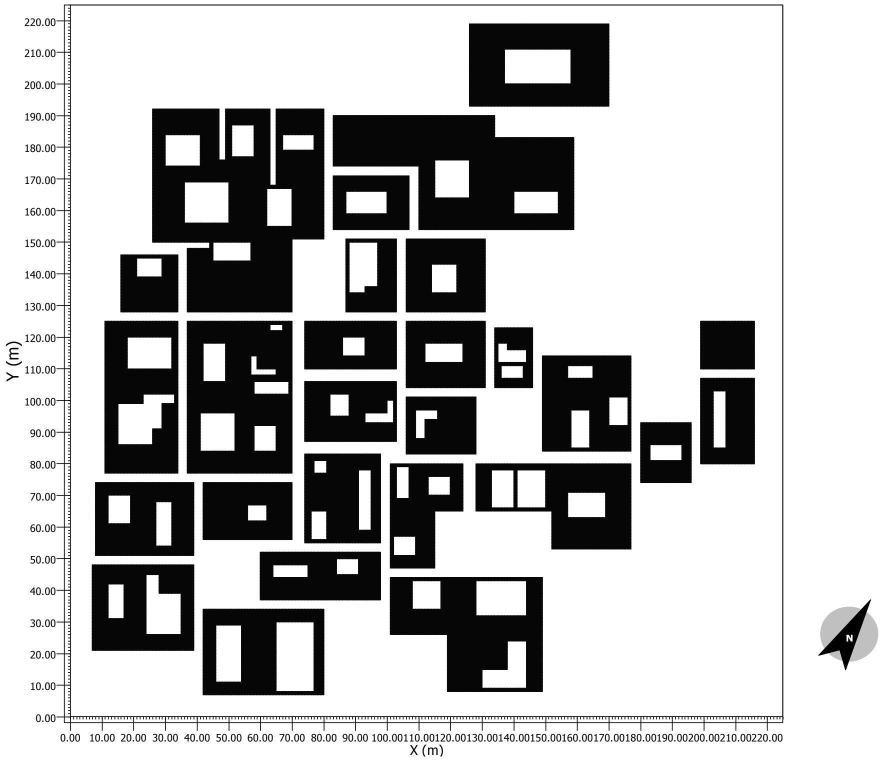

Figure 4.6 Orthogonal configuration modeled in ENVI-met

The third of the configurations is one that represented a highly structured configuration resembling the grid-iron configuration. The layout was produced by creating a formal and equally spaced building layout. The footprint of the buildings is equal and the alleyways were set at a width of 4m. The 4m width represents the widest of the alleyways in the Bastakiyah configuration. It is also the recommendation for a low speed urban context boulevard, avenue, or street in a sustainable urban development (Farr, 2008). The footprint of the buildings was calculated by subdividing the overall volume of the Bastakiyah configuration to equal parcels, knowing that the spacing between the buildings is 4m and the height of the buildings is 3.5. Open spaces and courtyards were eliminated but the overall volume of the buildings was maintained and surrounded by the total area of open spaces. Figure 4.7 shows the ENVI-met layout of the third configuration, referred to as the Volume Ortho from here on.

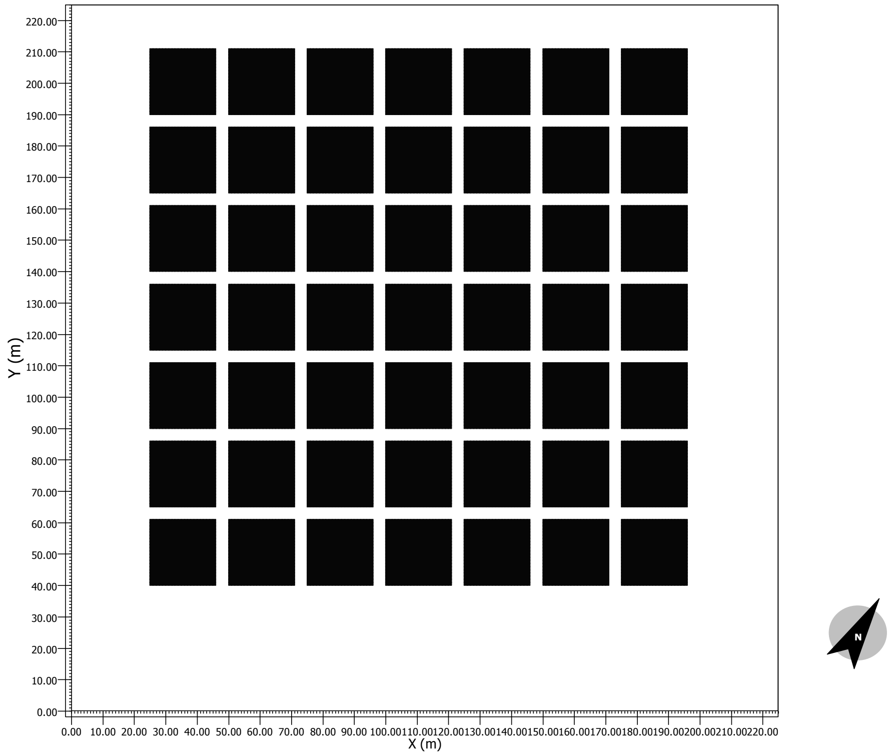

Figure 4.7 Volume Ortho configuration modeled in ENVI-met

For each of the three models, the chosen dates for simulations were selected to represent the winter, summer, and autumn solstices. December 21st 2010, June 21st 2010, and September 21st 2010 are the exact dates respectively. Spring was considered to be similar to autumn and thus excluded to reduce time required for the simulations. Those dates were selected to give a better idea of the distribution throughout the year instead of only choosing the hottest and coldest days as peek temperature and wind variation values. Furthermore, from the simulation results, only results from 06:00 till 18:00 were tabulated. However, the actual simulation runs were set up to run from 04:00 till 20:00. This allowed for buffer timing before 06:00 and after 18:00 overcoming one of the challenges faced throughout the simulation. This process was to ensure that the results are not compromised by the initialization spin-up at the beginning of the simulation, when all the build-up of energy is being calculated. Although there was no indication for the need for a buffer at the end of the simulation, it was considered just to be on the safe side. The timing of the day selected for the tabulated results covered a range of 12 hours during daytime and was uniform across all three seasons regardless of the sunrise and sunset timings. This was to ensure yet another level of consistency amongst the three seasons.

The configuration files used to run the simulations included climatic details as mentioned in the previous section.

Some of the challenges faced during the simulations were errors that needed to be rectified. Some errors related to the model drawing itself, and others related to the model numerical set-up. Most of these errors related directly to the complexity and size of the model.

Errors related to the drawings were easily detected through error files in which the location of the error was clear. Such errors required redrawing the area and reducing some of the complexities such as staggered grids and alleyway widths. Other errors which related to numerical overload and instability required changing the time-step of the simulation. The time-step was directly related to the solar height. Because the simulation is run in a city with higher solar angle, the time steps were reduced from the default values.

The biggest challenge of all was the duration it took for every simulation to run accurately with no errors. The simulation running time ranged from 6-7 days per simulation.

4.4 Software Validation

Validation of the software was achieved by referencing recent papers from 2006 till 2010, for researchers who used the software as a primary or secondary simulation software. Okeil (2010) used ENVI-met for air flow behavior simulation, whereas Fahmy and Sharples (2009) used it as a primary software to study green structures. Thapar and Yannas (2008) used the software to measure temperature variations and wind speed around specific urban forms, similar to the intentions of this research but on a smaller scale. Thapar and Yannas (2008) used the software to substantiate field measurement findings. The ENVI-met simulation results gave similar trends found by field measurements, only “the simulated values were much lower than those measured” (Thapar and Yannas, 2008). They suggested that ENVI-met is useful to get an idea of the impact of urban forms, vegetation and water bodies in terms of temperature and wind flow. Hedquist et al. (2009), used ENVI-met along with field measurements and CFD software and reported accurate results in terms of temperature variations in high density areas. It was able to accurately simulate the impact of building heights and shading on surface temperature.

CHAPTER FIVE

RESULTS AND DISCUSSION

5.0 Results and Discussion

5.1 Data Extraction and Tabulation

After running the simulations, the result files were visualized and snapshots of the simulated timeframes were obtained. Details such as temperature gradients and wind contours were extracted. Temperature variations are represented in color gradients in Kelvin. Wind is represented in iso-lines indicating wind speed and direction instead of vectors to ensure clarity and legibility of the result snapshots. The values were extracted from a horizontal cutting plane close to the ground surface.

Numerical data was then extracted using Excel. Each file included over 50,600 coordinate entries, each representing the values at a simulated grid point. The size of the files reached a size of 122MB. The extracted data was reorganized. Furthermore, points with values of zero temperature and/or wind were excluded. Those values represent grid points within buildings where calculated temperature and wind values realistically render zero values (Appendix B). The extracted numerical data was summarized in 6 files, one per configuration and one per season. These files contained information showing the daily averages, standard deviation, maximum values, minimum values, and sky-view factor (Appendices C and D).

In order to further understand the temperature behavior throughout the three different configurations, it was important to verify that wind is a factor in this investigation and that the simulation accounts for its effect. Another set of simulations was carried out with wind speed approaching zero. The initial wind speed input was changed to 0.1m/s. This was the least value of wind with which the software ran the simulations without errors.

Numerical data extracted in Excel are represented graphically by mapping the daily averages for each of the configurations. Each graph includes three configurations showing both wind scenarios (wind speed of 3.6m/s and 0.1m/s). The graphs in the following section show temperature and wind trends and fluctuations throughout the day.

5.2 Results

June data analysis shown in Figure 5.1 revealed that all three configurations have the same temperature variation trends throughout the day. The difference is in the value of the temperature for the Orthogonal configuration, which registered higher values by 2-3K than both the Bastakiyah and Volume Ortho configurations. The temperature values in the three configurations with wind speed of 0.1m/s demonstrate fluctuating and higher temperature values.

The wind graph shown in Figure 5.2 registered similar trends across the three configurations; however the wind speed of the Volume Ortho configuration was recorded at about 0.1 m/s higher than the other two configurations. In the no wind speed scenario (wind at 0.1 m/s), average wind speed values were less and fluctuated more.

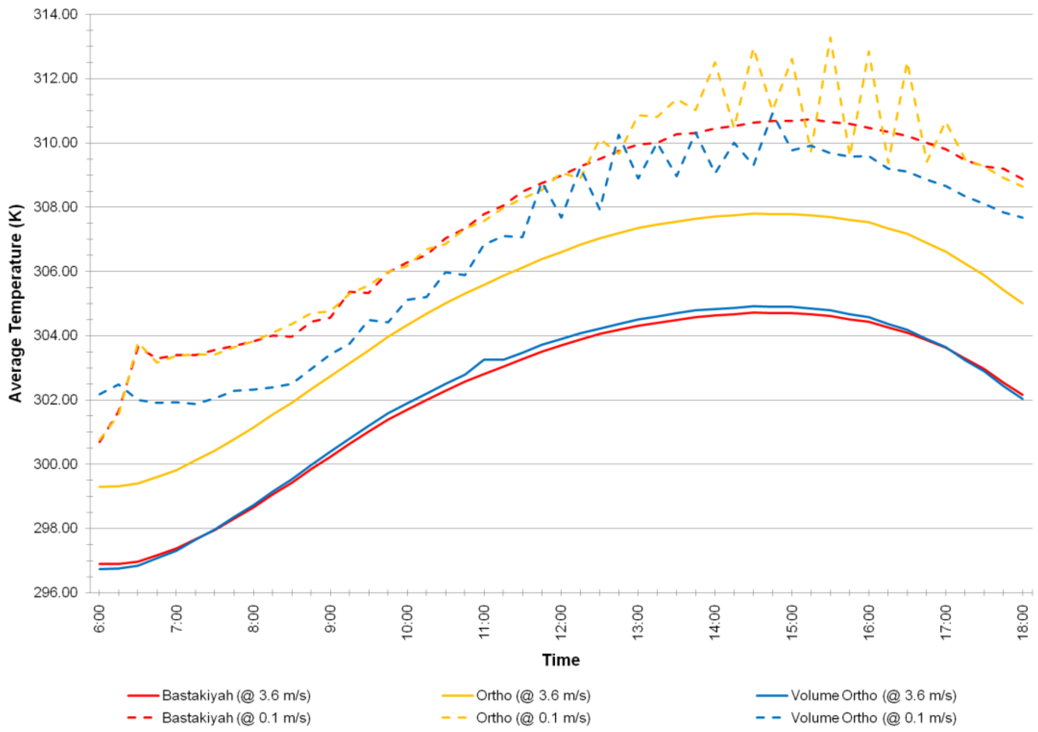

Figure 5.1 Daily average temperatures (K) for Bastakiyah, Ortho, and Volume Ortho configurations in June for both 3.6m/s and 0.1m/s initial wind speed scenarios

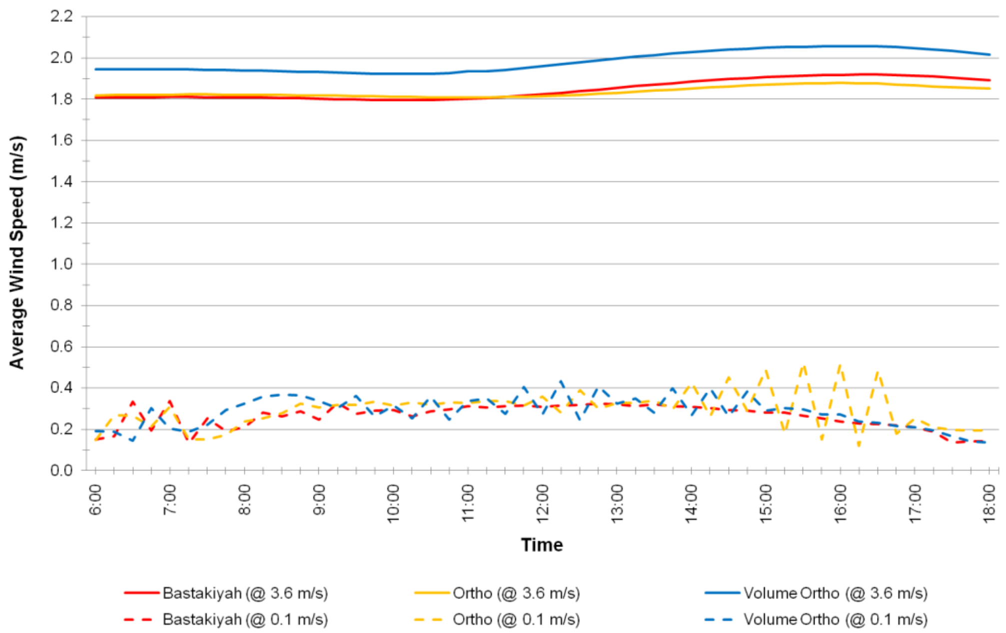

Figure 5.2 Daily average wind speeds (m/s) for Bastakiyah, Ortho, and Volume Ortho configurations in June for both 3.6m/s and 0.1m/s initial wind speed scenarios.

December analysis shown in the graphs in Figure 5.3 revealed that as with the June graph, the temperature trends are similar across the three configurations. Average temperature readings showed almost negligible differences and the averages ranges are in the order of 0.1K. In the case of no wind scenario, temperatures recorded higher values for all three configurations with the same trend. The Volume Ortho configuration showed the lowest temperature variation of the three in the order of around 1K. Wind trends shown in Figure 5.4 are similar between the three configurations with the Orthogonal configuration recording around 0.1m/s higher than both the Bastakiyah and Volume Ortho. In the case of no wind, the highest fluctuation was recorded by the Volume Ortho configuration and it occurred earlier in the day.

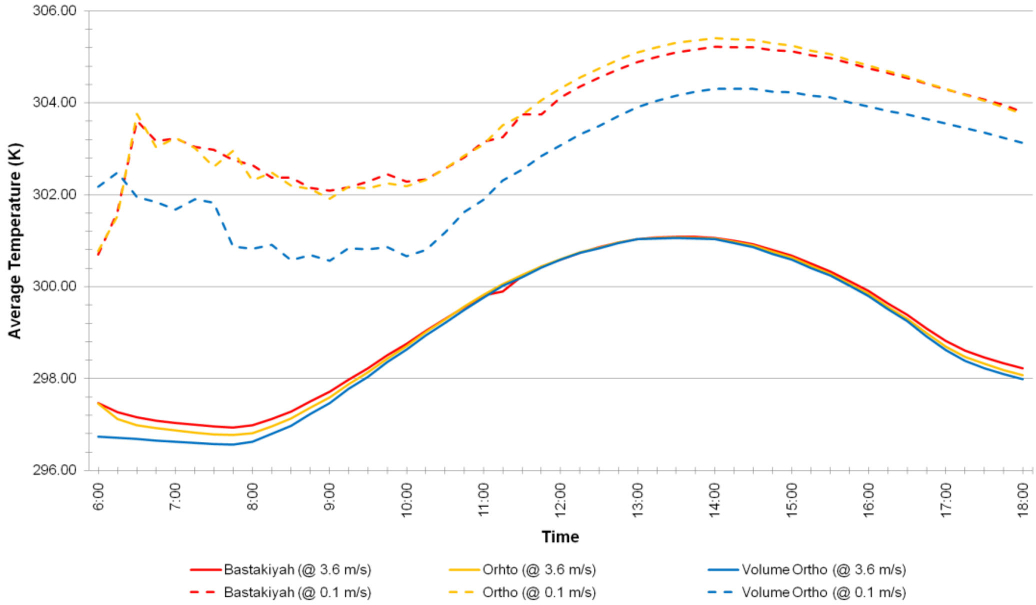

Figure 5.3 Daily average temperatures (K) for Bastakiyah, Ortho, and Volume Ortho configurations in December for both 3.6m/s and 0.1m/s initial wind speed scenarios

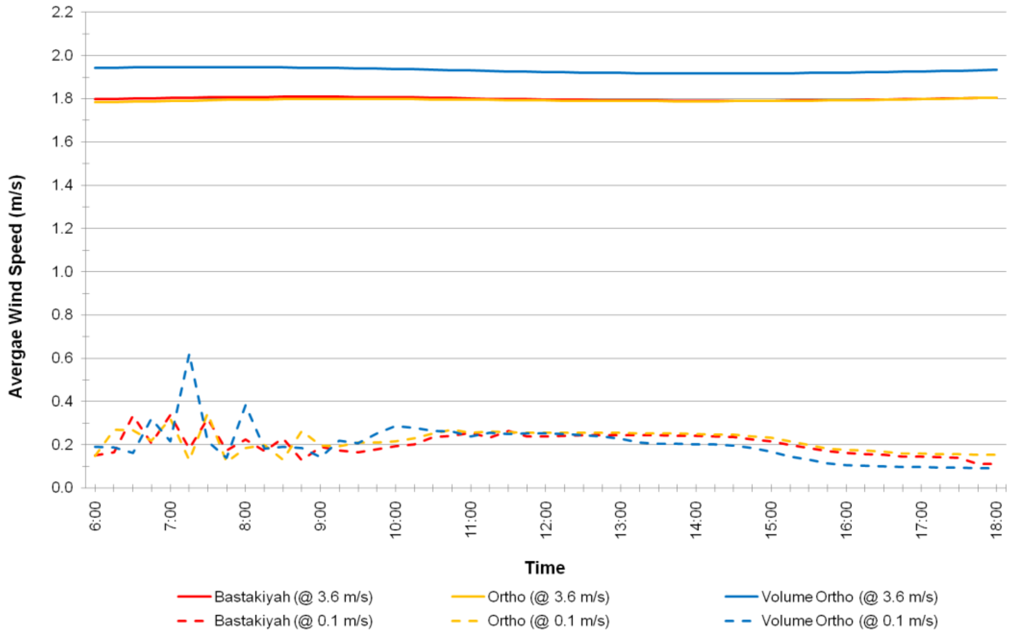

Figure 5.4 Daily average wind speed (m/s) for Bastakiyah, Ortho, and Volume Ortho configurations in December for both 3.6m/s and 0.1m/s initial wind speed scenarios.

In September, analysis revealed as shown in Figure 5.5 that the Bastakiyah configuration showed lower temperature values than both the Orthogonal and Volume Ortho configuration. The difference is in the order of about 0.5K. In the no wind scenario the temperature trends across the three configurations are almost the same with more fluctuation occurring in the Volume Ortho configuration. As for wind speeds, the graph shown in Figure 5.6 reveals that there the wind is more varied than in June and December. The Bastakiyah configuration recorded lower wind speed than the Orthogonal configuration which in turn is lower than wind speeds of the Volume Ortho configuration. In the no wind scenario, wind speed values across the three configurations are approximate with the highest fluctuation occurring in the Volume Ortho configuration around mid-day.

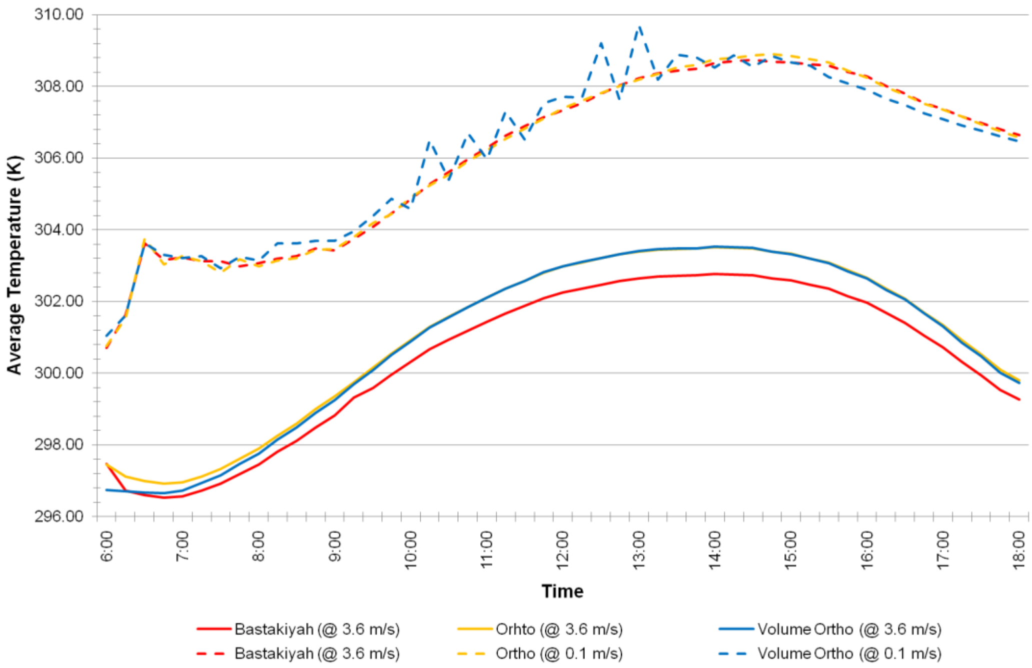

Figure 5.5 Daily average temperature (m/s) for Bastakiyah, Ortho, and Volume Ortho configurations in September for both 3.6m/s and 0.1m/s initial wind speed scenarios.

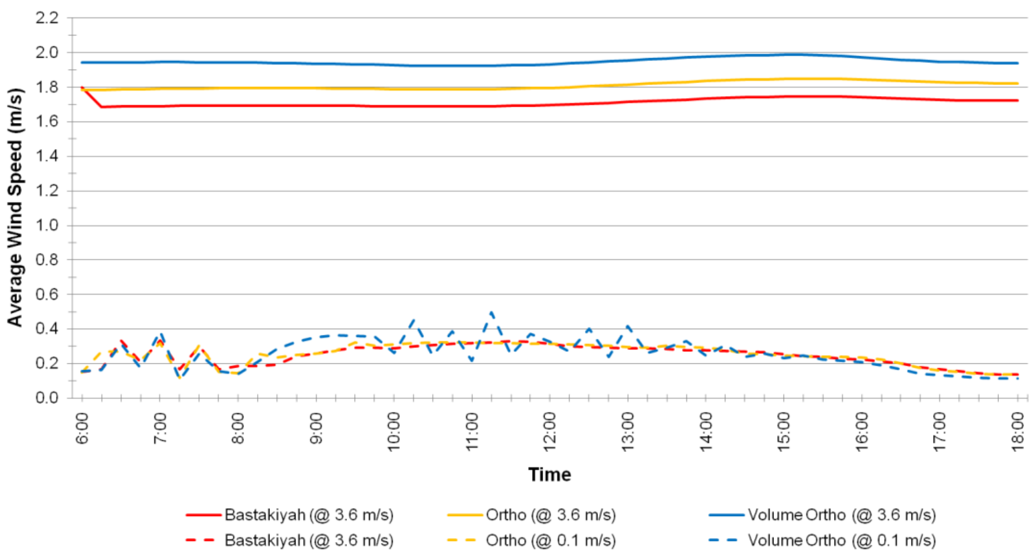

Figure 5.6 Daily average wind speed (m/s) for Bastakiyah, Ortho, and Volume Ortho configurations in September for both 3.6m/s and 0.1m/s initial wind speed scenarios.

5.3 Summary of Results for the Different Configurations

The results were summarized and tabulated in a matrix of configurations and seasons. Table 5.1 shows the summary which includes average temperature and wind speed for both wind scenarios, as well as the standard deviation for each.

Table 5.1 Matrix summarizing data of the three configurations across three seasons

Time of Year	June				Sept				December			
Configuration	**Avg T**	**Stdv**	**Avg W**	**Stdv**	**Avg T**	**Stdv**	**Avg W**	**Stdv**	**Avg T**	**Stdv**	**Avg W**	**Stdv**
Bastakiyah 3.6m/s	28.948	2.638	1.848	0.047	27.285	2.153	1.712	0.025	26.003	1.482	1.800	0.006
Bastakiyah 0.1m/s	34.436	2.951	0.262	0.059	32.950	2.310	0.249	0.061	30.541	1.181	0.207	0.052
Ortho 3.6 m/s	31.750	2.884	1.836	0.024	27.887	2.295	1.810	0.023	25.935	1.542	1.794	0.005
Ortho 0.1 m/s	34.733	3.321	0.294	0.097	32.958	2.339	0.254	0.064	30.583	1.270	0.219	0.050
Volume Ortho 3.6 m/s	29.061	2.716	1.982	0.051	27.814	2.396	1.949	0.020	25.830	1.631	1.931	0.011
Volume Ortho 0.1 m/s	33.459	3.059	0.285	0.076	33.056	2.291	0.257	0.097	29.505	1.330	0.203	0.090

The graphs shown in Figures 5.7 and 5.8 represent the temperature and wind averages with their standard deviations for the 3.6m/s wind speed scenario, respectively.

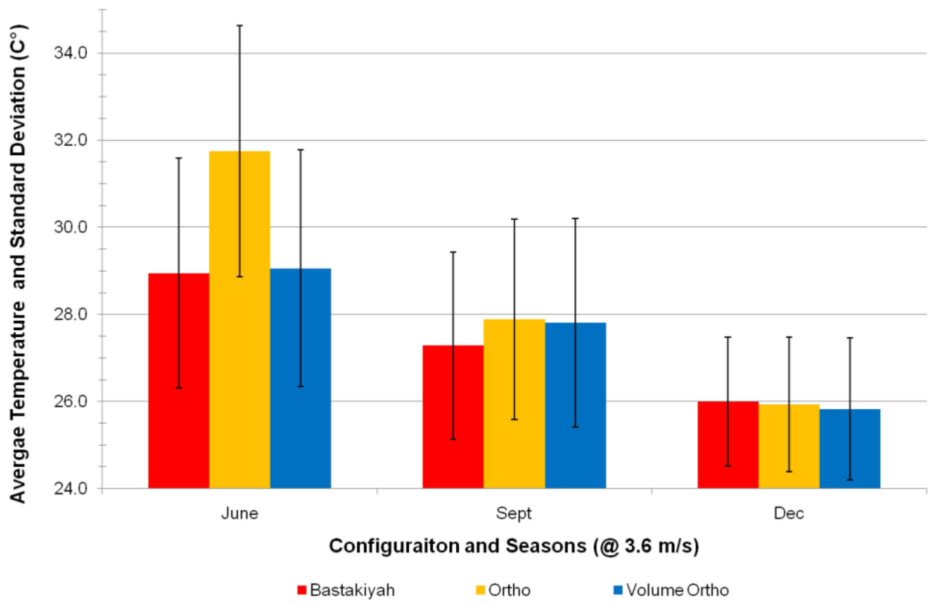

Figure 5.7 Average temperatures and standard deviations for Bastakiyah, Ortho, and Volume Ortho configurations in the three seasons for initial wind speed of 3.6m/s.

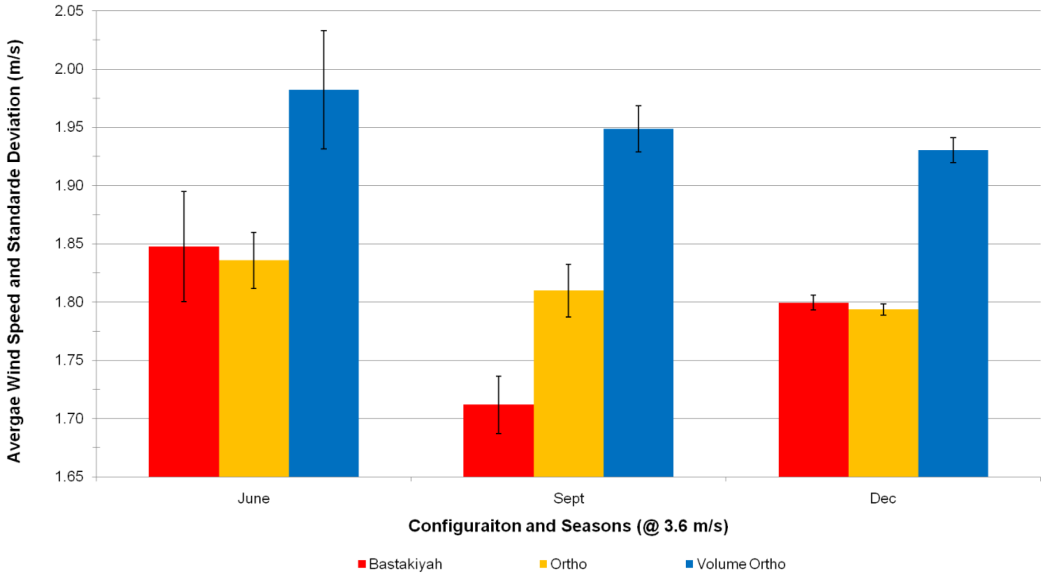

Figure 5.8 Average wind speeds and standard deviations for Bastakiyah, Ortho, and Volume Ortho configurations in the three seasons for initial wind speed of 3.6m/s.

No wind scenario (0.1 m/s) temperature and wind speed averages are shown in the graphs in Figures 5.9 and 5.10 respectively.

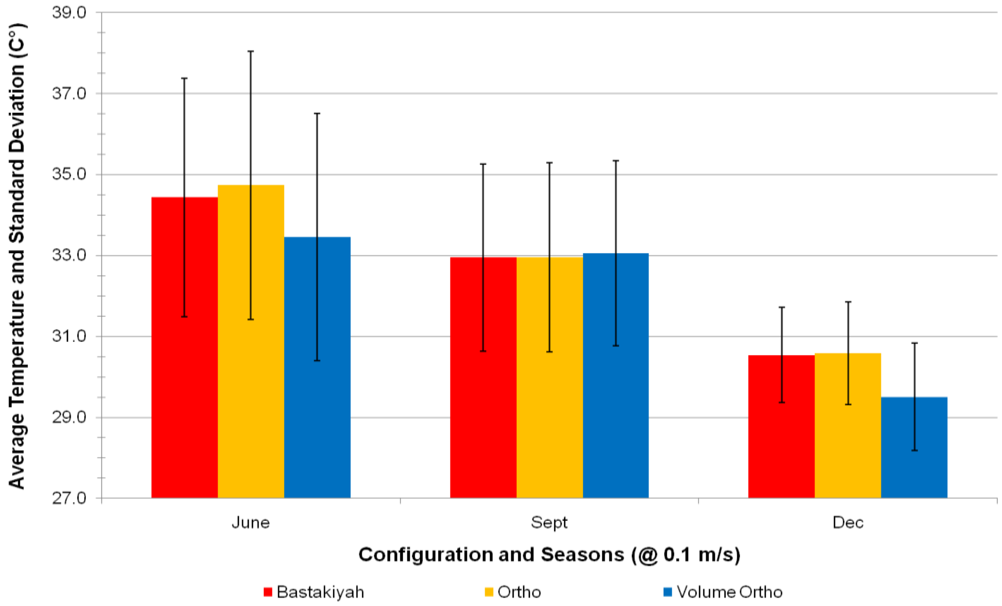

Figure 5.9 Average temperatures and standard deviations for Bastakiyah, Ortho, and Volume Ortho configurations in the three seasons for initial wind speed of 0.1 m/s.

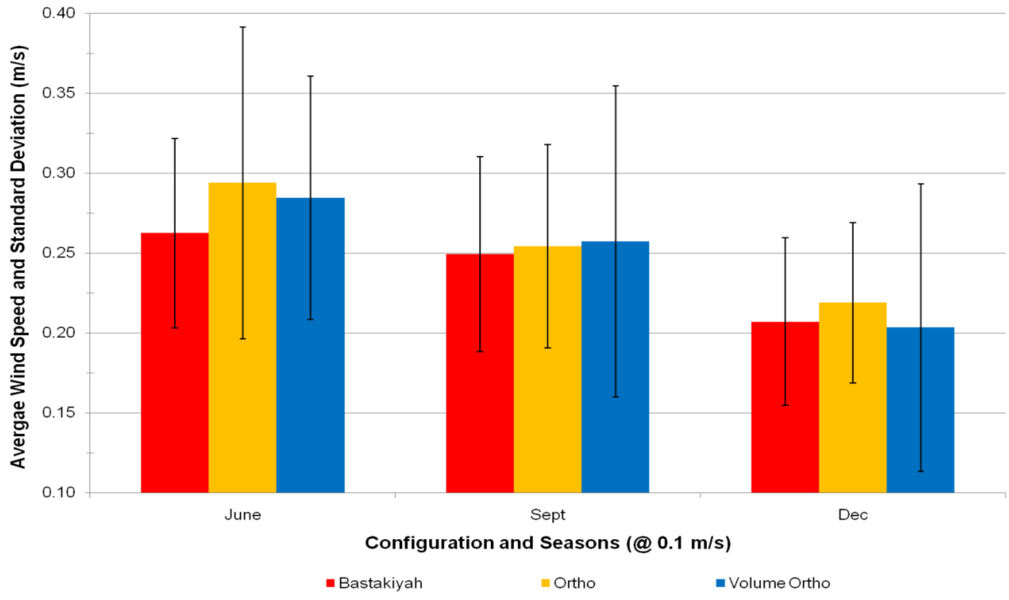

Figure 5.10 Average wind speeds and standard deviations for Bastakiyah, Ortho, and Volume Ortho configurations in the three seasons for initial wind speed of 0.1 m/s.

The data was also summarized in Table 5.2 and shown in Figure 5.11 in terms of differentiation percentages to demonstrate the extent of variation between the reported temperature and wind values and initial temperature input values.

Table 5.2 Summary of differential percentages from initial temperature and wind speed

Time of Year	June		Sept		Dec	
Configuration	Temp	Wind	Temp	Wind	Temp	Wind
Bastakiyah (3.6 m/s)	9.54%	48.68%	14.73%	52.45%	18.74%	50.01%
no wind (0.1m/s)	-7.61%	-162.48%	-2.97%	-149.40%	4.56%	-107.05%
Ortho (3.6 m/s)	0.78%	49.01%	12.85%	49.72%	18.95%	50.18%
no wind (0.1m/s)	-8.54%	-193.91%	-2.99%	-154.19%	4.43%	-119.05%
Volume Ortho (3.6 m/s)	9.19%	44.94%	13.08%	45.87%	19.28%	46.37%
no wind (0.1m/s)	-4.56%	-184.63%	-3.30%	-103.39%	7.80%	-103.39%

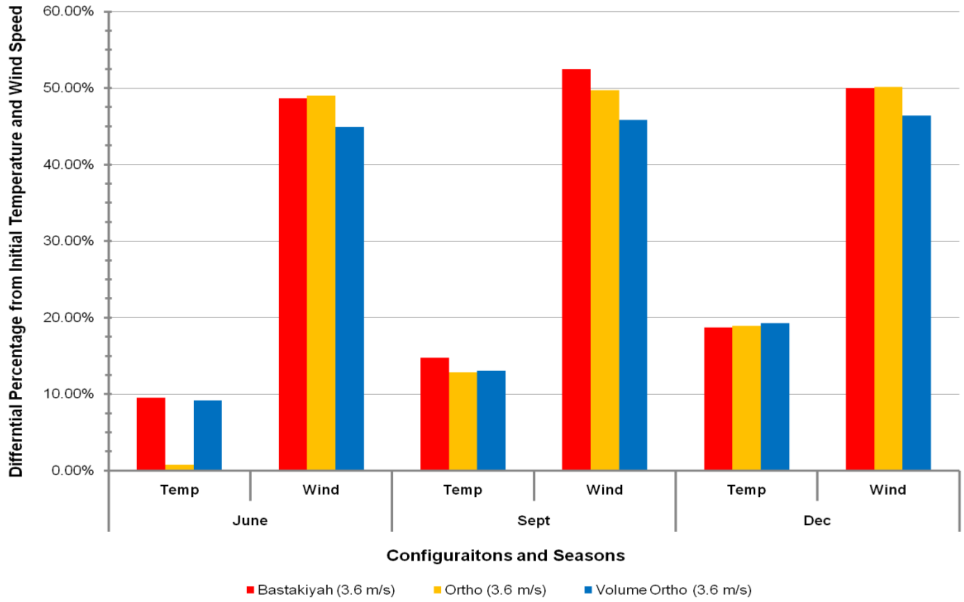

Figure 5.11 Differential percentages from initial temperature and wind input for Bastakiyah, Ortho, and Volume Ortho configurations in the three seasons for initial wind speed of 3.6m/s.

An additional simulation was carried out using wind speed of 7.0m/s instead of 3.6 m/s in June to understand the effect of increasing the wind speed on temperature variation. Table 5.3 shows the values of temperature and wind variations and their standard deviations in all the three wind scenarios for all three configurations. The values shown in the table represent a time frame between 10:00 and 16:00. Figures 5.12 and 5.13 show the average temperature trends across the three configurations comparing the behavior in three initial wind scenarios (0.1m/s, 3.6m/s, 7m/s). Appendix E shows the tabulated data from 10:00-16:00 for initial wind of 7.0m/s in June.

Table 5.3 Summary of temperature and wind averages in the three configurations using three initial wind values in June

	Time of Year	June			
	Configuration	**Average Temp**	**Stnd Dev**	**Average Wind**	**Stnd Dev**
Bastakiyah	no wind (0.1m/s)	**308.146**	1.169	**0.297**	0.023
	wind (3.6 m/s)	**303.858**	0.946	**1.855**	0.047
	high wind (7.0 m/s)	**303.089**	1.306	**3.436**	0.032
Ortho	no wind (0.1m/s)	**309.849**	2.102	**0.341**	0.089
	wind (3.6 m/s)	**304.900**	2.884	**1.836**	0.024
	high wind (7 m/s)	**303.090**	1.276	**3.436**	0.033
Volume Ortho	no wind (0.1m/s)	**308.524**	1.700	**0.320**	0.058
	wind (3.6 m/s)	**304.060**	0.930	**1.992**	0.050
	high wind (7 m/s)	**303.259**	1.332	**3.683**	0.033

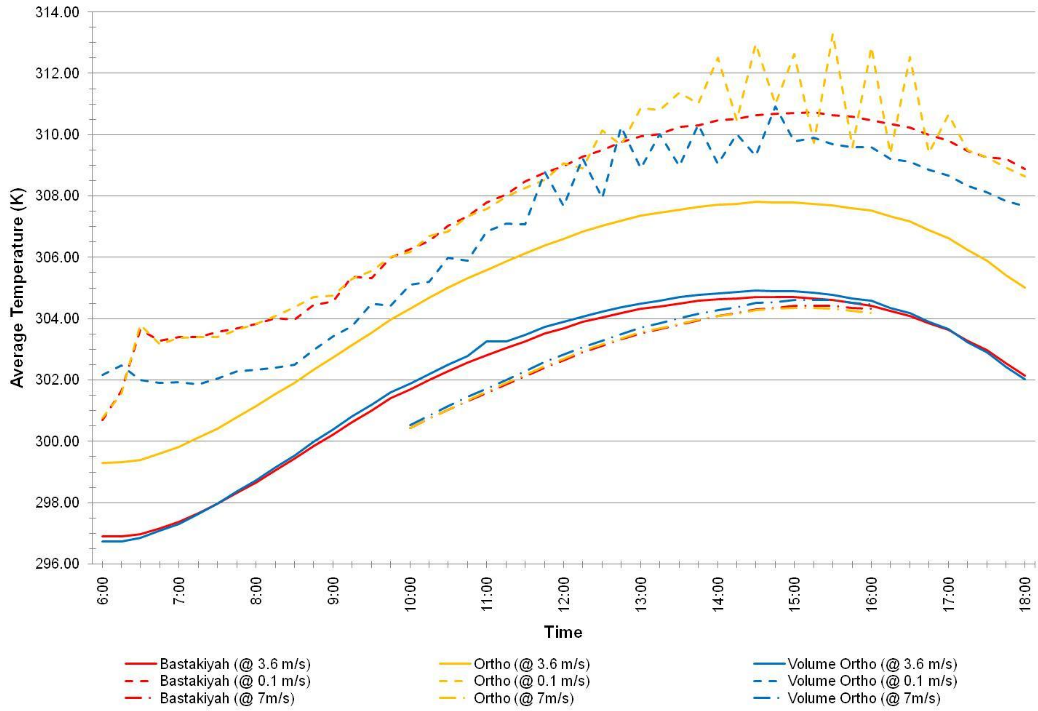

Figure 5.12 Average temperature trends for the three configurations in three initial wind speed scenarios (0.1, 3.6, and 7 m/s) in June from 10:00-16:00

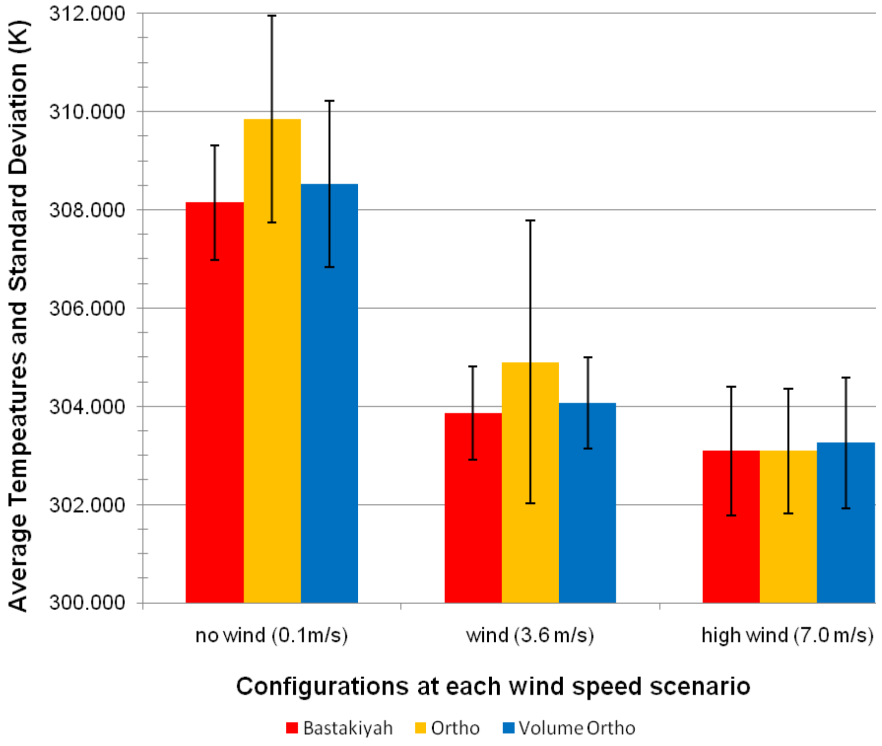

Figure 5.13 Comparison of average temperature and standard deviation in all three wind scenarios (0.1m/s, 3.6m/s, and 7m/s)

The sky-view factor for the three configurations was also calculated and tabulated in the Table 5.4 below. The sky-view factor for the three different configurations is illustrated in ENVI-met snapshots in Figures 5.14-5.16. The sky-view factors are presented on a scale from 0 to 1. The closer the value is to one, it indicates more exposure to the horizontal sky plane.

Table 5.4 Sky-view factor values for all three configurations

Sky-view Factor	Bastakiyah	Ortho	Volume Ortho
Average	0.8353156	0.812568	0.848728977
Maximum	1	1	1
Minimum	0.1389	0.1821	0.5123

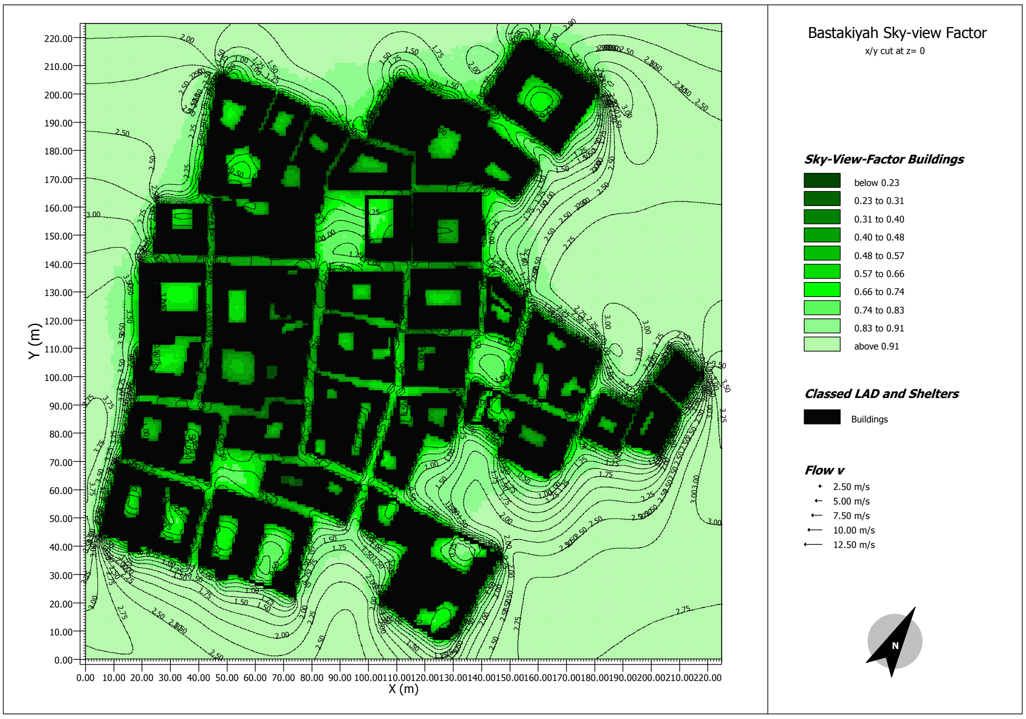

Figure 5.14 Bastakiyah configuration sky-view factor gradient

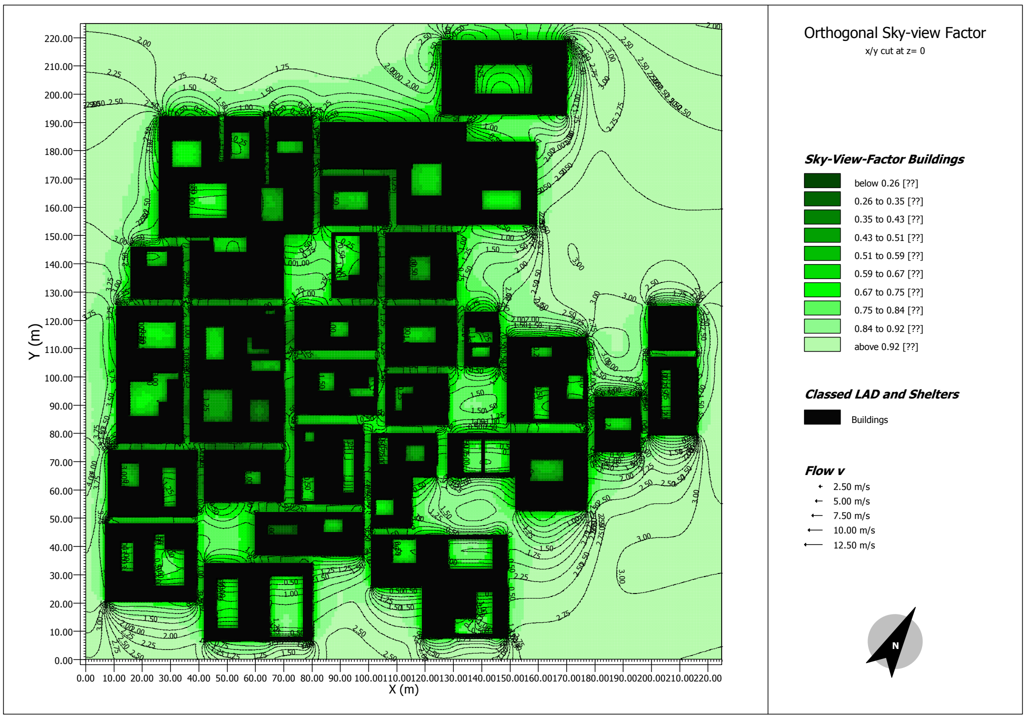

Figure 5.15 Orthogonal configuration sky-view factor gradient

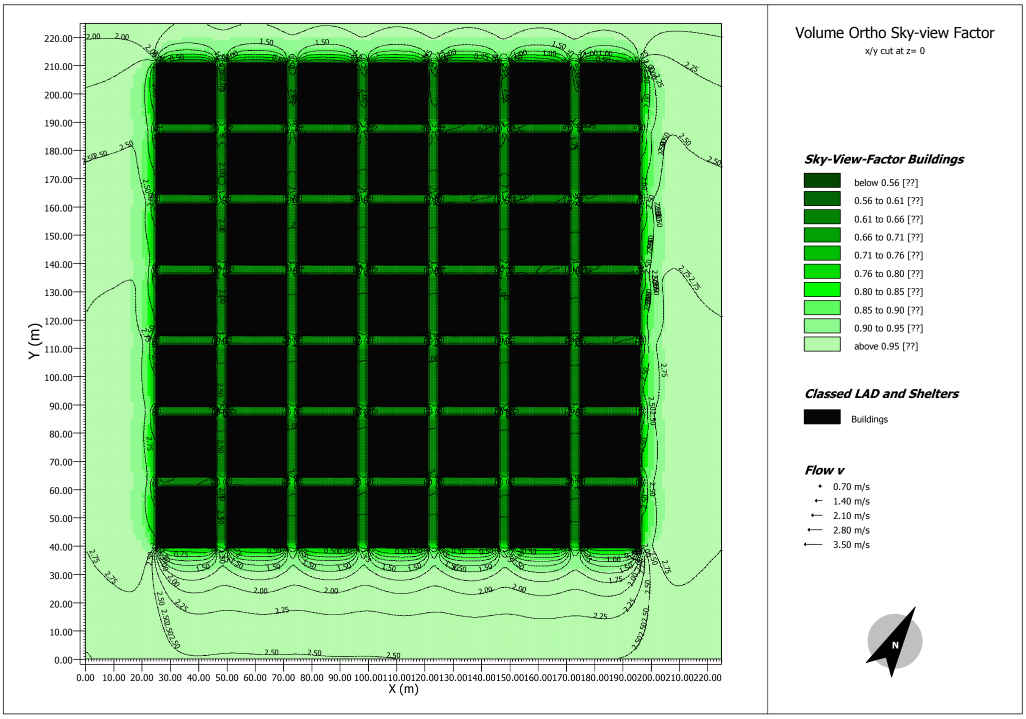

Figure 5.16 Volume Ortho configuration sky-view factor gradient

5.4 Discussion of Results

In the Bastakiyah configuration with a sky-view factor of 0.84 in June and initial wind speed of 3.6m/s the temperature decreased by 9.54% from initial temperature of 305.15K with a standard deviation of 2.64K and daily average temperature of 302.1K and max daily average of 304.72K occurring at 14:30. The wind speed decreased by 48.7% from initial wind speed with standard deviation of 0.047K.

In the case of no wind scenario (initial wind speed at 0.1m/s), the temperature increased by 7.61% from initial temperature of 305.15K with a standard deviation of 2.95K and daily average temperature of 307.59K and max daily average of 310.73K occurring at 15:15. The wind speed increased by 162.5% from initial wind speed with standard deviation of 0.059K.

In September and initial wind speed of 3.6m/s, the temperature decreased by 14.73% from initial temperature of 305.15K with a standard deviation of 2.15K and daily average temperature of 300.44K and max daily average of 302.77K occurring at 14:00. Wind speed decreased by 52.45% from initial wind speed with standard deviation of 0.025K.
As for the case of no wind (initial wind speed at 0.1m/s), the temperature increased by 2.97% from initial temperature of 305.15K with a standard deviation of 2.31K and daily average temperature of 306.1K and max daily average of 308.75K occurring at 14:30. Wind speed increased by 149.4% from initial wind speed with standard deviation of 0.061K.

As for December and initial wind speed of 3.6m/s, the temperature decreased by 18.74% from initial temperature of 305.15K with a standard deviation of 1.48K and daily average temperature of 299.1K and max daily average of 301.1K occurring at 13:30. Wind speed decreased by 50% from initial wind speed with standard deviation of 0.006K.
In the no wind scenario (0.1 m/s), the temperature decreased by 7.61% from initial temperature of 305.15K with a standard deviation of 1.18K and daily average temperature of 303.7K and max daily average of 305.2K occurring at 14:00. Wind speed increased by 107.1% from initial wind speed with standard deviation of 0.052K.

Looking at the Orthogonal configuration with a sky-view factor of 0.81, the results showed for the month of June and initial wind speed of 3.6 m/s, the temperature decreased by 0.78% from initial temperature of 305.15K with a standard deviation of 2.88K and daily average temperature of 304.9K and max daily average of 307.8K occurring at 14:30. Wind speed decreased by 49% from initial wind speed with standard deviation of 0.024K.
In the case of the no wind scenario (0.1 m/s), the temperature increased by 8.54% from initial temperature of 305.15K with a standard deviation of 3.32K and daily average temperature of 307.88K and max daily average of

313.3K occurring at 15:30. Wind speed increased by 193.9% from initial wind speed with standard deviation of 0.097K.

In September and initial wind speed of 3.6m/s, the orthogonal configuration showed decreased temperature by 12.85% from initial temperature of 305.15K with a standard deviation of 2.295K and daily average temperature of 301.04K and max daily average of 303.5K occurring at 14:00. Wind speed decreased by 49.7% from initial wind speed with standard deviation of 0.023K.

As for the 0.1m/s initial wind speed case, the temperature increased by 2.99% from initial temperature of 305.15K with a standard deviation of 2.34K and daily average temperature of 306.1K and max daily average of 308.9K occurring at 14:45. Wind speed increased by 154.2% from initial wind speed with standard deviation of 0.064K.

In December and initial wind speed of 3.6m/s, the temperature decreased by 18.95% from initial temperature of 305.15K with a standard deviation of 1.54K and daily average temperature of 299.09K and max daily average of 301.08K occurring at 13:30. Wind speed decreased by 50.2% from initial wind speed with standard deviation of 0.005K.

In the case of no wind (0.1m/s), the temperature decreased by 4.43% from initial temperature of 305.15K with a standard deviation of 1.27K and daily average temperature of 303.7K and max daily average of 305.4K occurring at 14:00. Wind speed increased by 119.1% from initial wind speed with standard deviation of 0.005K.

The Volume Ortho configuration with a sky-view factor of 0.85 in the month of June and initial wind speed of 3.6m/s, the results showed that the temperature decreased by 9.2% from initial temperature of 305.15K with a standard deviation of 2.72K and daily average temperature of 302.2K and max daily average of 304.9K occurring at 14:30. Wind speed decreased by 44.94% from initial wind speed with standard deviation of 0.051K.

As for the case of 0.1 m/s initial wind speed, the temperature increased by 4.56% from initial temperature of 305.15K with a standard deviation of 3.059K and daily average temperature of 306.6K and max daily average of 310.9K occurring at 14:45. Wind speed increased by 184.6% from initial wind speed with standard deviation of 0.076K.

As for September and initial wind speed of 3.6m/s the Volume Ortho results showed that the temperature decreased by 13.1% from initial temperature of 305.15K with a standard deviation of 2.4K and daily average temperature of 300.96K and max daily average of 303.5K occurring at 14:00. Wind speed decreased by 45.9% from initial wind speed with standard deviation of 0.02K.

In the no wind scenario (0.1m/s initial wind speed), the temperature increased by 3.3% from initial temperature of 305.15K with a standard deviation of 2.29K and daily average temperature of 306.2K and max daily average of 309.7K occurring at 13:00. Wind speed increased by 157.3% from initial wind speed with standard deviation of 0.097K.

In the case of December and initial wind speed of 3.6m/s, the temperature decreased by 19.28% from initial temperature of 305.15K with a standard deviation of 1.63K and daily average temperature of 298.98K and max daily average of 301.1K occurring at 13:30. Wind speed decreased by 46.4% from initial wind speed with standard deviation of 0.01K.

With no wind (0.1m/s) the temperature decreased by 7.8% from initial temperature of 305.15K with a standard deviation of 1.33K and daily average temperature of 302.66K and max daily average of 304.3K occurring at 14:00. Wind speed increased by 103.4% from initial wind speed with standard deviation of 0.09K.

The average temperature difference between the initial temperature and reported data in these simulations range from 2-5K. These are in accordance to reported data by Bourbia and Boucheribah (2010), where the difference between rural and the measured urban street temperature in a semi-arid climate was between 3-6C°. Shashua-bar et al. (2004) reported a temperature difference between narrow deep spaces and a reference meteorological station reading to be 2.1 K. Thapar and Yannas (2008) reported a temperature difference between a street canyon of 1.8:1 and a reference station to be 4-6K.

From the results presented in the previous section, the following will provide observations regarding the three configurations in comparison to each other with discussion of the possible causes for these findings. The maximum temperatures reported in the previous section will be used to select the corresponding visual snapshots to discuss the findings. The result analysis focused on the month of June as it is important to understand temperature behavior in summer when temperature reductions are most critical. Furthermore, June showed greater variation in temperature amongst the three configurations than the other seasons.

The Bastakiyah configuration recorded the lowest average temperature value of the three configurations in June. It showed decreased wind speed from the Volume Ortho configuration, but temperature was slightly less. The standard deviation for the Bastakiyah configuration of both temperature and wind are slightly less than the Volume Ortho standard deviation. Looking at the Bastakiyah and Volume Ortho snapshot at 14:30 in Figure 5.17, it revealed that the temperature south of the Bastakiyah configuration is around 1K cooler that the remainder of the configuration indicating that there are cooler areas within the configuration that helped in slightly reducing the overall average temperature of the configuration. On the other hand, the Volume Ortho configuration snapshot in Figure 5.18

showed that the highest temperatures are confined within the entire configuration and bound by the edges of the grid.

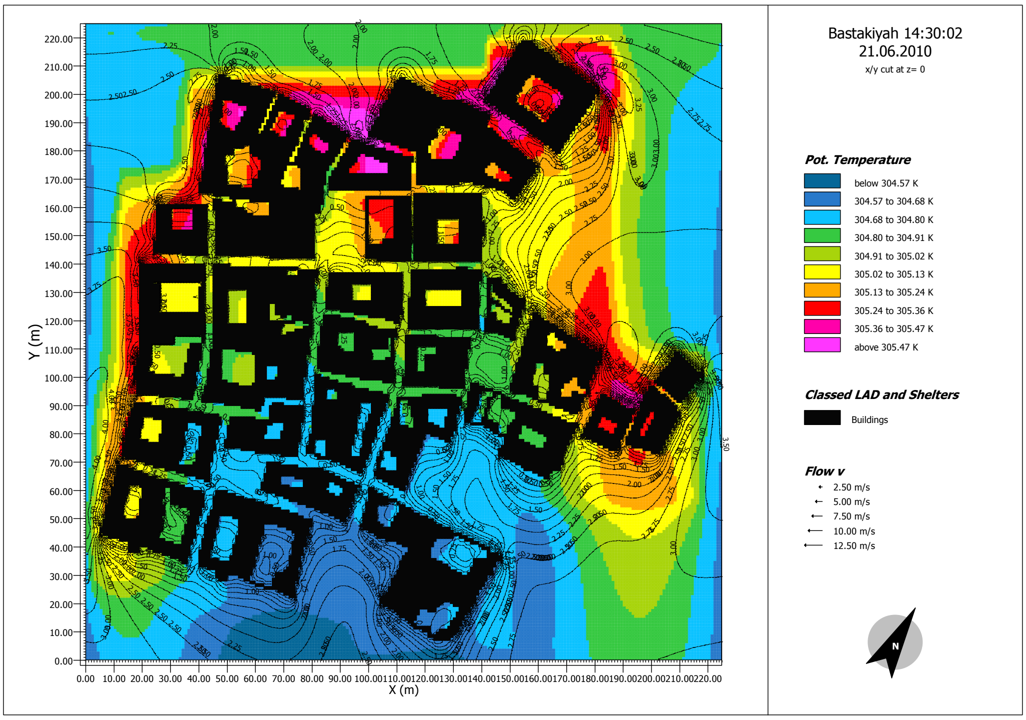

Figure 5.17 Snapshot of temperature gradient in Bastakiyah at 14:30 in June showing a difference in temperature values across the configuration (initial wind speed at 3.6m/s).

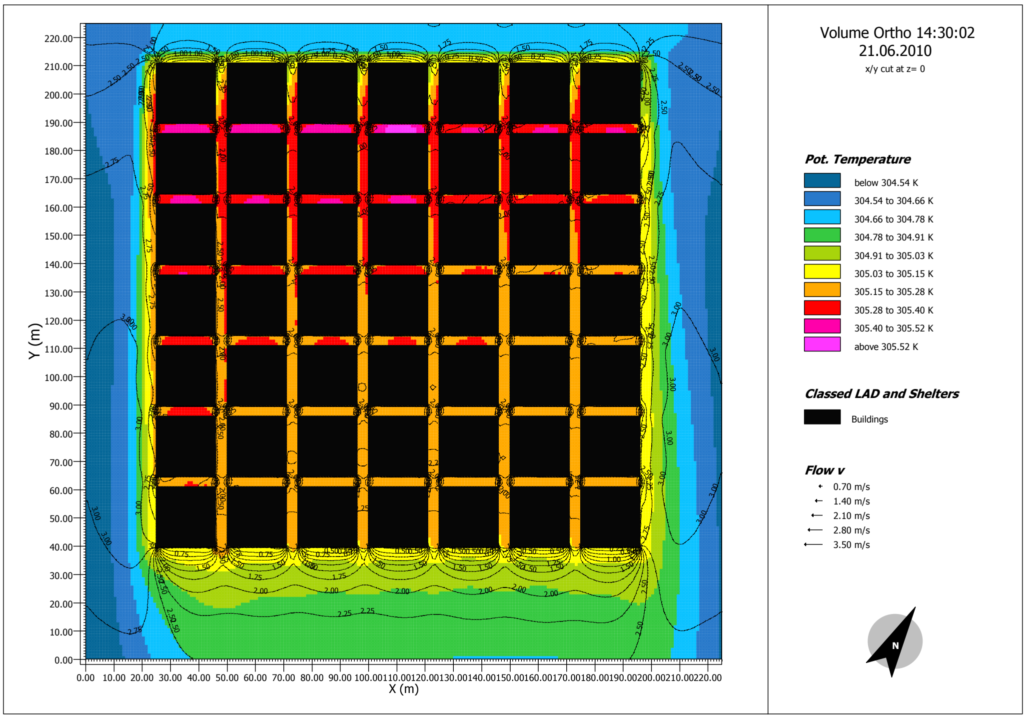

Figure 5.18 Snapshot of temperature gradient in Volume Ortho at 14:30 in June showing high temperature occurring throughout the entire configuration (initial wind speed 3.6m/s).

In the Volume Ortho configuration, the wind speed is higher than that of the Bastakiyah configuration by about 4%, yet it did not record lower average temperature than the Bastakiyah configuration. The increased wind speed in Volume Ortho did not contribute in reducing the average temperature as expected. We also find that the standard deviation is slightly higher for both wind and temperature than those in the Bastakiyah configuration. The Volume Ortho snapshot showed that the roads that are perpendicular to the wind direction recorded the least wind speed. The highest wind speed occurred on the peripheral edges of the configuration and along and through roads aligned with the wind direction. The low wind speed in the perpendicular roads (approaching the value of zero) cancelled out the effect of the high peripheral wind speed in reducing the temperature. This is why the temperature in Volume Ortho was not lower relative to Bastakiyah to correspond with its higher wind speed. Both parallel and perpendicular roads recorded similar high temperature values. The effect of having roads aligned to the prevailing wind or perpendicular to it rendered the same results in terms of temperature values. Figures 5.19 and 5.20 show wind variations in the Bastakiyah configuration and Volume Ortho configuration, respectively.

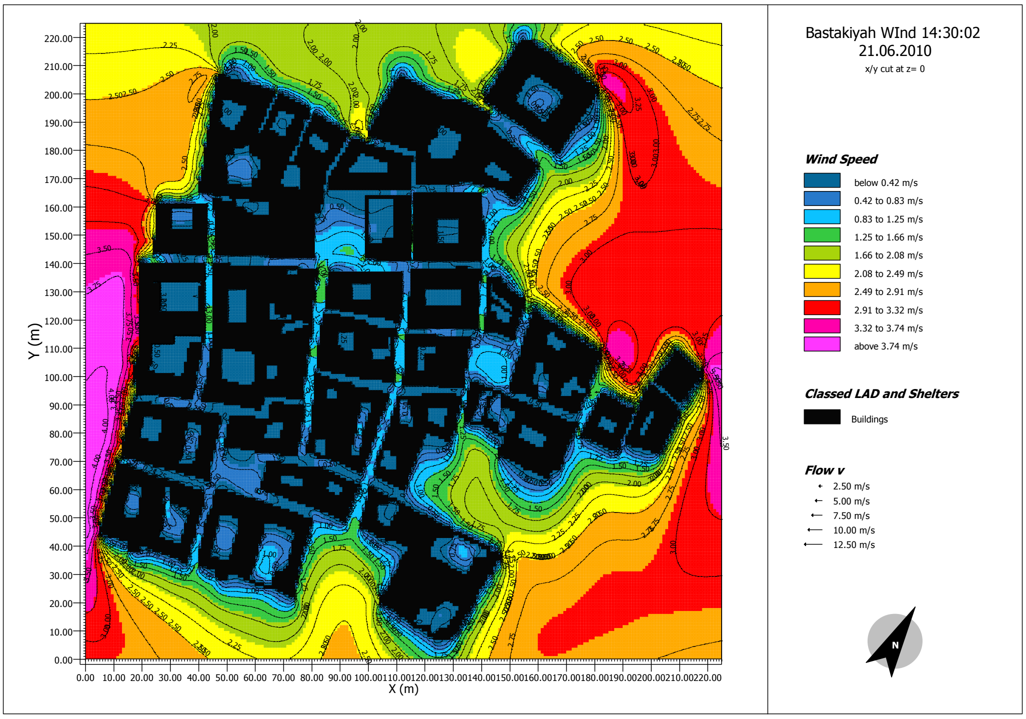

Figure 5.19 Snapshot of wind contours in Bastakiyah at 14:30 in June showing the distribution of wind throughout the configuration (initial wind at 3.6m/s).

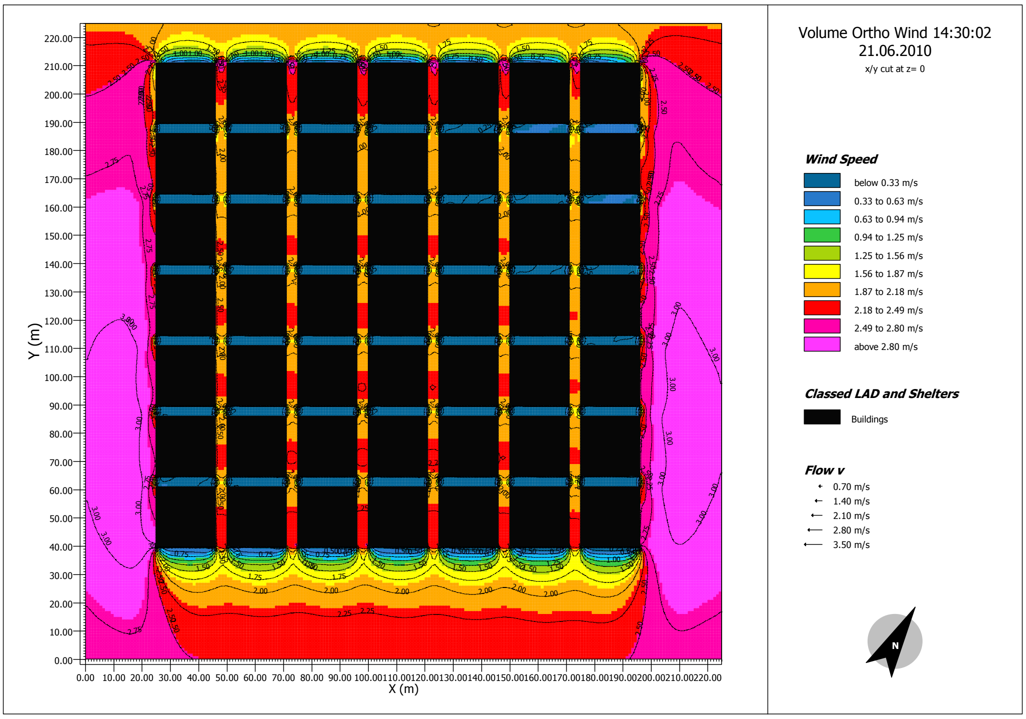

Figure 5.20 Snapshot of wind contours in Volume Ortho at 14:30 in June showing the distribution of wind throughout the configuration (initial wind at 3.6m/s)

In order to illustrate the magnitude of temperature variation, snapshots of both Bastakiyah and Volume Ortho were studied for a wind input of 0.1m/s. The lowered wind speed reveals more of the surface temperature behavior without the wind factor, and could help explain the variations. It was found that the behavior of temperature and wind is similar to that happening with wind speed of 3.6 m/s. Namely, the Volume Ortho configuration recorded higher wind speed but higher temperature values than in the Bastakiyah configuration. The standard deviation of the Bastakiyah configuration is slightly lower than that of Volume Ortho.

It is evident from the snapshots that in the Bastakiyah configuration, the increased wind speed occurred around the configuration and not through alley-ways and semi enclosed open spaces. The high temperatures were recorded in those areas and more evenly distributed throughout the configuration. In the Volume Ortho configuration, the wind standard deviation is higher than that of the Bastakiyah configuration. This is reflected in the snapshot, where wind speeds are scattered throughout the configuration. This created a hotspot at one edge of the configuration, with a recorded highest temperature within the hotspot to be higher than the highest temperature in the Bastakiyah configuration. Figures 5.21 and 5.22 show the temperature behavior in Bastakiyah and Volume Ortho configuration respectively, and Figures 5.23 and 5.24 show the wind behavior in Bastakiyah and Volume Ortho configurations respectively.

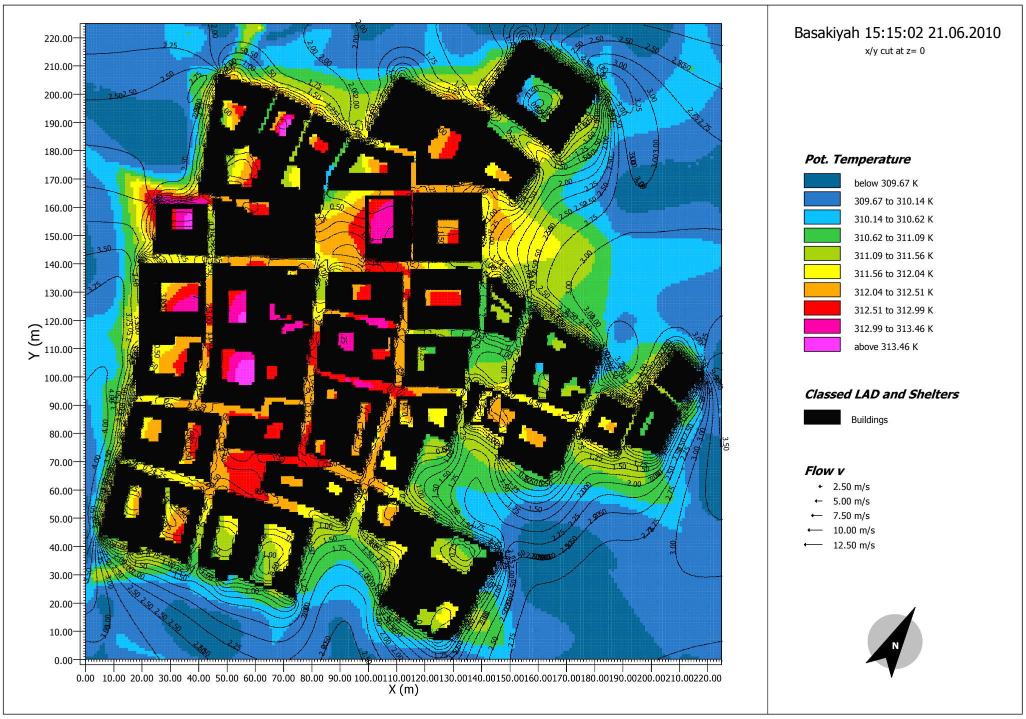

Figure 5.21 Snapshot of temperature variation in Bastakiyah at 15:15 in June in absence of wind (0.1 m/s) showing the distribution of temperature throughout the configuration.

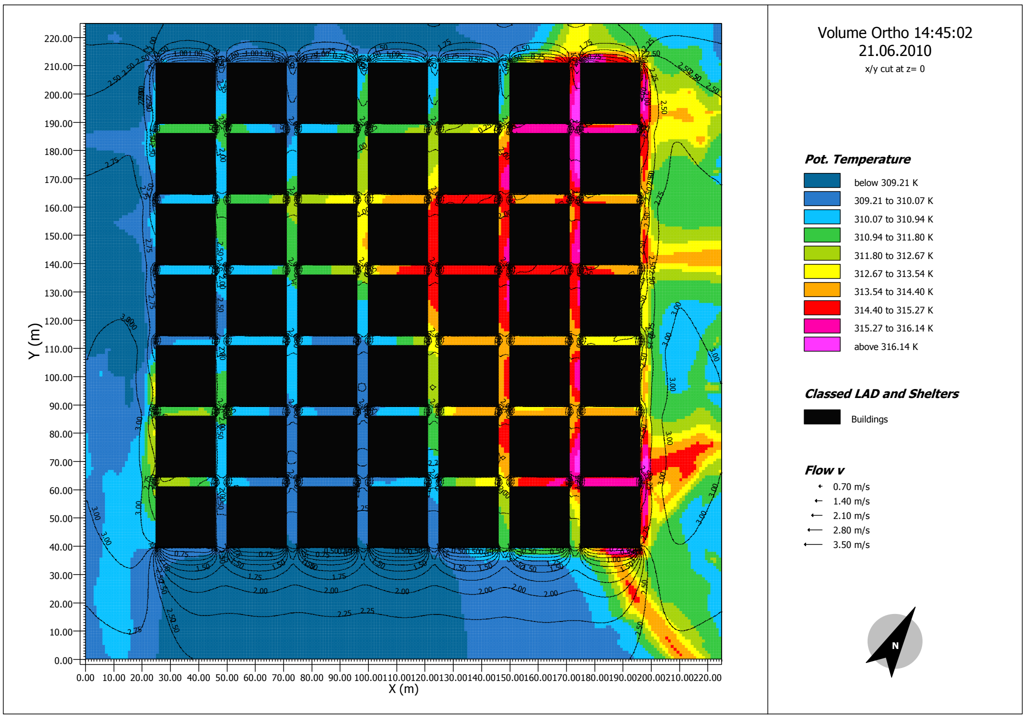

Figure 5.22 Snapshot of temperature variation in Volume Ortho at 14:45 in June in absence of wind (0.1 m/s) showing the distribution of temperature in one part of the configuration.

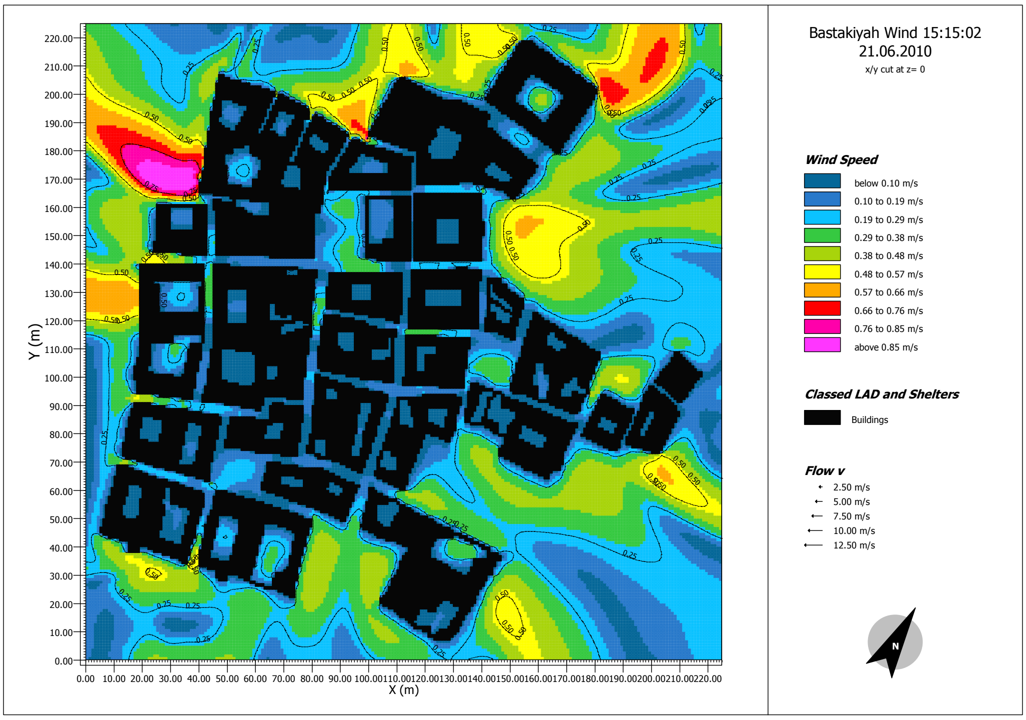

Figure 5.23 Snapshot of wind behavior in Bastakiyah at 15:15 in June in absence of wind (0.1 m/s)

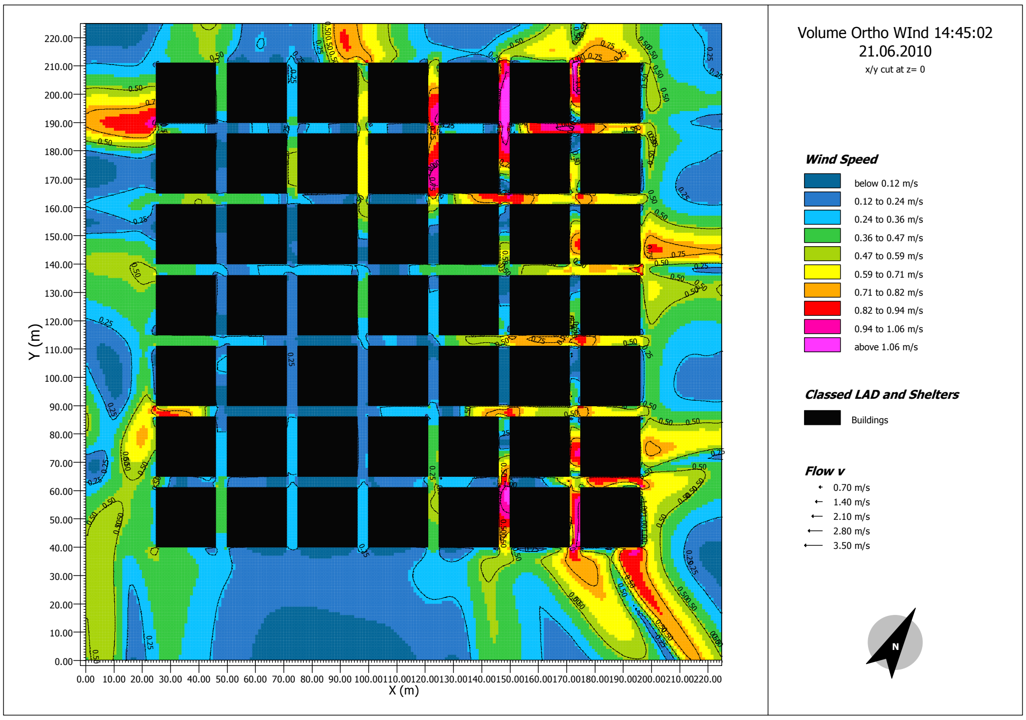

Figure 5.24 Snapshot of wind behavior in Volume Ortho at 14:45 in June in absence of wind (0.1 m/s).

In June, The Orthogonal configuration recorded a highest temperature of all three configurations with the highest decrease in wind speed. The Orthogonal average temperature was higher than the Bastakiyah configuration although wind speeds are almost similar in both. The wind standard deviation of the orthogonal configuration is double of Bastakiyah's.

The lack of observed trend with regards to wind speed and temperature variation, and the fact that the wind did not assist in heat transfer out of the configuration, the sky-view factor provided a plausible explanation with regard to the consistently higher temperature of the Orthogonal configuration than the other two, though wind speeds were not always the lowest. Comparing between the Bastakiyah and Orthogonal configuration, it was found that the sky-view factor of the Bastakiyah is higher than that of the Orthogonal, 0.84 and 0.81 respectively. The sky-view factor of the Orthogonal configuration indicated that the surfaces are less exposed to the sky. Therefore, radiation, which is usually released more by higher exposure to the sky, is trapped within the configuration. The lack of radiation release due to a smaller sky-view factor, and the lack of heat transfer from the lower wind speed were conducive in increasing temperature readings in the Orthogonal configuration.

Comparisons were also drawn between the Orthogonal and Bastakiyah configuration with the 0.1m/s scenario, where wind and temperature variations are exaggerated.

In this case, the standard deviation of the Orthogonal configuration is half of that in the Bastakiyah configuration. By definition, this means there is higher fluctuation of wind in the Orthogonal configuration than there is in the Bastakiyah. This fluctuation in wind speed caused the semi-enclosed areas to be higher in temperature creating hot-spots. The shape of the configuration contributed in the lack of wind circulation in those areas.

Figures 5.25 and 5.26 show the temperature distribution and wind flow in the absence of wind (0.1m/s) respectively.

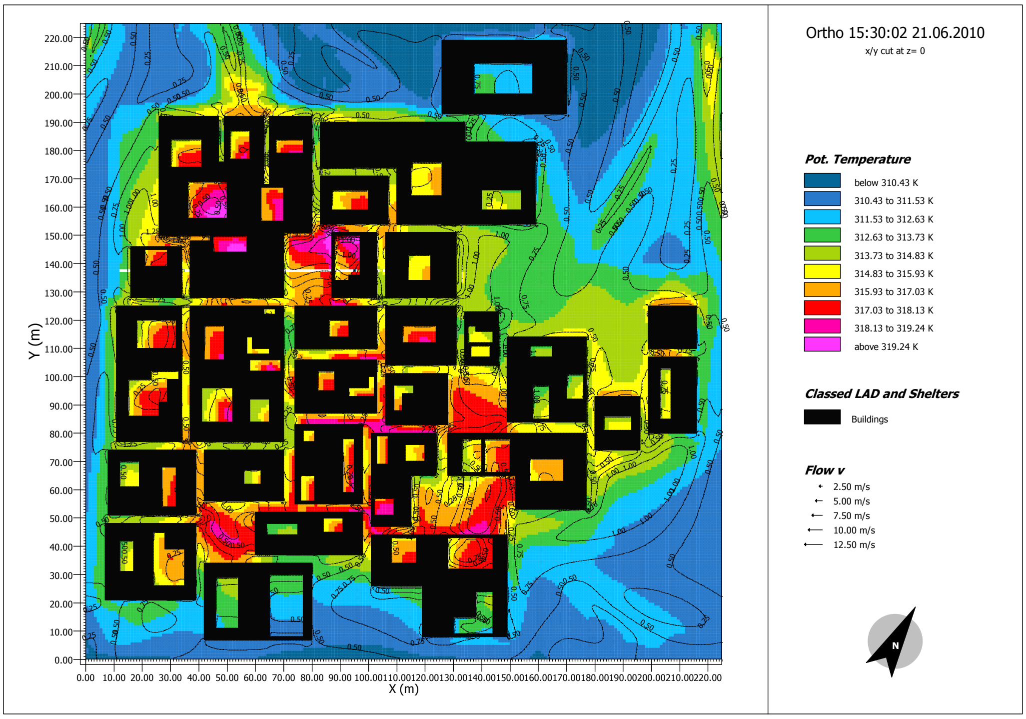

Figure 5.25 Snapshot of temperature variation in Orthogonal configuration at 15:30 in June in absence of wind (0.1 m/s).

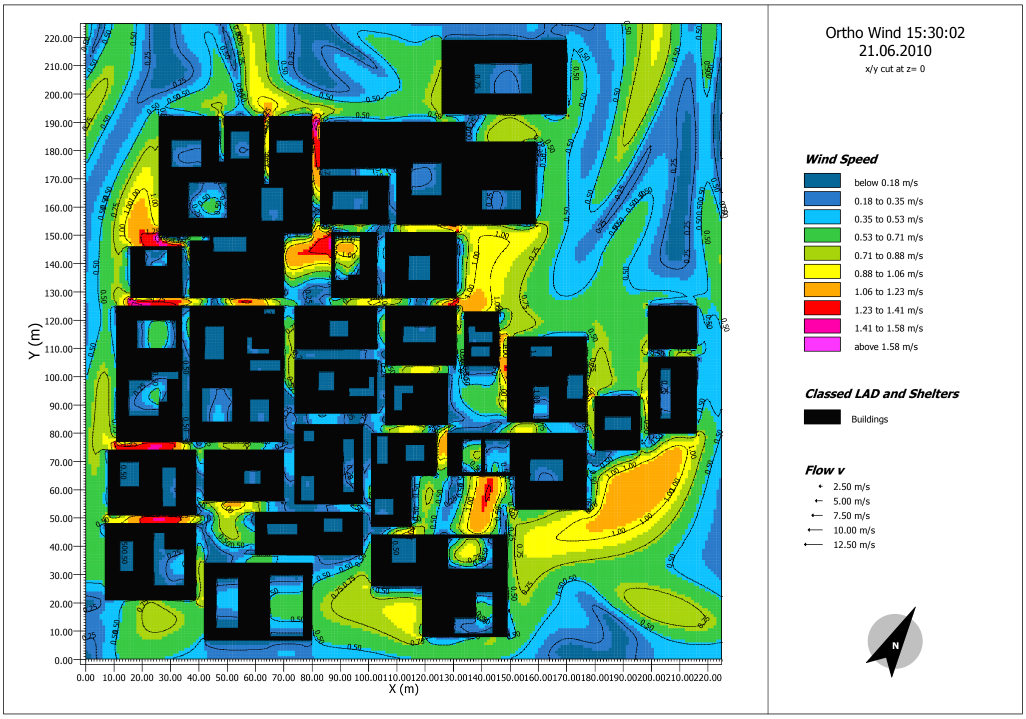

Figure 5.26 Snapshot of wind behavior in Orthogonal configuration at 15:30 in June in absence of wind (0.1 m/s).

In September, the Orthogonal and Volume Ortho had temperatures, with the highest wind speed occurring in the Volume Ortho configuration. Bastakiyah showed the least average temperature value though it had the lowest wind speed of all three configurations.

Temperatures recorded in December were similar in all three configurations though the Volume Ortho configuration showed the highest wind speed. The Volume Ortho temperature behavior did not correspond to its higher wind speed in comparison to the other configurations. The reasoning of this behavior may be explained along the same justification presented in June. The higher wind speed in the Volume Ortho configuration was compromised by the lack of wind in the perpendicular roads to wind direction. Figure 5.27 and 5.28 illustrates wind behavior in both bastakiyah and Volume Ortho configurations in December with initial wind speed of 3.6m/s.

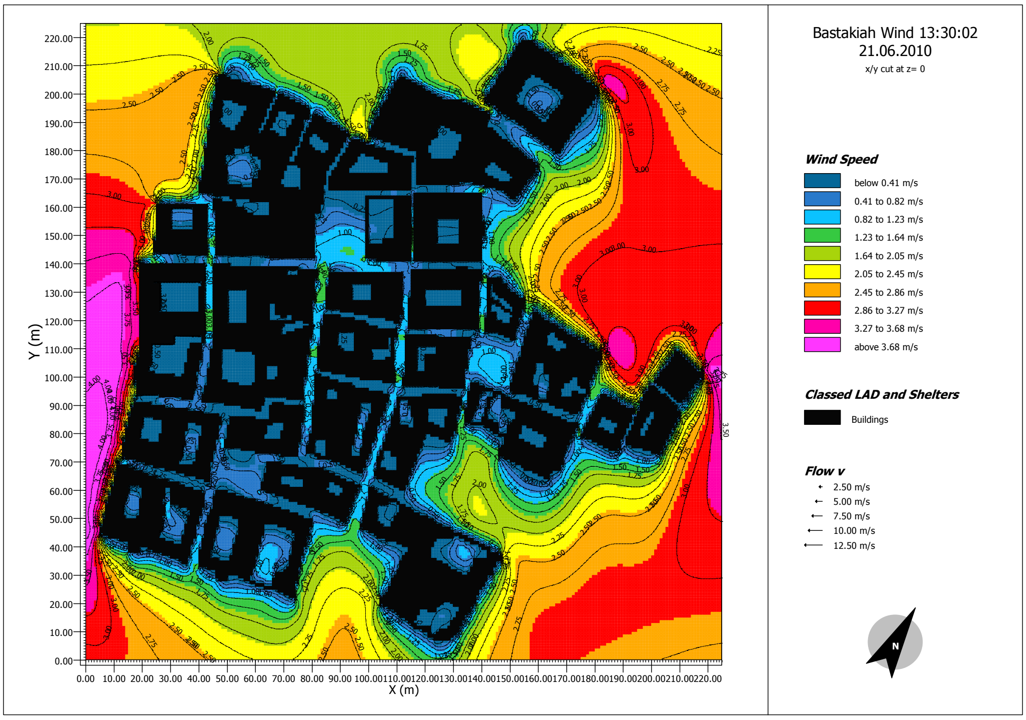

Figure 5.27 Snapshot of wind behavior in Bastakiyah configuration at 13:30 in December with initial wind speed of 3.6m/s

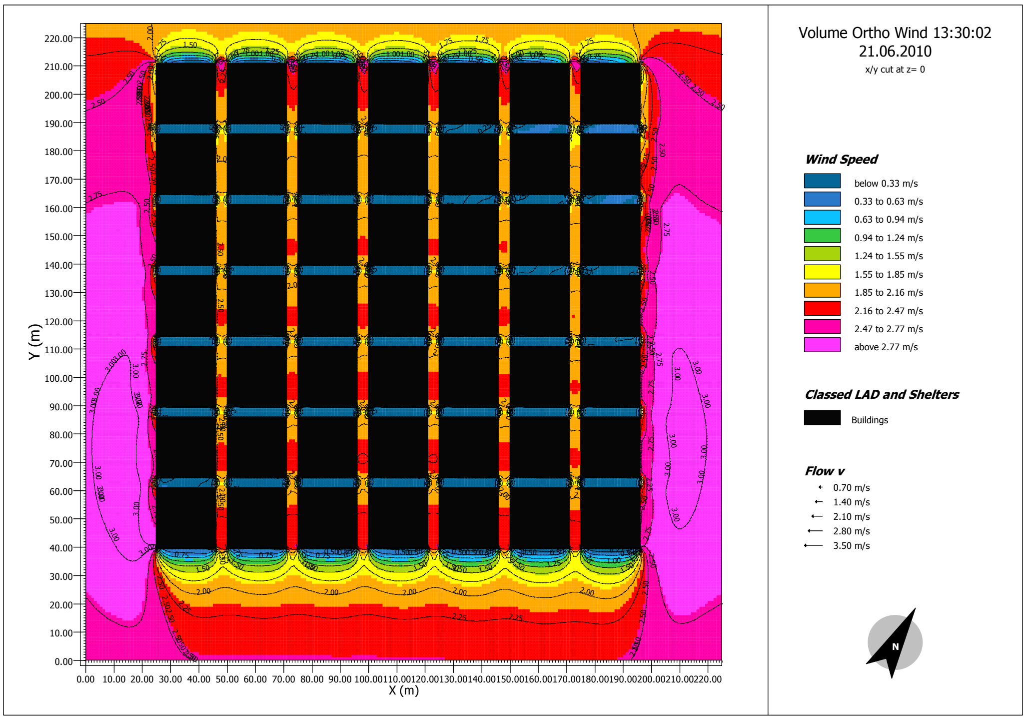

Figure 5.28 Snapshot of wind behavior in Volume Ortho configuration at 13:30 in December with initial wind speed of 3.6m/s

Appendices F-H provide the full range of ENVI-met snapshots showing temperature variations for the three configurations and in three seasons for initial wind speed of 3.6, 0.1, and 7m/s. The snapshots are illustrated for every two hours and the remainder is available in soft copy.

CHAPTER SIX

CONCLUSIONS AND RECOMMENDATIONS

6.0 Conclusion and future work

6.1 Conclusion

This study showed that the urban configuration affects the urban micro-climate. After previous research has substantiated that street geometry influences the micro-climate, this study showed that various urban configurations affect the urban micro-climate in different manners. Beyond the one-to-one relationship between the single elements and buildings of the city, the overall interaction of all the components plays a role in the temperature readings.

Prominent Trends

The coolest configuration was the Bastakiyah. It recorded the least average temperature (sometimes similar) of all configurations in all seasons and under the various wind conditions (0.1m/s, 3.6 m/s, 7m/s). This was despite the fact that it recorded different average wind speeds relative to other configurations. In some instances the wind speed was lower than in others, and in other instances it was intermediate.

The highest average wind speed was recorded by the Volume Ortho configuration in all three seasons. However, this did not contribute in reducing its temperature relative to the other configurations. This was due to the effect the configuration had on the behavior of the wind.

The warmest configuration was the Orthogonal configuration. It recorded the highest average temperature of all configurations in June with a lower wind speed in the initial 3.6m/s wind speed scenario and the greatest wind speed increase in the 0.1m/s wind speed scenario. This is mainly because the configuration did not allow the wind to behave in a way conducive to lowering the temperature.

Reducing the wind speed input to 0.1 m/s resulted in increased temperature in all configurations across all the seasons. Whereas, doubling the wind speed to 7.0 m/s did not reduce the average temperatures substantially from the 3.6 m/s wind speed scenario. It was found that there seems to be a threshold after which increasing the wind to a certain value, it stops becoming effective in reducing temperature values substantially. The results from these specific configurations are expected to hold under a wide range of wind speeds, and even in other locations with varying wind speeds.

In this research, it is safe to conclude that it is not the wind, though an influencing factor in temperature change, but it is the configurations that played a more significant role in temperature variations. As such the input wind did not impact temperature variations. This study showed that the configuration shape was the factor in manipulating the wind within it which became independent of the input wind speeds. Thus, the wind behavior is seen as a resultant of the configuration shape.

Given the specific location of the site, these specific climatic conditions and the alignment of the prevailing wind direction parallel to the majority of the streets, the Bastakiyah configuration is best suited as an urban form.

The Bastakiyah configuration was cooler in summer and autumn, but not colder in winter as it recorded very similar temperatures as the other configurations. The Volume Ortho configuration did not perform up to par with respect to its higher wind speeds in reducing the average temperature. Further, the Orthogonal configuration did not perform as an intermediate solution between the two configurations and consistently recorded unexplained higher temperatures.

By comparing the results between the presence and absence of wind, it was confirmed that the wind had the effect of eliminating major temperature fluctuations and therefore reducing the occurrence of hot spots. It contributed to a smoother distribution of temperature throughout the entire site.

Orientation of the configuration is not seen to be significant in terms of its alignment to the sun; however, it is in terms of the wind direction. The orientation of the majority of roads and streets towards the wind contributed in flushing out the temperature.

In this research, it was found that the urban configuration on the whole is the primary factor affecting temperature variation. With the Orthogonal configuration not resulting in substantial benefits over the Bastakiyah configuration, and with the Volume Ortho configuration resulting in values that are counter to thermal comfort in terms of higher winds and no resultant reduction in temperature, it was concluded that the Bastakiyah configuration performs best under all circumstances. The Bastakiyah configuration is selected as the recommended configuration not only for its thermal behavior, but also for the other sustainability dimensions it promotes. It responds best to the cultural aspect of the society and at the same time to the climatic conditions of the city.

6.2 Recommendations for Future Work

This research has been specifically carried out in the city of Dubai. The orientation of the configurations of the existing site was oriented towards the wind direction. The fact that the variations are minor between the configurations does not mean they may be interchangeable in terms of their performance. It is recommended that designers capitalize on those minor differences. The findings from this research can be implemented in areas related to urban planning of cities, linking between good planning practices with sustainability and environmental consciousness. Some future work that could be carried out would involve repeating the simulations for configurations that are oriented oblique or against the wind direction. Also, simulating the configurations in various latitudes may be explored in order to further understand the behavior of these configurations in different climatic conditions.

Some other suggestions for future work include:

- The Volume Ortho configuration itself could also be altered. Some investigations could explore the effect of reducing or increasing the spacing of the roads and compare the results to those obtained in this research.
- Extend the duration of the simulation to incorporate nocturnal temperature variations.
- Investigate changing the shape of buildings and/or alignment to funnel wind into the configuration without compromising its effective energy in reducing temperature values.
- Investigate the effect of building and material properties and color, as well as the impact of thermal mass in these three configurations.
- Detailed investigation of the effect of sky-view factor when measured as an average of a configuration or portion of a city as a whole. The balance between SVF and shadow casting is also worthy of investigation.

- More rigorous research in the field of urban heat islands and micro-climatic responsive design must be encouraged and carried out by regulating authorities in order to establish the best suiting urban configurations to the city with the least negative impact to the environment and climatic variations. Regulating authorities might need to revise the current regulations which promote dispersed planning.
- Establish research departments with simulation and laboratories as testing facilities to increase investigations in the field of urban heat islands in the United Arab Emirates.

REFERENCES

Ahmed, K. S., 2003. Comfort in urban spaces: defining the boundaries of outdoor thermal comfort for the tropical urban environments. *Energy and Buildings*, 35, 103-110. Available from: www.elsevier.com/locate/enbuild [Accessed 15 December 2010].

Akbari, H. 2005. Energy Saving Potentials and Air Quality Benefits of Urban Heat Island Mitigation. Available from: http://www.osti.gov/bridge/servlets/purl/860475-UlH-WIq/860475.PDF [Accessed 10 July 2010].

Ali-Toudert, F., Mayer, H., 2006. Numerical study on the effects of aspect ratio and orientation of an urban street canyon on outdoor thermal comfort in hot and dry climate. *Building and Environment,* 40, 94-108. Available from: www.elsevier.com/locate/buildenv [Accessed 5 June 2010].

Arnfield, A. J., 2003. Two decades of urban climate research: a review of turbulence, exchanges, of energy and water, and the urban heat island. *International Journal of Climatology,* 23, 1-26. Available from: www.interscience.wiley.com [Accessed 20 September 2010].

Bourbia, F., Boucheriba, F., 2010. Impact of street design on urban microclimate for semi arid climate (Constantine). *Renewable Energy,* 35, 343-347. Available from: www.elsevier.com/locate/renene [Accessed 10 January 2011].

Bretz, S., Akbari, H., Rosenfeld, A., 1998. Practical issues for using solar-reflective materials to mitigate urban heat islands. *Atmospheric Environment*, 32: 1, 95-10. Available from: www.elsevier.com [Accessed 15 August 2010].

Che-Ani, A. I., Shahmohamadi, P., Sairi, A., Mohd-Nor, M. F. I., Zain, M. F. M., Surat, M., 2009. Mitigating the urban heat island effect: some points without altering existing city planning. *European Journal of Scientific Research*, 35 (2), 204- 216. Available from: www.eurojournals.com/ejsar.htm [Accessed 15 October 2009].

Eliasson, I., 1996. Urban nocturnal temperatures, street geometry and land use. *Atmospheric Environment,* 30:3, 379-392. Available from: www.elsevier.com [Accessed 15 August 2010].

Elnahas, M. M., Williamson, T.J., 1997. An improvement of the CTTC model for predicting urban air temperatures. *Energy and Buildings*, 25, 41-49. Available from: www.elsevier.com/locate/enbuild [Accessed 15 December 2010].

Emmanuel R., Johansson, E., 2006. Influence of urban morphology and sea breeze on hot humid microclimate: the case of Colombo, Sri Lanka. *Climate Research*, 30, 189-200. Available from: www.int-res.com [Accessed 20 August, 2010].

Environmental Protection Agency (EPA), 2009. *Basic information: What is sustainability?* [online]. EPA. Available from: www.epa.gov/sustainability/basicinfo.htm#sustainability [Accessed 15 September 2010].

Fahmy, M., Sharples, S., 2009. On the development of an urban passive thermal comfort system in Cairo, Egypt. *Building and Environment,* 44, 1907-1916. Available from: www.elsevier.com/locate/buildenv [Accessed 2 June 2010].

Farr, D., 2008. *Sustainable Urbanism: Urban Design with Nature.* New York: John Wiley & Sons

Figuerola, P., Mazzeo, N., 1998. Urban-rural temperature differences in Buenos Aires. *International Journal of Climatology,* 18, 1709-1723. Available from: http://www.coaps.fsu.edu/pub/williams/AGC_presentation/Grindin_2009/Figuerola_1998.pdf [Accessed 20 Feb 2011].

Golany, G., 1996. Urban design morphology and thermal performance. *Atmospheric Environment,* 30:3, 455-465. Available from: www.elsevier.com [Accessed 20 September 2010].

Hamdi, R., Schayes, G., 2008. Sensitivity study of the urban heat island intensity to urban characteristics. *International Journal of Climatology,* 28, 973-982. Available from: www.interscience.wiley.com [Accessed 20 June 2010].

Hamdi, R., Shayes, G., 2009. Sensitivity study of the urban heat island intensity to urban characteristics. In: *The seventh International Conference on Urban Climate.* Available from: http://www.meteo.be/meteo/download/de/3040061/pdf/rmi_scpub-1233.pdf [Accessed 15 November 2010].

Hedquist, B. C., Sabatino, S., Fernando, H.J.S., Leo. L.S., Brazel, A.J., 2009. Results from the Pheonix Arizona urban heat island experiment. In: *7th International Conference on Urban Climate.* Available from: http://www.ide.titech.ac.jp/~icuc7/extended_abstracts/pdf/384812-1-090518233339-002.pdf. [Accessed 15 December 2010].

Johansson, E., 2006. Influence of urban geometry on outdoor thermal comfort in a hot dry climate: A study in Fez, Morocco. *Building and Environment*, 41, 1326-1338. Available from: www.sciencedirect.com [Accessed 15 October 2009].

Kolokotroni, M., Giannitsaris, I., Watkins, R., 2006. The effect of London urban heat island on building summer cooling demand and night ventilation strategies. *Solar Energy,* 80, 383-392. Available from: www.sciencedirect.com [Accessed 10 October 2009].

Kolokotsa, D., Psomas, A., Karapidakis, E., 2009. Urban heat island in southern Europe: The case study of Hania, Crete. *Solar Energy*, 83, 1871-1883. Available from: www.sciencedirect.com [Accessed 15 October 2009].

Landsberg, H., 1981. *The Urban Climate* [online]. New York: Academic Press. Available from: http://books.google.com/books?id=zkKHiEXZGBIC&printsec=frontcover&dq=the+urban+climate&hl=en&ei=b8C9TYDDCtmS4gbMyqi5BQ&sa=X&oi=book_result&ct=result&resnum=1&ved=0CCkQ6AEwAA#v=onepage&q&f=false [Accessed 20 October 2010].

Mills, G., 1997. The radiative effects of building groups on single structures. *Energy and Buildings,* 25, 51-61. Available from: www.elsevier.com/locate/enbuild [Accessed 12 June 2010].

Montavez, J. P., Rodriguez, A., Jimenez, J., 2000. A study of the urban heat island of Granada. *International Journal of Climatology*, 20, 899-911. Available from: http://adsabs.harvard.edu/abs/2000IJCli..20..899M [Accessed 10 November 2010].

Morris, C. J. G., Simmonds, I., Plummer, N., 2001. Quantification of the influences of wind and cloud on the nocturnal urban heat island of a large city. *Journal of Applied Meteorology,* 40, 169-182. Available from: http://journals.ametsoc.org/doi/abs/10.1175/1520-0450(2001)040%3C0169%3AQOTIOW%3E2.0.CO%3B2 [Accessed 15 December 2012].

Moughtin, C., Shirley, P., 2005. *Urban Design: Green Dimensions.* 2^{nd} ed. Oxford: Architectural Press.

Oke, T. R., 1973. City size and urban heat island. *Atmospheric Environment,* 7, 769-779. Available from: www.elsevier.com [Accessed 30 June 2010].

Oke, T.R. 1995. The heat island characteristics of the urban boundary layer: Characteristics, causes and effects. In J.E. Cermak, A.G. Davenport, E.J. Plate, and D.X. Viegas (eds). *Wind Climate in Cities*, pp. 81–107 [online]. Netherlands: Kluwer Academic. Available from: http://books.google.com/books?id=fYcjrJhiucgC&printsec=frontcover&dq=Wind+Climate+in+Cities&hl=en&ei=tMC9TYK8H9GL4gbJzLC5BQ&sa=X&oi=book_result&ct=result&resnum=1&ved=0CCkQ6AEwAA#v=onepage&q&f=false [Accessed 15 December 2010].

Okeil, A., 2010. A holistic approach to energy efficient building forms. *Energy and Buildings.* Available from: www.elsevier.com/locate/enbuild [Accessed 7 June 2010].

Olroyd-Robinson, K., 2006. Urban Architecture of Al-Bastakiyah. In: Damluji, S., ed. *The Architecture of the United Arab Emirates.* Reading: Garnet Publishing Ltd, pp. 179-203.

Panao, M., Goncalves, H., Ferrao, P., 2008. Optimization of the urban building efficiency potential for mid-latitude climates using a genetic algorithm approach. *Renewable Energy,* 33, 887-896. Available from: www.elsevier.com/locate/renene [Accessed 3 January 2011].

Prado, R. T. A., Ferreira, F. L., 2005. Measurement of albedo and analysis of its influence the surface temperture of building roof materials. *Energy and Buildings*, 37, 295-300. Available from: www.sciencedirect.com [Accessed 15 October 2009].

Poreh, M., 1996. Investigation of heat islands using small scale models. *Atmospheric Environment,* 30(3), 467-474. Available from: www.elsevier.com [Accessed 17 June 2010].

Ratti, C., Raydan, D., Steemers, K., 2003. Building form and environmental performance: archetypes, analysis and an arid climate. *Energy and Buildings,* 35, 49-59. Available from: www.elsevier.com/locate/enbuild [Accessed 12 June 2010].

Sakakibara, Y., Sato, T., 2008. Relationship between urban-rural temperature differences after sunset and urban geometry. *Geographical Reports of Tokyo Metropolitan University,* 43, 57-68. Available from: http://www.repository.lib.tmu.ac.jp/dspace/bitstream/10748/3799/1/20005-43-012.pdf [Accessed 15 December 2010].

Seaman, N., Ludwig, F., Donall, E., Warner, T., Bhumralkar, C., 1989. Numerical studies of urban planetary boundary-layer structure under realistic synoptic conditions. *Journal of Applied Meteorology,* 28, 760-781. Available from: http://adsabs.harvard.edu/abs/1989JApMe..28..760S [Accessed 15 August 2010].

Shashua-Bar, L., Tzamir, Y., Hoffman, M., 2004. Thermal effects of building geometry and spacing on the urban canopy layer microclimate in a hot-humid climate in summer. *International Journal of Climatology,* 24, 1729- 1742. Available from: www.interscience.wiley.com [Accessed 15 June 2010].

Stone, B. Jr., Rodgers, M., 2001. Urban form and thermal efficiency: How the design of cities influences the urban heat island effect*. Journal of the American Planning Association*, 67:2, 186-198. Available from: http://www.informaworld.com [Accessed 27 March 2011].

Synnefa, A., Santamouris, M., Akbari, H., 2007a. Estimating the effect of using cool coatings on energy loads and thermal comfort in residential buildings in various climatic conditions. *Energy and Buildings*, 39, 1167-1174. Available from: www.sciencedirect.com [Accessed 15 October 2009].

Synnefa, A., Santamouris, M., Apostolakis, K., 2007b. On the development, optical properties and thermal performance of cool colored coatings for the urban environment. *Solar Energy*, 81, 488-497. Available from: www.sciencedirect.com [Accessed 15 October 2009].

Takebayashi, H., Moriyama, M., 2009. Study on the urban heat island mitigation effect achieved by converting to grass-covered parking. *Solar Energy*, 83, 1211-1223. Available from: www.sciencedirect.com [Accessed 15 October 2009].

Thapar, H., Yannas, S., 2008. Microclimate and urban form in Dubai. In: *25th Conference on Passive and Low Energy Architecture (PLEA 2008).* Available from: http://architecture.ucd.ie/Paul/PLEA2008/content/papers/oral/PLEA_FinalPaper_ref_491.pdf [Accessed 15 August 2010].

Unger, J., 2004. Intra-urban relationship between surface geometry and urban heat island: review and new approach. *Climate Research,* 27, 253-264. Available from: www.int-res.com [Accessed 20 December 2010].

Voogt, J., 2004. Urban heat islands: Hotter cities [online]. Available from: http://www.actionbioscience.org/environment/voogt.html [Accessed 15 December 2010].

Wanphen, A., Nagano, K., 2009. Experimental study of the performance of porous materials to moderate the roof surface temperature by its evaporative cooling effect. *Building and Environment*, 44, 338-351. Available from: www.elsevier.com/locate/buildenv [Accessed 15 October 2009].

Wong, N. H., Yu, C., 2005. Study of green areas and urban heat island in a tropical city. *Habitat International*, 29, 547-558. Available from: www.elsevier.com/locate/habitatint [Accessed 15 October 2009].

Yamashita, S., Sekine, K., Shoda, M., Yamashita, K., Hara, Y., 1986. On relationships between heat island and sky view factor in the cities of Tama River Basin, Japan. *Atmospheric Environment,* 20:4, 681-686. Available from: www.elsevier.com [Accessed 15 June 2010].

Yilmaz, H., Toy, S., Irmak, M.A., Yilmaz, S., Bulut, Y., 2008. Determination of temperature differences between asphalt concrete, soil and grass surfaces of the City of Erzurum, Turkey. *Atmosphera*, 21(2), 135-146. Available from: http://www.ejournal.unam.mx/atm/Vol21-2/ATM002100202.pdf [Accessed 15 October 2009].

BIBLIOGRAPHY

AboulNaga, M., Elsheshtawy, Y., 2001. Environmental Sustainability Assessment of Buildings in Hot Climates: The case of the UAE. *Renewable Energy,* 24, 553-563. Available from www.elsevier.nt/locate/renene [Accessed 15 August 2010].

Balazs, B., Hall, T., Roth, M., Norford, L., 2009. Microclimate in a high-rise residential development in Singapore. In: *7th International Conference on Urban Climate.* Available from: http://censam.mit.edu/publications/balazs.pdf [Accessed 15 December 2010].

Clifton, K., Ewing, R., Knaap, G., Song, Y., 2008. Quantitative Analysis of Urban Form: A multidisciplinary review. *Journal of Urbanism: International Research on Placemaking and Urban Sustainability,* 1:1, 17-45. Available from: http://www.informaworld.com/smpp/content~db=all?content=10.1080/17549170801903496 [Accessed 17 August 2010].

Environmental Protection Agency (EPA), 2009. *Reducing urban heat islands: Compendium of strategies, Urban heat island basics* [online]. EPA. Available from: http://www.epa.gov/heatisld/about/index.htm [Accessed 15 September 2010].

Giridharan, R., Ganesan, S., Lau, S.S.Y., 2004. Daytime urban heat island effect in high-rise and high-density residential developments in Hong Kong. *Energy and Buildings*, 36, 525-534. Available from: www.sciencedirect.com [Accessed 15 October 2009].

Giridharan, R., Lau, S.S.Y., Givoni, G., 2007. Urban design factors influencing heat island intensity in high-rise high-density environments in Hong Kong. *Building and Environment*, 42, 3669-3684. Available from: www.elsevier.com/locate/buildenv [Accessed 15 October 2009].

Golden, J. S., 2004. The built environment induced urban heat island effect in rapidly urbanizing arid regions – A sustainable urban engineering complexity. *Environmental Sciences*, 1:4, 321-349. Available from: www.sciencedirect.com [Accessed 15 October 2009].

Hung, T., Uchihama, D., Ochi, S., Yasuoka, Y., 2006. Assessment with satellite data of the urban heat island effects in Asian mega cities. *International Journal of Applied Earth Observation and Geoinformation,* 8, 34-48. Available from:www.elsevier.com/locate/jag [Accessed 15 January 2011].

Jabareen, Y., 2006. Sustainable Urban Forms: Their Typologies, Models, and Concepts. *Journal of Planning Education and Research,* 26, 38-52. Available from: http://jpe.sagepub.com [Accessed 17 August 2010].

Kidder, S., Essenwanger, O., 1995. The effects of clouds and wind in nocturnal cooling rates between urban and rural areas. *Journal of Applied Meteorology,* 34, 2440-2448. Available from: http://amsu.cira.colostate.edu/Kidder/Oskar.pdf [Accessed 15 December 2010].

Leder, S., Pereira, F., Claro, A., Ramos, M., 2006. Impact of Urban Design on Daylight Availability. In: *23rd Conference on Passive and Low Energy Architecture.* Available from: http://www.unige.ch/cuepe/html/plea2006/Vol1/PLEA2006_PAPER209.pdf [Accessed 15 August 2010].

Lee, D. O., 1979. The influence of atmospheric stability and the urban heat island on urban-rural wind speed differences. *Atmospheric Environment,* 13, 1175-1180. Available from: http://www.sciencedirect.com [Accessed 15 December 2010].

Memon, R. A., Leung D.Y.C., Chunho, L., 2008. A review on the generation, determination, and mitigation of urban heat island. *Journal of Environmental Sciences*, 20, 120-128. Available from: www.sciencedirect.com [Accessed 15 October 2009].

Roberts, S., 2008. Effects of climate change on the built environment. *Energy Policy,* 36, 4552-4557. Available from: www.elsevier.com/locate/enpol [Accessed 10 October 2009].

Sasaki, K., Mochida, A., Yoshino, H., Watanbe, H., Yoshida, T., 2008. A new method to select appropriate countermeasures against heat-island effects according to the regional characteristics of heat balance mechanism. *Journal of Engineering and Industrial Aerodynamics,* 96, 1629-1639. Available from: www.elsevier.com/locate/jweia [Accessed 20 February 2011].

Yannas, S., 2001. Toward more sustainable cities. *Solar Energy*, 70 (3), 281-294. Available from: www.elsevier.com/locate/solener [Accessed 15 October 2009].

http://www.urbanheatislands.com/home

http://heatisland.lbl.gov/learn/

APPENDICES

Appendix A

Table A.1 Che-Ani (2009) summary of factors affecting the occurrence of Urban Heat Islands

Factors			Possible Effects
Meteorological Factors	Temperature		Since current meteorological conditions associated with heat island intensification are also associated with intense pollution episodes in cities, higher temperatures and changes in cloud cover in the future could lead to higher rates of smog formation, and lower wind speeds may tend to keep pollutants concentrated over urban areas
	Cloud Cover		
	Wind		
Urban Parameters	Location of City	Mountain Ranges & Altitude	Different locations within a given region may vary greatly in their temperature, wind conditions, humidity, precipitation, fog, inversion prevalence and so on. Such variations may be caused by differences in distance from the sea, altitude, direction of slopes, and the general topography of the area (Givoni, 1998).
		Topography	
		Rivers & Other Water Bodies	
	City Size		Increasing of city size is caused higher population & density. Two of the factors that cause the UHI phenomenon depend upon the size and density of the population & its standard of living (vehicular traffic, intensity of heating in the winter & air conditioning in the summer and industrial plants) (Givoni, 1998).
	Density of the Built-up Area (Givoni, 1998)	Land Coverage	The fraction of land covered by buildings in a given area is a relevant factor in evaluating the climatic effect of urbanization. Some architectural details of the buildings, color of their roofs, can change completely the direction of the effect of buildings on the urban radiant balance & temperature.
		Distance between Buildings	Either across streets or within an urban block greatly affects the ventilation conditions, both outdoors & indoors.
		Average Height of Buildings	Higher buildings reduce the ground-level wind speed more than do lower buildings.
	Urban Geometry		1. Increased friction created by a rough urban surface reduces horizontal airflow in the city; 2. The complex geometry of the urban surface changes the urban radiation budget. During the day vertical canyon walls trap short-wave radiation. Night-time losses of infrared energy are also retarded due to the decreased sky view below roof level (Oke, 1981).
	Population Size		Higher population annually increase millions kilo calorie energy in urban thermal temperature from biological activities. Producing lots of energy from these activities is caused UHI (Alijani and Safavi, 2007).
	Wind Speed		UHI intensity is inversely proportional to macro-level wind speed. However, urban wind flows are usually weak at macro-level.
	Anthropogenic Heat		Space heating, manufacturing, transportation, lighting and human and animal metabolisms warm the urban atmosphere by conduction, convection, and radiation (Oke, 1981).
	Surface Waterproofing		1. Buildings and paved streets quickly shed precipitation into catchment basins, creating an evaporation deficit in the city; 2. Urban surface cover enhances sensible heat transfer and suppresses latent heat flux (Oke, 1981).
	Thermal Properties of Fabric		The greater diurnal absorption of short-wave radiation in urban areas by urban construction materials such as concrete and asphalt.
	Land uses		Different types of land uses (Commercial, Residential, Industrial, Parks, Airport and so on) have different influence on urban climate. Increasing the centralization of population in an area of city and anthropogenic heat can be of the most important factors for producing heat (Commercial area).
	Air Pollution		1. Reducing the incident flux of short-wave (i.e. solar) radiation; 2. Re-emitting long-wave (i.e. infrared) radiation from the urban surface downward to where it is retained by the ground; and 3. Absorbing long-wave radiation from the urban surface, effectively warming the ambient air (Oke, 1981).

Appendix B

Data Extraction Progress (sample) – remaining files available in soft copy

Table B.1 Data extraction process- remaining files included in soft copy

	A	B	C	D	E	F
1	x(m)	y(m)	Pot. Temperature (	Wind Speed (m/	Pot. Temperature (K)	Wind Speed (m/s)
2	0.5	0.50 29	7.4208	6295	7.4208	6295
3	0.5	1.50 29	7.4229	6435	7.4229	6435
4	0.5	2.50 29	7.4248	6578	7.4248	6578
5	0.5	3.50 29	7.4267	6725	7.4267	6725
6	0.5	4.50 29	7.4286	6875	7.4286	6875
7	0.5	5.50 29	7.4305	7029	7.4305	7029
8	0.5	6.50 29	7.4323	7187	7.4323	7187
18789	78.5	217.5	296.7327	1.8255	296.7327	1.8255
18790	95.5	217.5	296.7327	1.8272	296.7327	1.8272
18791	193.5	0 218.5	0 296.7328	0 2.2987	296.7328	2.2987
18792	194.5	0 218.5	0 296.7328	0 2.2886	296.7328	2.2886
18793	195.5	0 218.5	0 296.7328	0 2.2782	296.7328	2.2782
18794	196.5	0 218.5	0 296.7328	0 2.2675	296.7328	2.2675
18795	197.5	0 218.5	0 296.7328	0 2.2568	296.7328	2.2568
18796	198.5	0 218.5	0 296.7328	0 2.2461	296.7328	2.2461
18797	79.5	217.5	296.733	1.8298	296.733	1.8298
50620	78.5	52.5	298.0501	0.1791	298.0501	0.1791
50621	70.5	45.5	298.0502	0.1933	298.0502	0.1933
50622	77.5	51.5	298.0504	0.1154	298.0504	0.1154
50623	72.5	45.5	298.0504	0.0542	298.0504	0.0542
50624	77.5	50.5	298.0505	0.0621	298.0505	0.0621
50625	71.5	45.5	298.0505	0.0791	298.0505	0.0791
50626	78.5	51.5	298.0506	0.1851	298.0506	0.1851
50627	Average				297.471831	1.79914764

Appendix C

Tabulated simulation results for the three configurations per season showing the daily temperature and wind speed including average, maximum, minimum temperature and standard deviations

Table C.1 Simulation results for Bastakiyah, Orthogonal and Volume Ortho in June with initial wind speeds of 3.6m/s and 0.1m/s

Configuration	Bastakiyah - 3.6 m/s		Bastakiyah - wind 0.1 m/s		Ortho - 3.6 m/s		Ortho - wind 0.1 m/s		Volume Ortho - 3.6 m/s		Volume Ortho - wind 0.1 m/s	
Time of Day	B Avg Temp (K)	B Avg Wind Speed	B Avg Temp (K)	B Avg Wind Speed	O Avg Temp (K)	O Avg Wind Speed	O Avg Temp (K)	O Avg Wind Speed	VO Avg Temp (K)	VO Avg Wind Speed	VO Avg Temp (K)	VO Avg Wind Speed
6:00	296.8963105	1.807680579	300.7006279	0.15130987	299.3056081	1.819044745	300.7694399	0.147185539	296.7392594	1.944007007	302.1773369	0.190942255
6:15	296.8952671	1.808544455	301.63493	0.165644641	299.3127286	1.819991204	301.5415657	0.269292067	296.7479032	1.944116972	302.4802558	0.187350096
6:30	296.973612	1.809246472	303.6418019	0.33219456	299.3988499	1.820858763	303.7934308	0.26685442	296.8463893	1.944085599	301.9989288	0.145328942
6:45	297.1652964	1.809731711	303.2843859	0.194447389	299.6025073	1.821583587	303.1722876	0.212902028	297.0809756	1.943893159	301.914869	0.303387122
7:00	297.3753844	1.80999223	303.3929902	0.337085311	299.8234537	1.822114996	303.3869908	0.307429261	297.3175632	1.943444221	301.9244177	0.202248824
7:15	297.6717068	1.809999668	303.4053954	0.132752736	300.1287664	1.822381797	303.407523	0.151938207	297.6493087	1.942996685	301.8666219	0.188630255
7:30	297.9588885	1.809164068	303.5597557	0.25364108	300.4234425	1.822341952	303.4089173	0.149944994	297.9685608	1.941790187	302.0454538	0.222560592
7:45	298.3209198	1.809164068	303.6759681	0.192122549	300.7907408	1.821991814	303.6399859	0.173109575	298.3616656	1.940596301	302.2832192	0.291934061
8:00	298.6600029	1.808281648	303.826828	0.210683041	301.1402614	1.821455692	303.8268784	0.236483615	298.7235925	1.939052128	302.3246197	0.325363981
8:15	299.0586458	1.807099041	304.0076416	0.280262371	301.5445328	1.820761945	304.0915708	0.254492326	299.1605926	1.937537764	302.3936536	0.359510411
8:30	299.4296277	1.805669194	303.9708105	0.263144814	301.9186082	1.81990954	304.3628211	0.276969834	299.5306924	1.935369321	302.4993048	0.367156575
8:45	299.8483756	1.804022211	304.4367924	0.287110979	302.3449293	1.818891191	304.7116798	0.323087383	299.9789967	1.933095623	302.9640435	0.364588741
9:00	300.2307615	1.802135708	304.5611249	0.246419529	302.7355399	1.81772965	304.7550934	0.305418105	300.3834654	1.930605882	303.4209223	0.335720888
9:15	300.6379612	1.800204831	305.3719412	0.328634415	303.1444895	1.816458934	305.3072123	0.31852848	300.8096153	1.92787282	303.7502235	0.304084116
9:30	301.0106784	1.79825098	305.3311033	0.276227308	303.5400096	1.815093361	305.5685713	0.31674106	301.2020862	1.925188586	304.4872967	0.36244664
9:45	301.3977577	1.796608807	305.9776048	0.290166983	303.9783574	1.813649271	305.9996901	0.332183818	301.596523	1.923131612	304.4148793	0.263908316
10:00	301.6951281	1.795771166	306.273675	0.292185783	304.3367586	1.812098751	306.1804753	0.315233016	301.8896819	1.922286657	305.1157837	0.314667739
10:15	301.9999821	1.795921441	306.5200178	0.263963055	304.6891728	1.810488645	306.6873318	0.331846294	302.2021055	1.922715651	305.2058263	0.251839202
10:30	302.2850682	1.797017883	307.0342844	0.288535087	305.0103532	1.809093187	306.8486553	0.318733282	302.5008453	1.924326007	305.979714	0.359227187
10:45	302.5719471	1.799021641	307.3398102	0.295617802	305.3163237	1.808317644	307.3323904	0.330175328	302.7862304	1.927148053	305.8886764	0.24738426
11:00	302.8105201	1.802022226	307.7909128	0.310770075	305.5876042	1.80831455	307.5724632	0.326648828	303.2474546	1.936682029	306.841797	0.336143484
11:15	303.0473606	1.806124019	308.052355	0.305049612	305.8625751	1.809006658	307.9750276	0.337697713	303.2474546	1.936682029	307.0999673	0.349471061
11:30	303.2701335	1.811140894	308.4874395	0.313547709	306.1196183	1.810377764	308.2634508	0.335730985	303.4688242	1.942799015	307.0716325	0.275520689
11:45	303.5124052	1.816685281	308.7559392	0.314022555	306.3881881	1.812417631	308.529637	0.316587674	303.7213024	1.95033509	308.780099	0.404173864
12:00	303.6942049	1.823029369	308.9751801	0.308660229	306.6046162	1.815016128	309.0702784	0.358422951	303.9009165	1.95881106	307.6768885	0.272925852
12:15	303.887986	1.83037562	309.2737569	0.315404132	306.8325713	1.818202072	308.8954927	0.280500196	304.0725848	1.967839427	309.226267	0.432031303
12:30	304.0522345	1.838230809	309.4942958	0.319282431	307.0261975	1.821977008	310.1312929	0.388243021	304.2257725	1.977195025	307.9287185	0.245171006
12:45	304.1871242	1.846314184	309.7545397	0.322984806	307.1914198	1.826220829	309.6650977	0.298136635	304.3656102	1.986687358	310.254181	0.406498872
13:00	304.3162708	1.854439305	309.9427276	0.322602527	307.3508158	1.830779655	310.8630312	0.328629758	304.501921	1.996096511	308.8969872	0.32355076
13:15	304.4013401	1.862454042	310.0074856	0.310663115	307.4545658	1.835665232	310.806353	0.328334594	304.5938559	2.005121452	310.0131749	0.349803581
13:30	304.4957203	1.870178323	310.2663691	0.31996036	307.5470298	1.840885048	311.3717664	0.339308929	304.6975526	2.013497559	308.9717939	0.280929459
13:45	304.5757913	1.87752061	310.3084334	0.312847494	307.63771	1.846167737	311.0215561	0.297791071	304.7850923	2.021158335	310.319625	0.399050579
14:00	304.6343508	1.884434418	310.4575459	0.308885281	307.7103897	1.8514769	312.5051052	0.426192406	304.8270521	2.028125966	309.051382	0.268933301
14:15	304.6626768	1.890849919	310.521167	0.301276253	307.7452273	1.856722398	310.4658843	0.262625893	304.8637369	2.034370593	310.0089592	0.398377194
14:30	304.7152296	1.896698614	310.6349636	0.29384056	307.8043285	1.861649518	312.9523364	0.452615913	304.9260698	2.039864866	309.3016622	0.262423211
14:45	304.7045073	1.901911519	310.6900554	0.291747299	307.7900266	1.866146329	311.0013756	0.291402967	304.9005323	2.044556627	310.9161709	0.382237177
15:00	304.7102706	1.906431209	310.6938541	0.281923379	307.7908196	1.870116938	312.6222981	0.489322423	304.9054483	2.048407999	309.7774512	0.289748329
15:15	304.6619524	1.910264979	310.7328835	0.282410295	307.7505541	1.873433323	309.7394679	0.179376369	304.8512223	2.051454053	309.9082095	0.303239265
15:30	304.6163759	1.913448793	310.6442524	0.26517959	307.7025838	1.875966241	313.2848642	0.523893607	304.7851954	2.053790135	309.6834655	0.298000118
15:45	304.5127893	1.915939425	310.590312	0.251866233	307.6032813	1.877580582	309.5943703	0.150849979	304.6623025	2.055395357	309.5836764	0.270782999
16:00	304.4322814	1.917708505	310.4747978	0.238206429	307.5258346	1.878204561	312.8559317	0.517200509	304.5809087	2.056251036	309.5969836	0.27259913
16:15	304.2512096	1.918624497	310.348515	0.229643529	307.3367503	1.877594499	309.3833306	0.11964538	304.3594726	2.056181502	309.2075069	0.238941337
16:30	304.100562	1.918500863	310.2217048	0.223760181	307.1715087	1.875403995	312.5237393	0.484453778	304.1774294	2.054971946	309.1063806	0.23186654
16:45	303.8563085	1.917015606	310.0050543	0.217995797	306.8928732	1.871538931	309.4062215	0.179795831	303.9074851	2.052256524	308.8564673	0.216581498
17:00	303.633852	1.913928855	309.8041425	0.210280627	306.6281948	1.866950982	310.6685685	0.2521873	303.6524566	2.047769144	308.6701733	0.209873805
17:15	303.2919938	1.909281616	309.4719146	0.187688899	306.2457617	1.861820202	309.4907434	0.208596065	303.2430635	2.041424292	308.340083	0.195637963
17:30	302.973239	1.903448342	309.2623619	0.135541133	305.8890217	1.857110166	309.2659335	0.197582103	302.9024983	2.033477969	308.1094943	0.167031874
17:45	302.5405662	1.89698388	309.2007443	0.141769582	305.4238799	1.853237504	308.9210381	0.195707693	302.4392231	2.024560813	307.8455696	0.141174233
18:00	302.1535077	1.890416478	308.8846649	0.141769582	305.009191	1.850157571	308.6473937	0.195707693	302.033826	2.015453821	307.6747604	0.135938509
Average	302.0976752	1.854557368	307.5856298	0.262484265	304.9001749	1.835804033	307.8833992	0.293912998	302.2106595	1.982132199	306.6092974	0.284631371
Max	304.7152296	1.918624497	310.7328835	0.337085311	307.8043285	1.878204561	313.2848642	0.523893607	304.9260698	2.056251036	310.9161709	0.432031303
Min	296.8952671	1.795771166	300.7006279	0.132752736	299.3056081	1.80831455	300.7694399	0.11964538	296.7392594	1.922286657	301.8666219	0.135938509
Standard Deviation	2.637735836	0.047302453	2.950911632	0.059270874	2.883598639	0.024166844	3.320729369	0.097476302	2.716102314	0.050720447	3.058842046	0.076208792
Skyview Factor	83.53156%				81.25680%				84.87290%			

Table C.2 Simulation results for Bastakiyah, Orthogonal and Volume Ortho in September with initial wind speeds of 3.6m/s and 0.1m/s

Configuration	Bastakiyah - wind 3.6 m/s		Bastakiyah - wind 0.1 m/s		Ortho - wind 3.6 m/s		Ortho - wind 0.1 m/s		Volume Ortho - 3.6 m/s		Volume Ortho - wind 0.1 m/s	
Time of Day	B Avg Temp (K)	B Avg Wind Speed	B Avg Temp (K)	B Avg Wind Speed	O Avg Temp (K)	O Avg Wind Speed	O Avg Temp (K)	O Avg Wind Speed	VO Avg Temp (K)	VO Avg Wind Speed	VO Avg Temp (K)	VO Avg Wind Speed
6:00	297.471831	1.79914764	300.7006279	0.15130987	297.453228	1.784083916	300.7694399	0.147185539	296.7392594	1.944007007	301.0389317	0.154656974
6:15	296.7225984	1.686181962	301.6348687	0.165647267	297.1178953	1.785331488	301.5414859	0.269303119	296.7103969	1.944128437	301.6063266	0.162749344
6:30	296.6013139	1.687495552	303.6168782	0.33397228	296.9894791	1.786722319	303.7646341	0.267916442	296.6805979	1.944193871	303.62356	0.315578555
6:45	296.5385723	1.688900036	303.1621492	0.207365451	296.9230482	1.788209388	303.029464	0.22039869	296.6560786	1.944307759	303.3098074	0.174220066
7:00	296.5656705	1.690380206	303.238013	0.335690781	296.9517398	1.789776593	303.2609775	0.318772364	296.7254615	1.94440957	303.2080567	0.385279477
7:15	296.7265998	1.691803561	303.1262505	0.166009443	297.1221319	1.791283644	303.1326228	0.120113174	296.9388016	1.944338383	303.2717919	0.108328869
7:30	296.9161347	1.692914814	303.1266685	0.299236808	297.3228118	1.79246024	302.8075394	0.308714926	297.156411	1.944052191	302.9289943	0.256769531
7:45	297.1920899	1.693747586	302.9857871	0.168114226	297.6149934	1.79334198	303.1756346	0.152626241	297.4792462	1.94337604	303.2444581	0.154606657
8:00	297.4615886	1.694279076	303.0733704	0.187863156	297.900339	1.793904722	302.9848306	0.1438047	297.7642218	1.942710566	303.1352802	0.140568627
8:15	297.8022779	1.694487068	303.1922046	0.188213139	298.2610612	1.794124944	303.141519	0.258136242	298.1420943	1.942056373	303.6195078	0.210220682
8:30	298.1185773	1.694405079	303.267347	0.192581717	298.5959594	1.794038134	303.2220563	0.236477489	298.4794413	1.940364025	303.6192696	0.284630653
8:45	298.4942624	1.694067748	303.4876093	0.244935284	298.9937353	1.793680968	303.4497959	0.250612235	298.9017036	1.938397584	303.6964563	0.32504168
9:00	298.8299769	1.693410764	303.4363772	0.259117417	299.3491901	1.792985352	303.4596727	0.259008844	299.2575475	1.936455996	303.6904272	0.353374672
9:15	299.3191974	1.692686315	303.7487151	0.278426349	299.7544799	1.792140905	303.8052257	0.274600044	299.6879909	1.934063645	303.9597685	0.364153338
9:30	299.5866992	1.691718092	304.0835264	0.292390186	300.1504086	1.791193149	304.1970214	0.323383615	300.0909089	1.931697267	304.3795924	0.361712421
9:45	299.9608751	1.690724565	304.4668195	0.291477332	300.5465865	1.790141202	304.4433271	0.302818143	300.5073285	1.929354278	304.876117	0.358384629
10:00	300.3125765	1.68957965	304.8454083	0.288906578	300.9189684	1.788928964	304.8974847	0.312469492	300.8895369	1.926801254	304.5851363	0.260426969
10:15	300.6641652	1.688368136	305.2689472	0.299810692	301.291231	1.787646212	305.246821	0.319533845	301.2719284	1.924328614	306.4953372	0.451124023
10:30	300.9342358	1.687492236	305.6153693	0.307956683	301.577182	1.786718808	305.548365	0.320859124	301.559017	1.922516636	305.4060336	0.247191713
10:45	301.1957652	1.687308042	305.9671856	0.313248647	301.8540896	1.786523783	305.9148873	0.324131754	301.8413093	1.921783877	306.7015664	0.387741924
11:00	301.4437172	1.687887372	306.2933199	0.317996427	302.1166216	1.787137179	306.2092982	0.321935967	302.115941	1.922112	305.9758645	0.216171718
11:15	301.6757801	1.68922392	306.6242799	0.324265379	302.36233	1.788552317	306.5328654	0.320703277	302.3691972	1.923475509	307.3062205	0.497410193
11:30	301.8730717	1.691182109	306.8939827	0.330168331	302.5712226	1.790625649	306.8171982	0.318612678	302.5763518	1.925748613	306.5138309	0.250266123
11:45	302.0952793	1.693720568	307.1364645	0.327870243	302.8064963	1.793313373	307.11105	0.316201831	302.817251	1.928901586	307.5398056	0.373732306
12:00	302.2569515	1.696834053	307.3391919	0.315569448	302.9776749	1.796609935	307.3952515	0.314523125	302.9912882	1.932729643	307.712765	0.324898731
12:15	302.3645633	1.700488791	307.5379922	0.30116056	303.0916145	1.800479576	307.6045327	0.311213285	303.1000734	1.937324041	307.7006333	0.269062288
12:30	302.4739664	1.704589544	307.8021082	0.295181547	303.2074506	1.804821458	307.8162524	0.307116394	303.2191128	1.94257417	309.2027215	0.401282284
12:45	302.5774975	1.70891508	308.0286421	0.291425336	303.3170695	1.809401341	308.0137816	0.301958441	303.3229042	1.94865801	307.6265769	0.239885912
13:00	302.6465379	1.71357801	308.2271287	0.28946854	303.3901696	1.814338456	308.1964686	0.297069885	303.4041556	1.954928286	309.7158351	0.415789349
13:15	302.6952882	1.718512102	308.3682635	0.287937262	303.4417864	1.819562679	308.3513862	0.293241667	303.4590005	1.961095191	308.1831012	0.260633276
13:30	302.7131459	1.723723104	308.4434753	0.283404735	303.4606942	1.825080095	308.5345524	0.303135255	303.4730456	1.96692722	308.8868765	0.290936997
13:45	302.7339059	1.728566505	308.5019042	0.276363434	303.4826749	1.830208294	308.5964642	0.295424877	303.4787382	1.972131262	308.810128	0.33089508
14:00	302.7683512	1.732843386	308.6555417	0.276932168	303.5191456	1.83473666	308.7568097	0.294264346	303.5305759	1.976549712	308.5250524	0.247548363
14:15	302.7479952	1.736635302	308.6983725	0.2743329	303.4975926	1.838751545	308.7956581	0.280048097	303.5117991	1.980272223	308.8682452	0.309083696
14:30	302.7398256	1.740018017	308.7450521	0.271119747	303.4889427	1.842333168	308.8599509	0.259979978	303.5015128	1.983401365	308.5437855	0.238869678
14:45	302.6492764	1.742860223	308.6922929	0.264808601	303.393069	1.845342499	308.8948491	0.254050678	303.386601	1.985695881	308.8503981	0.259474864
15:00	302.595174	1.744949459	308.679313	0.25418837	303.3357854	1.847554585	308.8566408	0.248477631	303.3284925	1.986825236	308.6771609	0.230333283
15:15	302.4710072	1.746005267	308.6233746	0.243915358	303.2043174	1.848672475	308.7600506	0.243853516	303.2001467	1.986469708	308.5742258	0.245282508
15:30	302.3595185	1.745793499	308.5825272	0.237721363	303.086273	1.848448256	308.6652379	0.240189477	303.0747304	1.984360075	308.2695399	0.223409961
15:45	302.1531485	1.744025405	308.4012887	0.227163058	302.8677683	1.846576195	308.4421645	0.238890223	302.8375836	1.9799311	308.0842811	0.217173296
16:00	301.9666589	1.740880955	308.2723923	0.222843959	302.6703128	1.843246848	308.2503714	0.234916837	302.6378277	1.97332292	307.9017577	0.208436443
16:15	301.6787004	1.737055198	308.0065055	0.212897019	302.365422	1.839196132	307.9749223	0.22412948	302.3320784	1.965720888	307.6506328	0.189251291
16:30	301.4029708	1.733290037	307.8007763	0.201434615	302.0734792	1.835209575	307.7619833	0.202096381	302.0507829	1.95841113	307.4774826	0.166373639
16:45	301.0449757	1.729767473	307.5397518	0.179541501	301.6944335	1.83147988	307.5176801	0.174096635	301.6624367	1.95246276	307.2530697	0.139427836
17:00	300.7173642	1.726916204	307.3692714	0.168276606	301.3475581	1.828460952	307.3588016	0.160252042	301.3067915	1.947920217	307.0941262	0.132486112
17:15	300.3127237	1.724774111	307.1684507	0.154810121	300.9191243	1.826192902	307.1544967	0.150580282	300.8556228	1.94452112	306.9171048	0.125422308
17:30	299.9484504	1.723072385	306.9890908	0.143175503	300.5334313	1.824391112	306.9532787	0.142785972	300.4694528	1.942044859	306.7672347	0.118631048
17:45	299.5357149	1.721717984	306.806081	0.137130809	300.0964264	1.822957071	306.7502062	0.137234768	300.0130631	1.940364095	306.6083767	0.115415696
18:00	299.2635971	1.721717984	306.6412441	0.137130809	299.8083078	1.822957071	306.5761016	0.137234768	299.7339106	1.939321917	306.4639332	0.115415696
Average	**300.4351054**	**1.711809024**	**306.100249**	**0.249398103**	**301.0370562**	**1.809997428**	**306.1081859**	**0.254185384**	**300.9640765**	**1.94872539**	**306.206065**	**0.257342057**
Max	302.7683512	1.79914764	308.7450521	0.335690781	303.5191456	1.848672475	308.8948491	0.324131754	303.5305759	1.986825236	309.7158351	0.497410193
Min	296.5385723	1.686181962	300.7006279	0.137130809	296.9230482	1.784083916	300.7694399	0.120113174	296.6560786	1.921783877	301.0389317	0.108328869
Standard Deviation	**2.152847821**	**0.024554336**	**2.309846577**	**0.0610474**	**2.294721983**	**0.022547224**	**2.338977039**	**0.063675431**	**2.395971641**	**0.019574026**	**2.291181705**	**0.097392635**
Skyview Factor	83.53156%				81.25680%				84.87290%			

Table C.3 Simulation results for Bastakiyah, Orthogonal and Volume Ortho in December with initial wind speeds of 3.6m/s and 0.1m/s

Configuration	Bastakiyah - 3.6 m/s		Bastakiyah - wind 0.1 m/s		Ortho - 3.6 m/s		Ortho - wind 0.1 m/s		Volume Ortho - 3.6 m/s		Volume Ortho - wind 0.1 m/s	
Time of Day	B Avg Temp (K)	B Avg Wind Speed	B Avg Temp (K)	B Avg Wind Speed	O Avg Temp (K)	O Avg Wind Speed (m/s)	O Avg Temp (K)	O Avg Wind Speed (m/s)	VO Avg Temp (K)	VO Avg Wind Speed	VO Avg Temp (K)	VO Avg Wind Speed
6:00	297.471831	1.79914764	300.7006279	0.15130987	297.453228	1.784083916	300.7694399	0.147185539	296.7392594	1.944007007	302.1773369	0.190942255
6:15	297.2716953	1.800037519	301.6348687	0.165647267	297.1178953	1.785331488	301.5414859	0.269303119	296.7103969	1.944128437	302.4800021	0.187381996
6:30	297.1513905	1.801081804	303.6168782	0.33397228	296.9894791	1.786722319	303.7646341	0.267916442	296.6805979	1.944193871	301.9451093	0.163635533
6:45	297.0862517	1.802278138	303.1621492	0.207365451	296.9217057	1.788209622	303.029464	0.22039869	296.6517891	1.944308884	301.8357028	0.32003603
7:00	297.0348263	1.803509371	303.2221611	0.33746033	296.8683262	1.78980465	303.2435101	0.319923663	296.6237	1.944463166	301.6787831	0.21671872
7:15	296.9933163	1.804674745	303.0360658	0.181271838	296.8254282	1.791458469	303.0155833	0.129480032	296.5965469	1.944606096	301.9047	0.6202
7:30	296.9579918	1.805743906	302.9805091	0.322047927	296.7891715	1.793012194	302.607986	0.34654762	296.5707662	1.944722544	301.83	0.215
7:45	296.9360265	1.806723472	302.7529917	0.17262778	296.7670255	1.794424526	302.9596915	0.120981812	296.5607938	1.944813593	300.8686014	0.139663944
8:00	296.9803242	1.807640793	302.6437276	0.225464322	296.8139241	1.79570056	302.3158839	0.186623074	296.626339	1.944838475	300.8176914	0.382055137
8:15	297.1209139	1.80837556	302.3754823	0.172242057	296.9620824	1.796870523	302.484018	0.199039045	296.8014085	1.944711657	300.9105158	0.182029377
8:30	297.2792076	1.80884609	302.3750633	0.231380558	297.1293936	1.797835616	302.2018238	0.131967863	296.9768445	1.944361255	300.5757268	0.191342584
8:45	297.5042734	1.809059476	302.1493776	0.130024028	297.3672696	1.798542439	302.1222849	0.26523864	297.2351981	1.943753555	300.6816832	0.184085201
9:00	297.7153052	1.809043807	302.0864489	0.191800102	297.5914209	1.799017802	301.9155331	0.196619576	297.4682372	1.942895302	300.5574589	0.14416924
9:15	297.9792895	1.808806766	302.1621737	0.174422477	297.8725975	1.799248847	302.1754011	0.194064849	297.775717	1.942038959	300.8306097	0.219551217
9:30	298.2212742	1.808344309	302.2834256	0.166022564	298.129815	1.799243675	302.1406129	0.212030843	298.0378786	1.941198455	300.8159517	0.20702816
9:45	298.5080652	1.807652163	302.4429992	0.180590611	298.4376101	1.799005459	302.2453094	0.210647025	298.3592728	1.939690574	300.8575888	0.252358327
10:00	298.7576465	1.806773287	302.2835922	0.1930226	298.7053994	1.798569432	302.1909191	0.215405943	298.6287167	1.938191592	300.6645187	0.288306229
10:15	299.0432048	1.805740177	302.3295731	0.203149746	299.0119085	1.797962413	302.3246053	0.229946367	298.9409663	1.936444678	300.8037452	0.277168152
10:30	299.2997306	1.804562992	302.5647619	0.235714253	299.2914612	1.79720544	302.5665151	0.253703296	299.218425	1.934343461	301.1812895	0.265676401
10:45	299.5621803	1.803252787	302.8221995	0.242666066	299.5731621	1.796315591	302.8536812	0.268637621	299.5007793	1.93226266	301.6274036	0.261172205
11:00	299.8020428	1.801853065	303.1531825	0.257108666	299.8231187	1.795411476	303.0953654	0.256990267	299.7643793	1.93039313	301.8914174	0.237805134
11:15	299.9	1.8	303.2525141	0.23447916	300.0617228	1.794536467	303.5141407	0.261511381	300.0168329	1.928682483	302.3110909	0.255850136
11:30	300.2342142	1.799218662	303.745962	0.265148139	300.249394	1.793692124	303.7335548	0.258018045	300.2096522	1.927000266	302.5396977	0.251268561
11:45	300.4350956	1.798027027	303.7469292	0.238018471	300.4450754	1.792879257	304.0514479	0.257251555	300.4173885	1.925394748	302.8429185	0.251941304
12:00	300.5933638	1.796887608	304.1166041	0.239422866	300.6043548	1.792102695	304.3150898	0.256673269	300.5834843	1.923880797	303.0801788	0.251691669
12:15	300.7385348	1.795804078	304.3571932	0.242456662	300.7495193	1.791373842	304.5579128	0.256030704	300.7365847	1.922488719	303.3139154	0.249698687
12:30	300.8551682	1.794797777	304.5522334	0.244385281	300.8514975	1.79071417	304.7499216	0.255518596	300.8311124	1.921255491	303.5040506	0.244601884
12:45	300.9590043	1.793881717	304.7252736	0.244650185	300.9582038	1.790126535	304.9339038	0.255125602	300.9465408	1.920168996	303.7099918	0.238156738
13:00	301.0356895	1.793064008	304.8842909	0.244472522	301.0353057	1.789613921	305.096704	0.254611428	301.0340479	1.91921897	303.9068481	0.228437214
13:15	301.0668185	1.792366595	304.9974448	0.244114779	301.0576125	1.789200563	305.2041628	0.253889341	301.0462151	1.91843547	304.0414452	0.211962801
13:30	301.0867018	1.791801843	305.1007151	0.243547858	301.0750132	1.788900399	305.3043998	0.252992016	301.06473	1.917837155	304.1576958	0.205610308
13:45	301.0781634	1.791370649	305.1617883	0.242661152	301.065082	1.788714683	305.3575837	0.251823919	301.0509328	1.917413885	304.2405969	0.204394155
14:00	301.0603541	1.791065086	305.2163178	0.24152435	301.0434826	1.788639911	305.4063139	0.250443365	301.0338998	1.917147537	304.3084411	0.20342098
14:15	300.9935965	1.790892299	305.2078786	0.23990938	300.9728965	1.78868353	305.3879965	0.248683331	300.9529313	1.917038852	304.301142	0.201544343
14:30	300.9185251	1.790860363	305.2035295	0.236040679	300.8927742	1.788854832	305.3749673	0.246621313	300.8635605	1.917105646	304.30213	0.196606221
14:45	300.7949616	1.790975769	305.1473765	0.225221659	300.7651545	1.789159532	305.2950019	0.239358823	300.7146568	1.917340176	304.2413447	0.183873234
15:00	300.6724473	1.791238911	305.1219045	0.216320846	300.6367694	1.789599639	305.2481074	0.23202539	300.5905694	1.917740629	304.2281252	0.168464335
15:15	300.4995852	1.791649456	305.0315319	0.199664561	300.4570316	1.790176913	305.1312228	0.214960582	300.4087172	1.918294391	304.1573273	0.146806387
15:30	300.3325134	1.792208804	304.9780195	0.18591831	300.2830649	1.790893781	305.0602614	0.198288044	300.2404612	1.919002703	304.1207525	0.130958818
15:45	300.1143505	1.792917425	304.8582747	0.171747491	300.0593456	1.791750191	304.9231073	0.18316173	300.0186236	1.919849144	304.011322	0.115155392
16:00	299.9059057	1.793774754	304.7559557	0.162814755	299.8410083	1.792747386	304.8082169	0.176433645	299.796515	1.920834529	303.9158831	0.105602965
16:15	299.6401777	1.794789708	304.6467446	0.156182909	299.563335	1.793894708	304.688206	0.173037972	299.5092507	1.921967783	303.8239814	0.103369361
16:30	299.3910391	1.795963823	304.5445244	0.153902217	299.3012854	1.795194041	304.5767676	0.169465115	299.2461473	1.923305904	303.753163	0.101154193
16:45	299.0920114	1.797291976	304.4105419	0.146851993	298.9873349	1.796644058	304.4324868	0.16090557	298.9143976	1.924838339	303.6482597	0.098992982
17:00	298.8191365	1.798757382	304.2932867	0.144678279	298.6990433	1.798231817	304.302139	0.159466541	298.6158605	1.926377526	303.5477098	0.097022835
17:15	298.6067607	1.800304108	304.1814426	0.142599462	298.4759423	1.799910166	304.172668	0.158180728	298.3876501	1.928078223	303.4481423	0.095290275
17:30	298.4534762	1.801851138	304.0688387	0.140651314	298.3163186	1.801603065	304.0416192	0.157095025	298.22694	1.929770685	303.3447904	0.093804743
17:45	298.3279752	1.803335302	303.9526971	0.111307743	298.1864131	1.803250147	303.9063066	0.154726608	298.0970028	1.931474613	303.2370654	0.092561185
18:00	298.2215842	1.803335302	303.7991833	0.111307743	298.0764698	1.803250147	303.7547543	0.154726608	297.9863143	1.933166828	303.1266616	0.091561927
Average	**299.1531417**	**1.79962407**	**303.6905562**	**0.207047175**	**299.0847321**	**1.793639081**	**303.7325043**	**0.219054644**	**298.9797762**	**1.930519956**	**302.6551124**	**0.203390397**
Max	301.0867018	1.809059476	305.2163178	0.33746033	301.0750132	1.803250147	305.4063139	0.34654762	301.06473	1.944838475	304.3084411	0.6202
Min	296.9360265	1.790860363	300.7006279	0.111307743	296.7670255	1.784083916	300.7694399	0.120981812	296.5607938	1.917038852	300.5574589	0.091561927
Standard Deviation	**1.482349968**	**0.0062063**	**1.181079434**	**0.052479555**	**1.541881557**	**0.004713176**	**1.269681267**	**0.050162186**	**1.631248831**	**0.010624374**	**1.329795453**	**0.089898598**
Skyview Factor	83.53156%				81.25680%				84.87290%			

Appendix D

Tabulated simulation results for the three seasons per configuration showing the daily temperature and wind speed including average, maximum, minimum temperature and standard deviations.

Table D.1 Simulation results for Bastakiyah in June, September, and December with initial wind speed of 3.6 m/s

21st of	June		Sept/ March		December	
Time of Day	J Avg Temp (K)	J Avg Wind Speed (m/s)	S Avg Temp (K)	S Avg Wind Speed (m/s)	D Avg Temp (K)	D Avg Wind Speed (m/s)
6:00	296.8963105	1.807680579	297.471831	1.79914764	297.471831	1.79914764
6:15	296.8952671	1.808544455	296.7225984	1.686181962	297.2716953	1.800037519
6:30	296.973612	1.809246472	296.6013139	1.687495552	297.1513905	1.801081804
6:45	297.1652964	1.809731711	296.5385723	1.688900036	297.0862517	1.802278138
7:00	297.3753844	1.80999223	296.5656705	1.690380206	297.0348263	1.803509371
7:15	297.6717068	1.809999668	296.7265998	1.691803561	296.9933163	1.804674745
7:30	297.9588885	1.809164068	296.9161347	1.692914814	296.9579918	1.805743906
7:45	298.3209198	1.809164068	297.1920899	1.693747586	296.9360265	1.806723472
8:00	298.6600029	1.808281648	297.4615886	1.694279076	296.9803242	1.807640793
8:15	299.0586458	1.807099041	297.8022779	1.694487068	297.1209139	1.80837556
8:30	299.4296277	1.805669194	298.1185773	1.694405079	297.2792076	1.80884609
8:45	299.8483756	1.804022211	298.4942624	1.694067748	297.5042734	1.809059476
9:00	300.2307615	1.802135708	298.8299769	1.693410764	297.7153052	1.809043807
9:15	300.6379612	1.800204831	299.3191974	1.692686315	297.9792895	1.808806766
9:30	301.0106784	1.79825098	299.5866992	1.691718092	298.2212742	1.808344309
9:45	301.3977577	1.796608807	299.9608751	1.690724565	298.5080652	1.807652163
10:00	301.6951281	1.795771166	300.3125765	1.68957965	298.7576465	1.806773287
10:15	301.9999821	1.795921441	300.6641652	1.688368136	299.0432048	1.805740177
10:30	302.2850682	1.797017883	300.9342358	1.687492236	299.2997306	1.804562992
10:45	302.5719471	1.799021641	301.1957652	1.687308042	299.5621803	1.803252787
11:00	302.8105201	1.802022226	301.4437172	1.687887372	299.8020428	1.801853065
11:15	303.0473606	1.806124019	301.6757801	1.68922392	299.9	1.8
11:30	303.2701335	1.811140894	301.8730717	1.691182109	300.2342142	1.799218662
11:45	303.5124052	1.816685281	302.0952793	1.693720568	300.4350956	1.798027027
12:00	303.6942049	1.823029369	302.2569515	1.696834053	300.5933638	1.796887608
12:15	303.887986	1.83037562	302.3645633	1.700488791	300.7385348	1.795804078
12:30	304.0522345	1.838230809	302.4739664	1.704589544	300.8551682	1.794797777
12:45	304.1871242	1.846314184	302.5774975	1.70891508	300.9590043	1.793881717
13:00	304.3162708	1.854439305	302.6465379	1.71357801	301.0356895	1.793064008
13:15	304.4013401	1.862454042	302.6952882	1.718512102	301.0668185	1.792366595
13:30	304.4957203	1.870178323	302.7131459	1.723723104	301.0867018	1.791801843
13:45	304.5757913	1.87752061	302.7339059	1.728566505	301.0781634	1.791370649
14:00	304.6343508	1.884434418	302.7683512	1.732843386	301.0603541	1.791065086
14:15	304.6626768	1.890849919	302.7479952	1.736635302	300.9935965	1.790892299
14:30	304.7152296	1.896698614	302.7398256	1.740018017	300.9185251	1.790860363
14:45	304.7045073	1.901911519	302.6492764	1.742860223	300.7949616	1.790975769
15:00	304.7102706	1.906431209	302.595174	1.744949459	300.6724473	1.791238911
15:15	304.6619524	1.910264979	302.4710072	1.746005267	300.4995852	1.791649456
15:30	304.6163759	1.913448793	302.3595185	1.745793499	300.3325134	1.792208804
15:45	304.5127893	1.915939425	302.1531485	1.744025405	300.1143505	1.792917425
16:00	304.4322814	1.917708505	301.9666589	1.740880955	299.9059057	1.793774754
16:15	304.2512096	1.918624497	301.6787004	1.737055198	299.6401777	1.794789708
16:30	304.100562	1.918500863	301.4029708	1.733290037	299.3910391	1.795963823
16:45	303.8563085	1.917015606	301.0449757	1.729767473	299.0920114	1.797291976
17:00	303.633852	1.913928855	300.7173642	1.726916204	298.8191365	1.798757382
17:15	303.2919938	1.909281616	300.3127237	1.724774111	298.6067607	1.800304108
17:30	302.973239	1.903448342	299.9484504	1.723072385	298.4534762	1.801851138
17:45	302.5405662	1.89698388	299.5357149	1.721717984	298.3279752	1.803335302
18:00	302.1535077	1.890416478	299.2635971	1.721717984	298.2215842	1.803335302
Average	**302.0976752**	**1.847508776**	**300.4351054**	**1.711809024**	**299.1531417**	**1.79962407**
Max	304.7152296	1.918624497	302.7683512	1.79914764	301.0867018	1.809059476
Min	296.8952671	1.795771166	296.5385723	1.686181962	296.9360265	1.790860363
Standard Deviation	**2.637735836**	**0.047302453**	**2.152847821**	**0.024554336**	**1.482349968**	**0.0062063**
Skyview Factor	83.53156%					

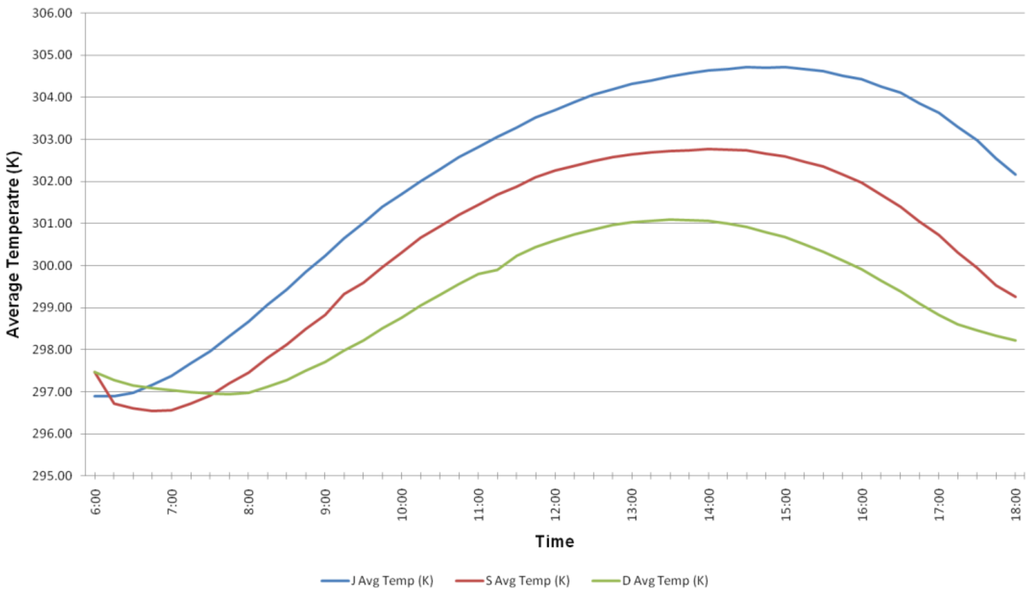

Figure D.1 Average temperature for Bastakiyah in three seasons

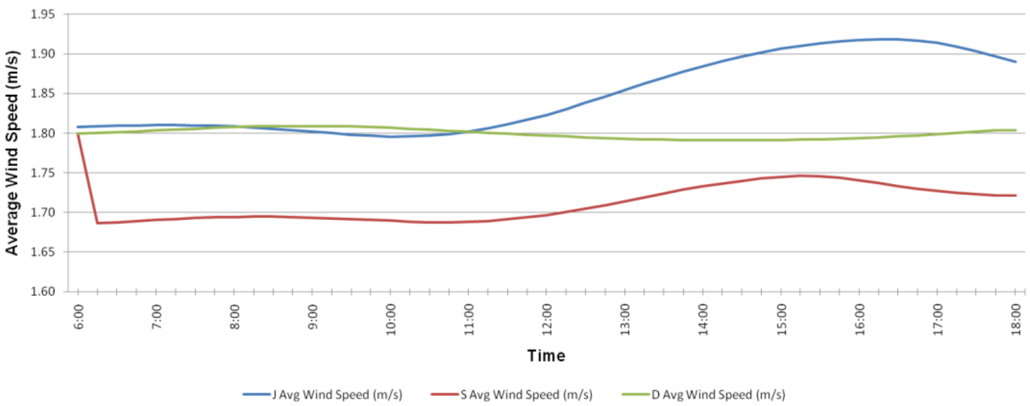

Figure D.2 Average wind speed for Bastakiyah in three seasons

Table D.2 Simulation results for Orthogonal in June, September, and December with initial wind speed of 3.6 m/s

21st of	June		Sept/ March		December	
Time of Day	J Avg Temp (K)	J Avg Wind Speed (m/s)	S Avg Temp (K)	S Avg Wind Speed (m/s)	D Avg Temp (K)	D Avg Wind Speed (m/s)
6:00	299.3056081	1.819044745	297.453228	1.784083916	297.453228	1.784083916
6:15	299.3127286	1.819991204	297.1178953	1.785331488	297.1178953	1.785331488
6:30	299.3988499	1.820858763	296.9894791	1.786722319	296.9894791	1.786722319
6:45	299.6025073	1.821583587	296.9230482	1.788209388	296.9217057	1.788209622
7:00	299.8234537	1.822114996	296.9517398	1.789776593	296.8683262	1.78980465
7:15	300.1287664	1.822381797	297.1221319	1.791283644	296.8254282	1.791458469
7:30	300.4234425	1.822341952	297.3228118	1.79246024	296.7891715	1.793012194
7:45	300.7907408	1.821991814	297.6149934	1.79334198	296.7670255	1.794424526
8:00	301.1402614	1.821455692	297.900339	1.793904722	296.8139241	1.79570056
8:15	301.5445328	1.820761945	298.2610612	1.794124944	296.9620824	1.796870523
8:30	301.9186082	1.81990954	298.5959594	1.794038134	297.1293936	1.797835616
8:45	302.3449293	1.818891191	298.9937353	1.793680968	297.3672696	1.798542439
9:00	302.7355399	1.81772965	299.3491901	1.792985352	297.5914209	1.799017802
9:15	303.1444895	1.816458934	299.7544799	1.792140905	297.8725975	1.799248847
9:30	303.5400096	1.815093361	300.1504086	1.791193149	298.129815	1.799243675
9:45	303.9783574	1.813649271	300.5465865	1.790141202	298.4376101	1.799005459
10:00	304.3367586	1.812098751	300.9189684	1.788928964	298.7053994	1.798569432
10:15	304.6891728	1.810488645	301.291231	1.787646212	299.0119085	1.797962413
10:30	305.0103532	1.809093187	301.577182	1.786718808	299.2914612	1.79720544
10:45	305.3163237	1.808317644	301.8540896	1.786523783	299.5731621	1.796315591
11:00	305.5876042	1.80831455	302.1166216	1.787137179	299.8231187	1.795411476
11:15	305.8625751	1.809006658	302.36233	1.788552317	300.0617228	1.794536467
11:30	306.1196183	1.810377764	302.5712226	1.790625649	300.249394	1.793692124
11:45	306.3881881	1.812417631	302.8064963	1.793313373	300.4450754	1.792879257
12:00	306.6046162	1.815016128	302.9776749	1.796609935	300.6043548	1.792102695
12:15	306.8325713	1.818202072	303.0916145	1.800479576	300.7495193	1.791373842
12:30	307.0261975	1.821977008	303.2074506	1.804821458	300.8514975	1.79071417
12:45	307.1914198	1.826220829	303.3170695	1.809401341	300.9582038	1.790126535
13:00	307.3508158	1.830779655	303.3901696	1.814338456	301.0353057	1.789613921
13:15	307.4545658	1.835665232	303.4417864	1.819562679	301.0576125	1.789200563
13:30	307.5470298	1.840885048	303.4606942	1.825080095	301.0750132	1.788900399
13:45	307.63771	1.846167737	303.4826749	1.830208294	301.065082	1.788714683
14:00	307.7103897	1.8514769	303.5191456	1.83473666	301.0434826	1.788639911
14:15	307.7452273	1.856722398	303.4975926	1.838751545	300.9728965	1.78868353
14:30	307.8043285	1.861649518	303.4889427	1.842333168	300.8927742	1.788854832
14:45	307.7900266	1.866146329	303.393069	1.845342499	300.7651545	1.789159532
15:00	307.7908196	1.870116938	303.3357854	1.847554585	300.6367694	1.789599639
15:15	307.7505541	1.873433323	303.2043174	1.848672475	300.4570316	1.790176913
15:30	307.7025838	1.875966241	303.086273	1.848448256	300.2830649	1.790893781
15:45	307.6032813	1.877580582	302.8677683	1.846576195	300.0593456	1.791750191
16:00	307.5258346	1.878204561	302.6703128	1.843246848	299.8410083	1.792747386
16:15	307.3367503	1.877594499	302.365422	1.839196132	299.563335	1.793894708
16:30	307.1715087	1.875403995	302.0734792	1.835209575	299.3012854	1.795194041
16:45	306.8928732	1.871538931	301.6944335	1.83147988	298.9873349	1.796644058
17:00	306.6281948	1.866950982	301.3475581	1.828460952	298.6990433	1.798231817
17:15	306.2457617	1.861820202	300.9191243	1.826192902	298.4759423	1.799910166
17:30	305.8890217	1.857110166	300.5334313	1.824391112	298.3163186	1.801603065
17:45	305.4238799	1.853237504	300.0964264	1.822957071	298.1864131	1.803250147
18:00	305.009191	1.850157571	299.8083078	1.822957071	298.0764698	1.803250147
Average	**304.9001749**	**1.835804033**	**301.0370562**	**1.809997428**	**299.0847321**	**1.793639081**
Max	307.8043285	1.878204561	303.5191456	1.848672475	301.0750132	1.803250147
Min	299.3056081	1.80831455	296.9230482	1.784083916	296.7670255	1.784083916
Standard Deviation	**2.883598639**	**0.024166844**	**2.294721983**	**0.022547224**	**1.541881557**	**0.004713176**
Skyview Factor	81.25680%					

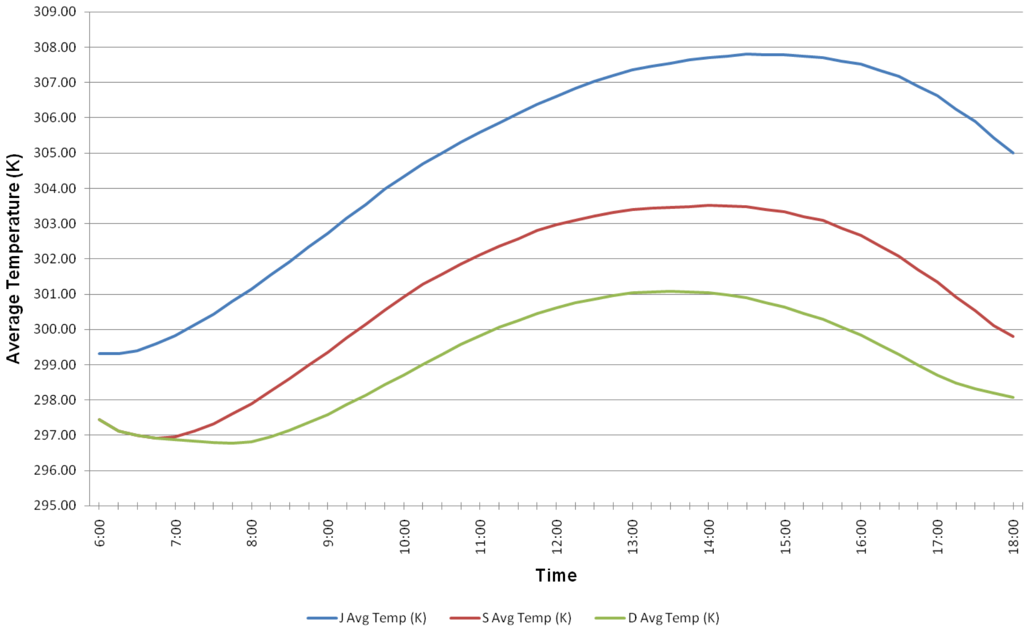

Figure D.3 Average temperature for Orthogonal in three seasons

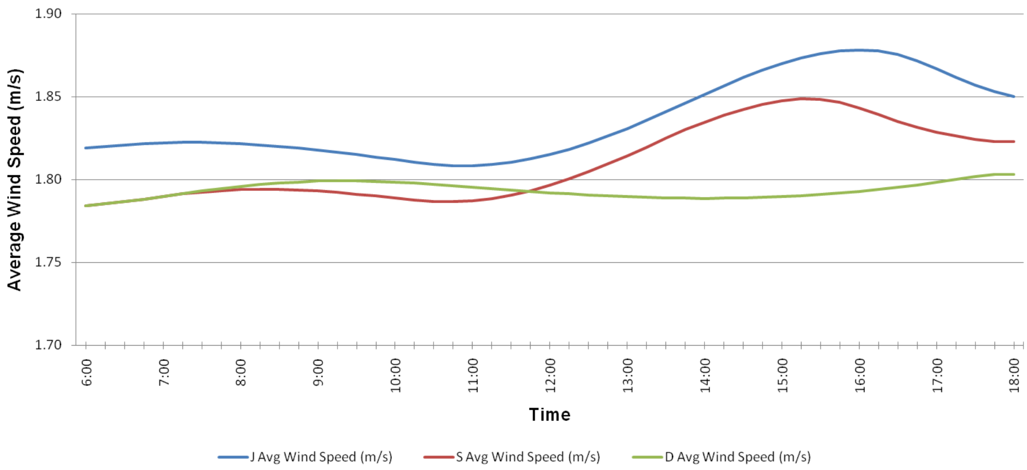

Figure D.4 Average wind speed for Orthogonal in three seasons

Table D.3 Simulation results for Volume Ortho in June, September, and December with initial wind speed of 3.6 m/s

21st of	June		Sept/ March		December	
Time of Day	J Avg Temp (K)	J Ag Wind Speed (m/s)	S Avg Temp (K)	S Avg Wind Speed (m/s)	D Avg Temp (K)	D Avg Wind Speed (m/s)
6:00	296.7392594	1.944007007	296.7392594	1.944007007	296.7392594	1.944007007
6:15	296.7479032	1.944116972	296.7103969	1.944128437	296.7103969	1.944128437
6:30	296.8463893	1.944085599	296.6805979	1.944193871	296.6805979	1.944193871
6:45	297.0809756	1.943893159	296.6560786	1.944307759	296.6517891	1.944308884
7:00	297.3175632	1.943444221	296.7254615	1.94440957	296.6237	1.944463166
7:15	297.6493087	1.942996685	296.9388016	1.944338383	296.5965469	1.944606096
7:30	297.9685608	1.941790187	297.156411	1.944052191	296.5707662	1.944722544
7:45	298.3616656	1.940596301	297.4792462	1.94337604	296.5607938	1.944813593
8:00	298.7235925	1.939052128	297.7642218	1.942710566	296.626339	1.944838475
8:15	299.1605926	1.937537764	298.1420943	1.942056373	296.8014085	1.944711657
8:30	299.5306924	1.935369321	298.4794413	1.940364025	296.9768445	1.944361255
8:45	299.9789967	1.933095623	298.9017036	1.938397584	297.2351981	1.943753555
9:00	300.3834654	1.930605882	299.2575475	1.936455996	297.4682372	1.942895302
9:15	300.8096153	1.92787282	299.6879909	1.934063645	297.775717	1.942038959
9:30	301.2020862	1.925188586	300.0909089	1.931697267	298.0378786	1.941198455
9:45	301.596523	1.923131612	300.5073285	1.929354278	298.3592728	1.939690574
10:00	301.8896819	1.922286657	300.8895369	1.926801254	298.6287167	1.938191592
10:15	302.2021055	1.922715651	301.2719284	1.924328614	298.9409663	1.936444678
10:30	302.5008453	1.924326007	301.559017	1.922516636	299.218425	1.934343461
10:45	302.7862304	1.927148053	301.8413093	1.921783877	299.5007793	1.93226266
11:00	303.2474546	1.936682029	302.115941	1.922112	299.7643793	1.93039313
11:15	303.2474546	1.936682029	302.3691972	1.923475509	300.0168329	1.928682483
11:30	303.4688242	1.942799015	302.5763518	1.925748613	300.2096522	1.927000266
11:45	303.7213024	1.95033509	302.817251	1.928901586	300.4173885	1.925394748
12:00	303.9009165	1.95881106	302.9912882	1.932729643	300.5834843	1.923880797
12:15	304.0725848	1.967839427	303.1000734	1.937324041	300.7365847	1.922488719
12:30	304.2257725	1.977195025	303.2191128	1.94257417	300.8311124	1.921255491
12:45	304.3656102	1.986687358	303.3229042	1.94865801	300.9465408	1.920168996
13:00	304.501921	1.996096511	303.4041556	1.954928286	301.0340479	1.91921897
13:15	304.5938559	2.005121452	303.4590005	1.961095191	301.0462151	1.91843547
13:30	304.6975526	2.013497559	303.4730456	1.96692722	301.06473	1.917837155
13:45	304.7850923	2.021158335	303.4787382	1.972131262	301.0509328	1.917413885
14:00	304.8270521	2.028125966	303.5305759	1.976549712	301.0338998	1.917147537
14:15	304.8637369	2.034370593	303.5117991	1.980272223	300.9529313	1.917038852
14:30	304.9260698	2.039864866	303.5015128	1.983401365	300.8635605	1.917105646
14:45	304.9005323	2.044556627	303.386601	1.985695881	300.7146568	1.917340176
15:00	304.9054483	2.048407999	303.3284925	1.986825236	300.5905694	1.917740629
15:15	304.8512223	2.051454053	303.2001467	1.986469708	300.4087172	1.918294391
15:30	304.7851954	2.053790135	303.0747304	1.984360075	300.2404612	1.919002703
15:45	304.6623025	2.055395357	302.8375836	1.9799311	300.0186236	1.919849144
16:00	304.5809087	2.056251036	302.6378277	1.97332292	299.796515	1.920834529
16:15	304.3594726	2.056181502	302.3320784	1.965720888	299.5092507	1.921967783
16:30	304.1774294	2.054971946	302.0507829	1.95841113	299.2461473	1.923305904
16:45	303.9074851	2.052256524	301.6624367	1.95246276	298.9143976	1.924838339
17:00	303.6524566	2.047769144	301.3067915	1.947920217	298.6158605	1.926377526
17:15	303.2430635	2.041424292	300.8556228	1.94452112	298.3876501	1.928078223
17:30	302.9024983	2.033477969	300.4694528	1.942044859	298.22694	1.929770685
17:45	302.4392231	2.024560813	300.0130631	1.940364095	298.0970028	1.931474613
18:00	302.033826	2.015453821	299.7339106	1.939321917	297.9863143	1.933166828
Average	**302.2106595**	**1.982132199**	**300.9640765**	**1.94872539**	**298.9797762**	**1.930519956**
Max	304.9260698	2.056251036	303.5305759	1.986825236	301.06473	1.944838475
Min	296.7392594	1.922286657	296.6560786	1.921783877	296.5607938	1.917038852
Standard Deviation	**2.716102314**	**0.050720447**	**2.395971641**	**0.019574026**	**1.631248831**	**0.010624374**
Skyview Factor	84.87290%					

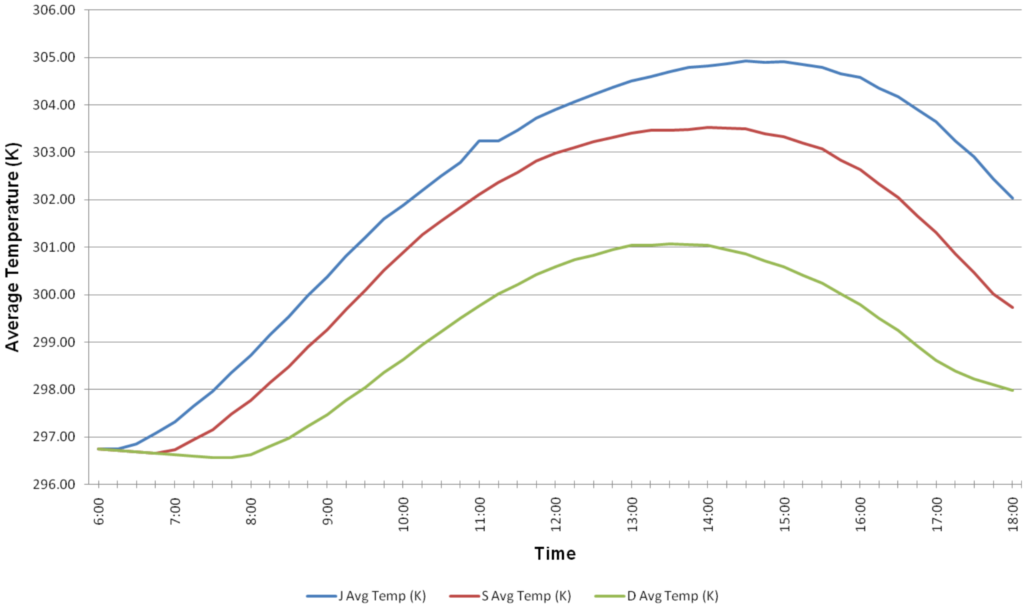

Figure D.5 Average temperature for Volume Ortho in three seasons

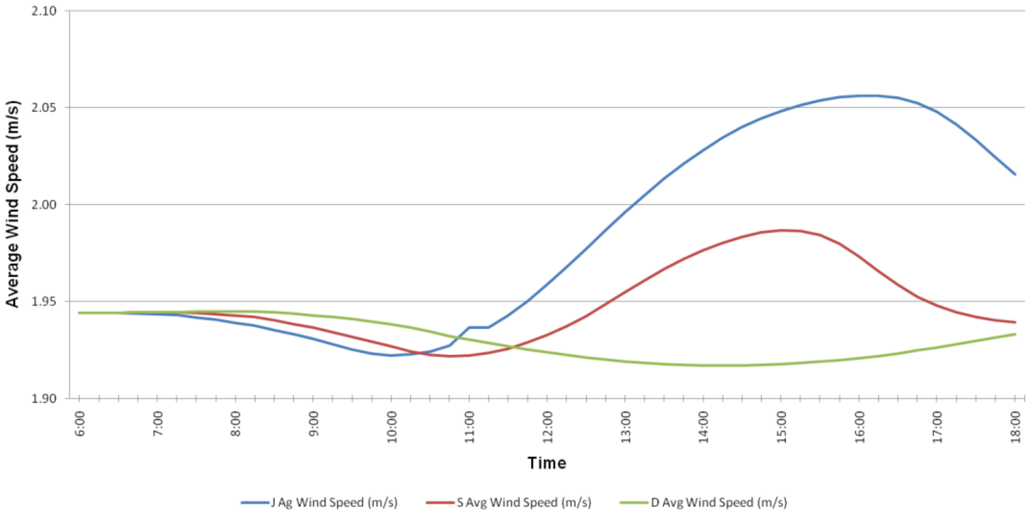

Figure D.6 Average wind speed for Volume Ortho in three seasons

Appendix E

Tabulated simulation results for three configurations in June from 10:00 – 16:00 with initial wind speed of 7.0 m/s showing the daily temperature and wind speed including average, maximum, minimum temperature and standard deviations.

Table E.1 Simulation results for Bastakiyah, Orthogonal, and Volume Ortho in June with initial wind speed 7.0 m/s from 10:00-16:00

Configuration	**Bastakiyah**		**Ortho**		**Volume Ortho**	
Time of Day	B Avg Temp (K)	B Avg Wind Speed	O Avg Temp (K)	O Avg Wind Speed	VO Avg Temp (K)	VO Avg Wind Speed
10:00	300.4421107	3.403869308	300.4447456	3.399065266	300.5383921	3.654255248
10:15	300.7333538	3.404285986	300.7416693	3.400136647	300.8400685	3.653200782
10:30	301.0183497	3.404628706	301.0387595	3.40112278	301.1484892	3.652239449
10:45	301.3108477	3.40490357	301.3404938	3.402022489	301.4506849	3.65134029
11:00	301.5742599	3.405099232	301.6153272	3.402826842	301.7098045	3.650503669
11:15	301.8560978	3.405281711	301.9046227	3.40362805	302.0073841	3.649942455
11:30	302.122131	3.405716613	302.1771995	3.40473003	302.2767711	3.649447146
11:45	302.412422	3.40689557	302.4634797	3.406595496	302.5906713	3.650340625
12:00	302.6412842	3.409194889	302.6887677	3.409475635	302.8278822	3.652489987
12:15	302.8933983	3.412539864	302.9431078	3.413244216	303.0593374	3.656574517
12:30	303.1150965	3.416668961	303.1601708	3.417682334	303.2768433	3.661439619
12:45	303.3208305	3.421343135	303.3605258	3.422578349	303.4932794	3.666625822
13:00	303.5217303	3.426489021	303.5578679	3.42790062	303.7000019	3.672347828
13:15	303.6638147	3.432017727	303.6949023	3.433740895	303.8464947	3.678801921
13:30	303.8071988	3.437982434	303.8288515	3.440006149	304.0081353	3.685833869
13:45	303.9529744	3.444531445	303.9656752	3.446353788	304.1597884	3.693215496
14:00	304.0822793	3.451263297	304.0830604	3.452701196	304.2716999	3.700512513
14:15	304.1777667	3.457653492	304.1647076	3.458967303	304.3770831	3.707327818
14:30	304.2973548	3.463587277	304.2802886	3.464926687	304.5077223	3.713535776
14:45	304.3478405	3.469221399	304.3169585	3.470650109	304.5450815	3.71924674
15:00	304.4127329	3.474739915	304.3571163	3.476258709	304.6137775	3.724630395
15:15	304.4187835	3.480177618	304.3519988	3.481679643	304.6166285	3.729792624
15:30	304.4196491	3.485302378	304.3263769	3.486614911	304.5993176	3.73450621
15:45	304.3607511	3.489674491	304.251448	3.490657425	304.5242561	3.738226593
16:00	304.3159276	3.489674491	304.1913371	3.490657425	304.4789176	3.738226593
Average	**303.0887594**	**3.4361097**	**303.0899783**	**3.4361689**	**303.2587405**	**3.6833842**
Max	304.4196491	3.4896745	304.3571163	3.4906574	304.6166285	3.7382266
Min	300.4421107	3.4038693	300.4447456	3.3990653	300.5383921	3.6494471
Standard Deviation	**1.3056830**	**0.0315593**	**1.2763265**	**0.0329332**	**1.3323140**	**0.0331827**

Appendix F

ENVI-met simulation snap shots of Bastakiyah, Orthogonal, and Volume Ortho configurations with initial wind speed of 3.6 m/s.

Note: Snapshots shown in 2 hour intervals from 06:00 -18:00 – remaining files are included in soft copy

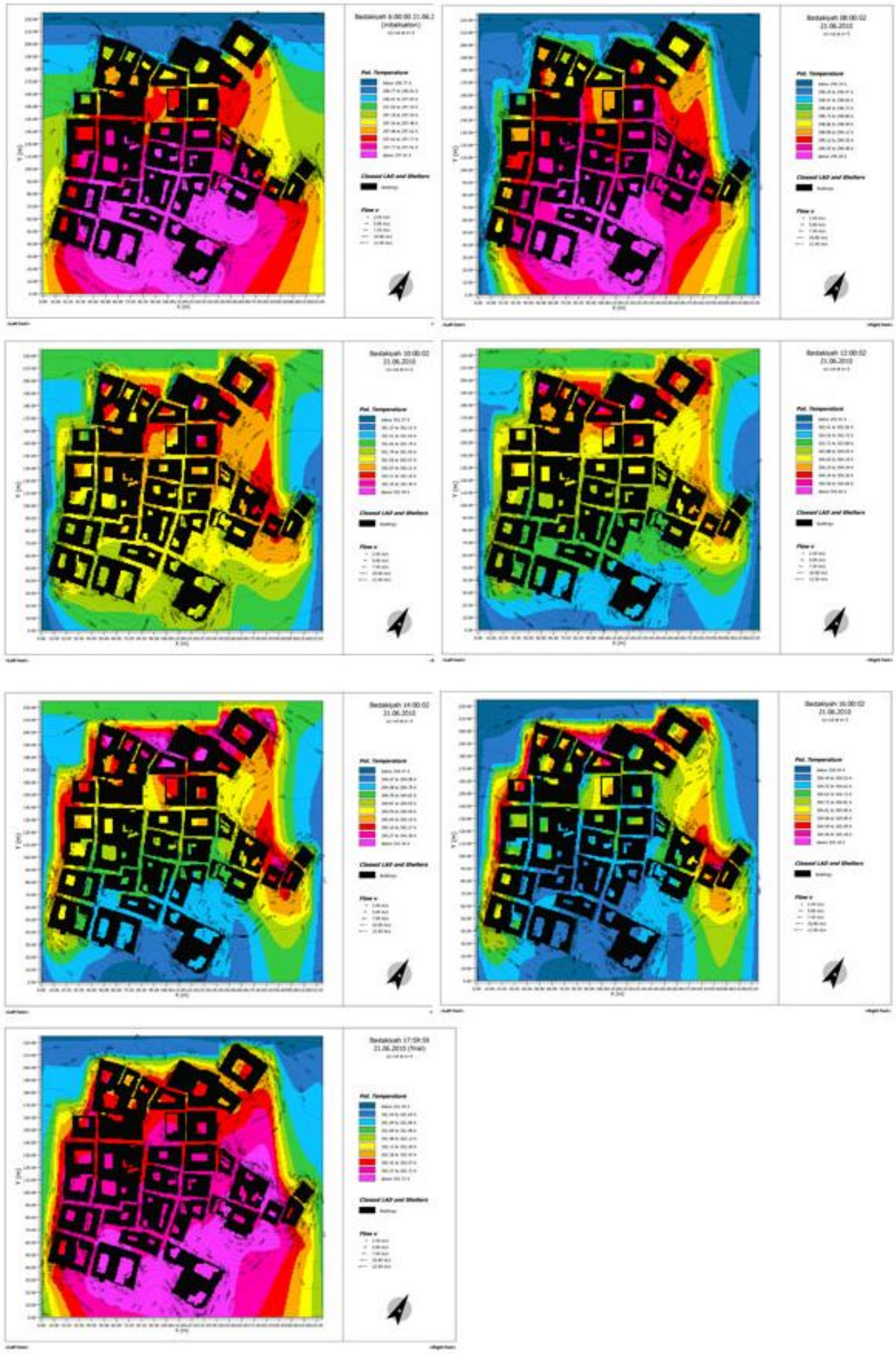

Figure F.1 Temperature gradient for Bastakiyah in June and initial wind speed 3.6m/s

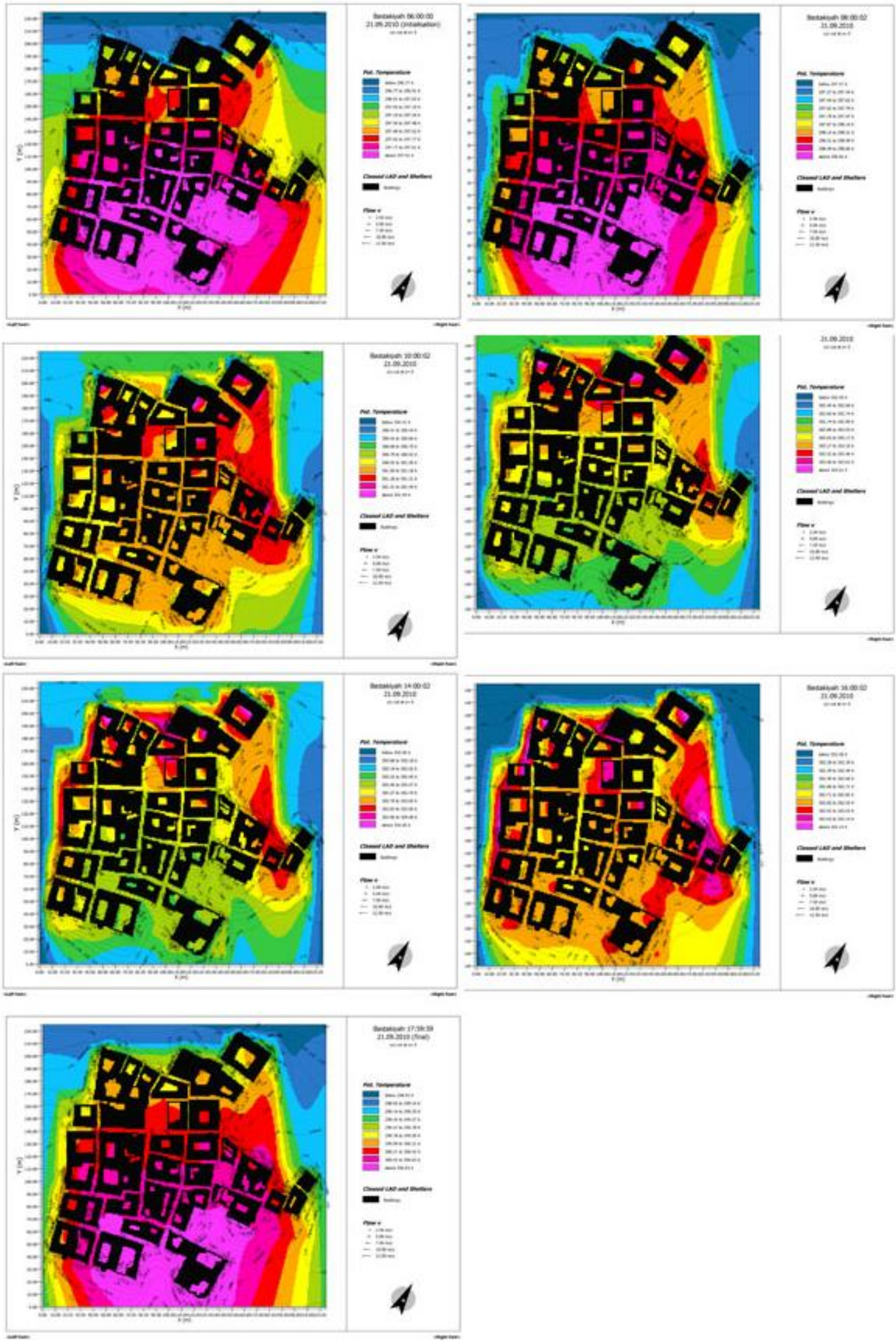

Figure F.2 Temperature gradient for Bastakiyah in September and initial wind speed 3.6m/s

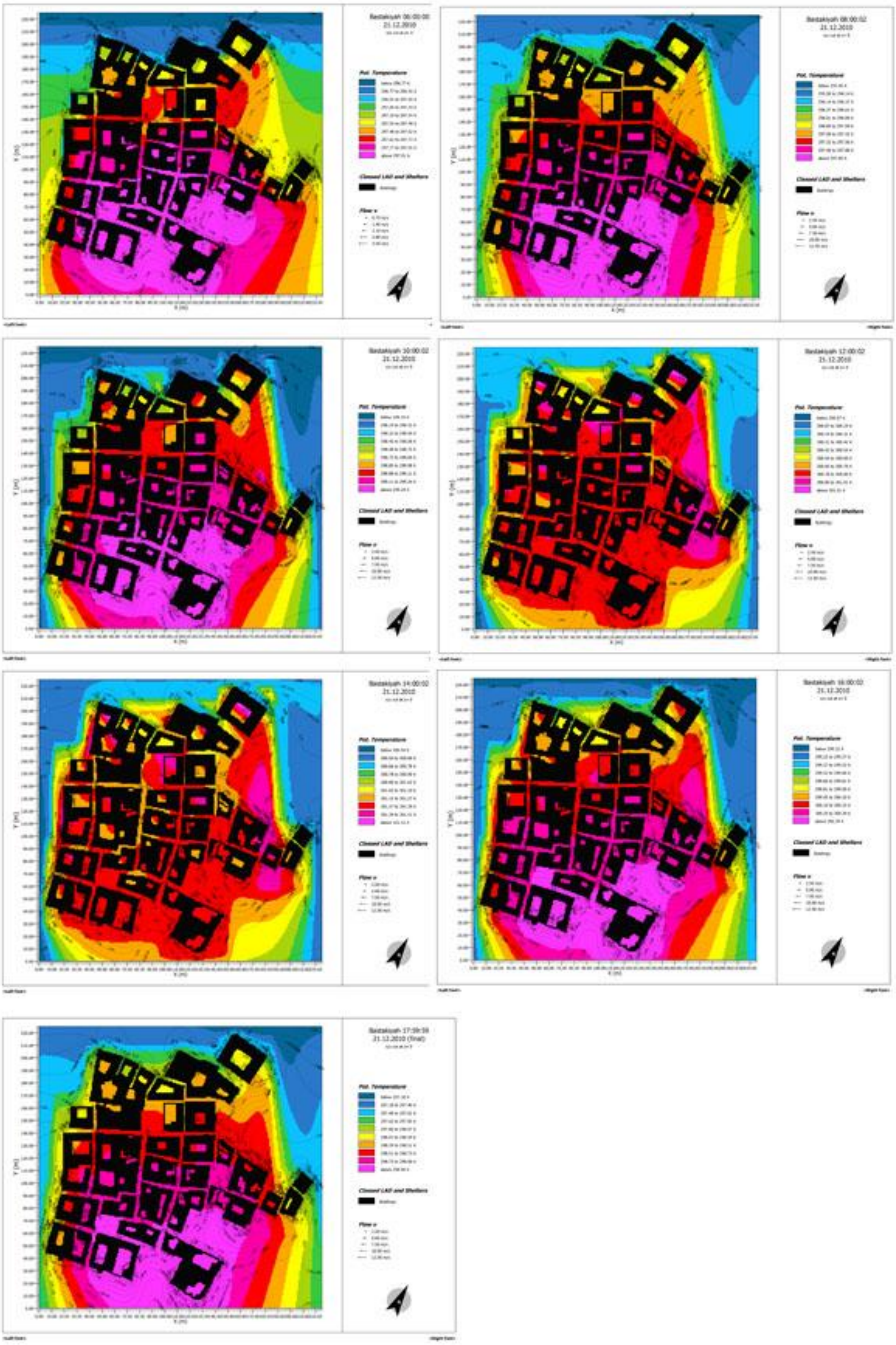

Figure F.3 Temperature gradient for Bastakiyah in December and initial wind speed 3.6m/s

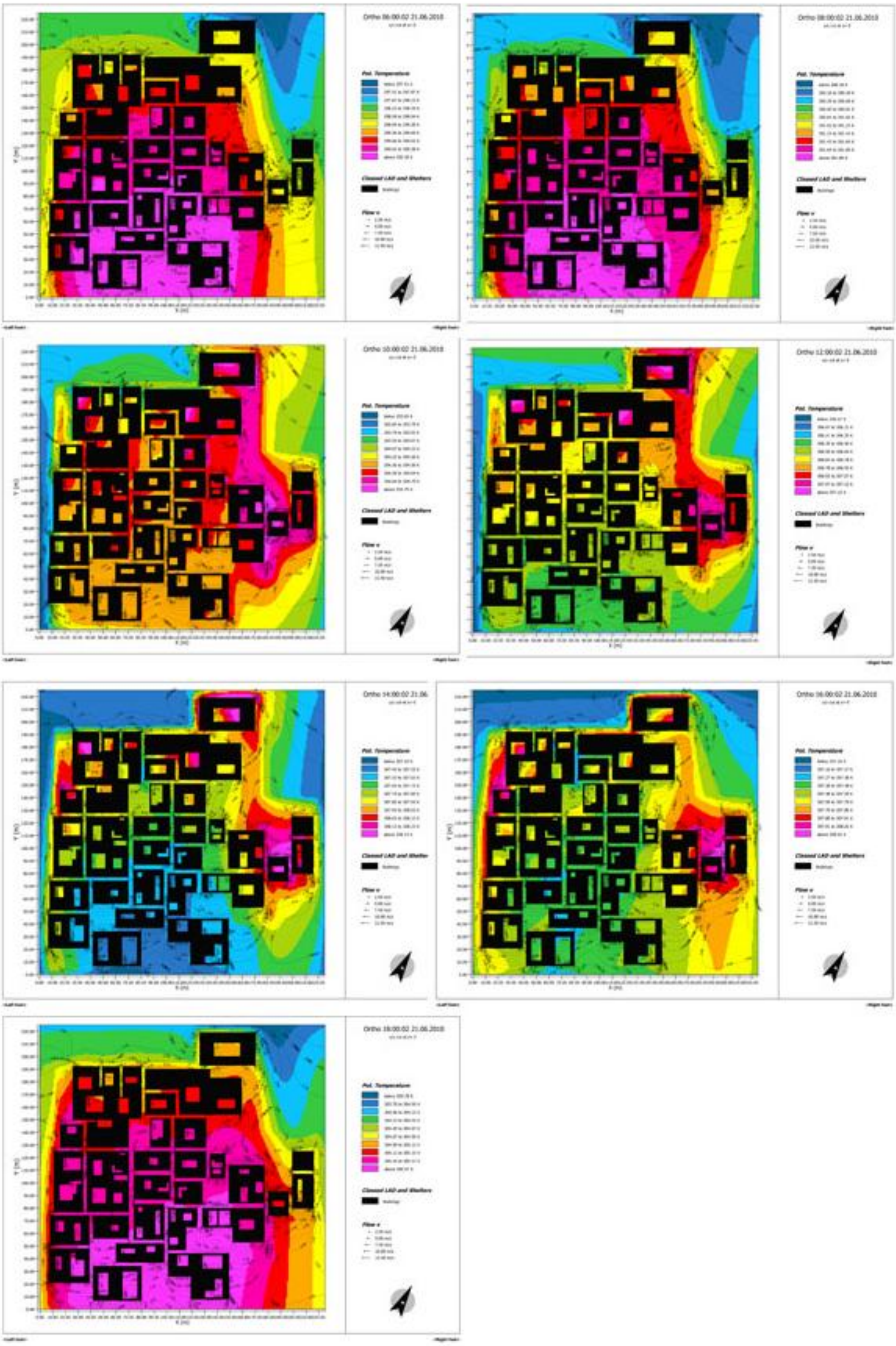

Figure F.4 Temperature gradient for Orthogonal in June and initial wind speed 3.6m/s

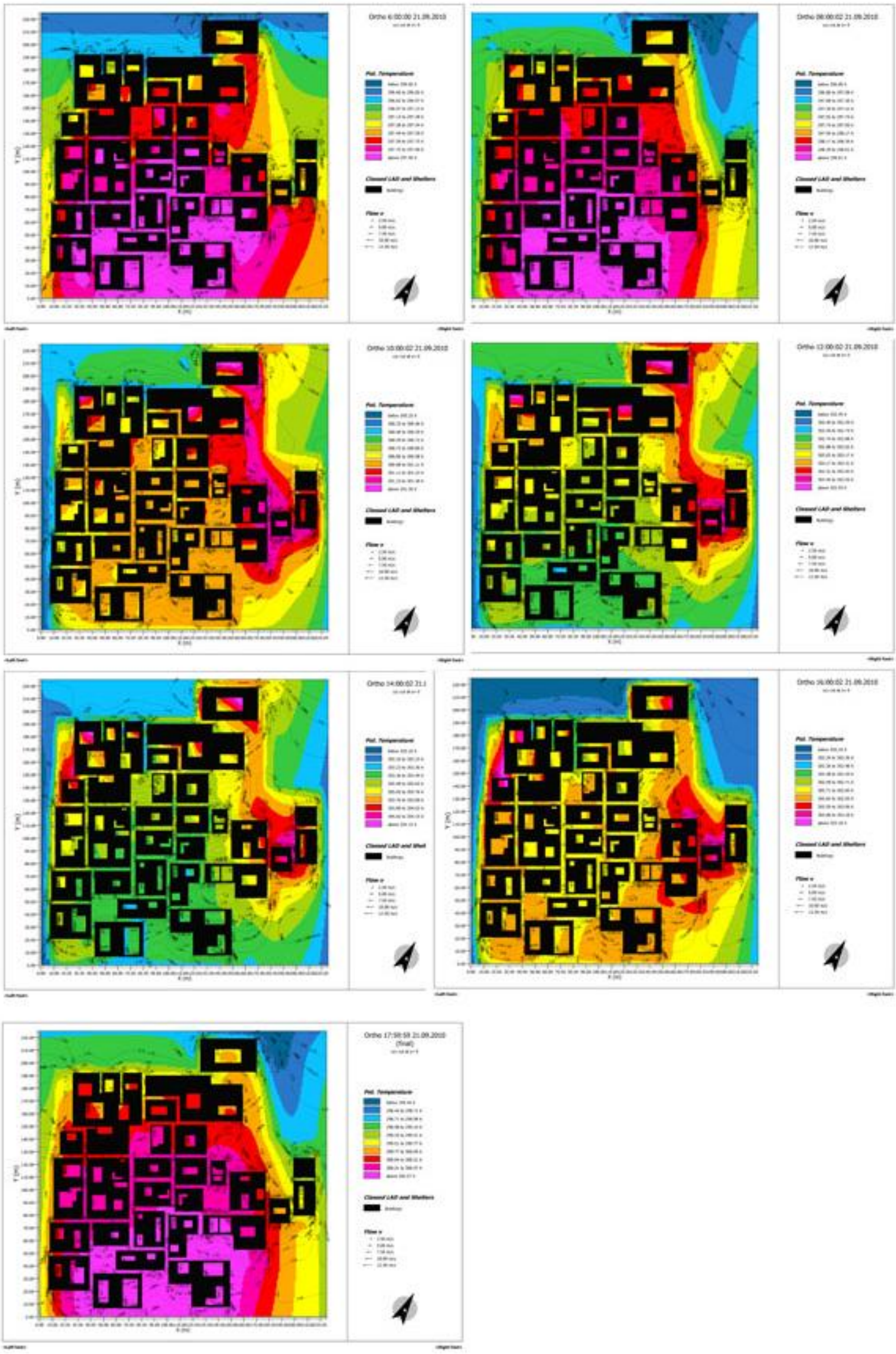

Figure F.5 Temperature gradient for Orthogonal in September and initial wind speed 3.6m/s

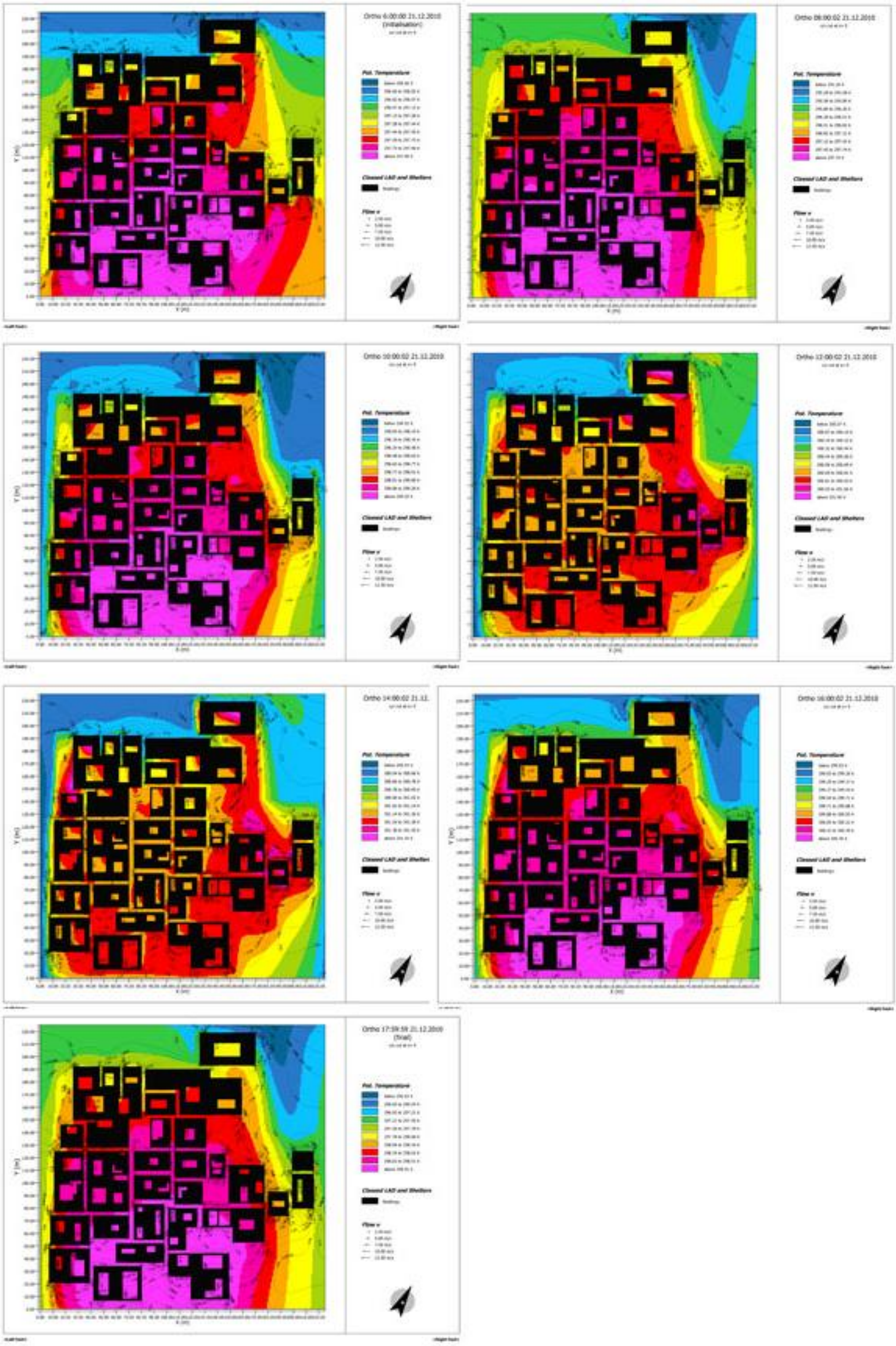

Figure F.6 Temperature gradient for Orthogonal in December and initial wind speed 3.6m/s

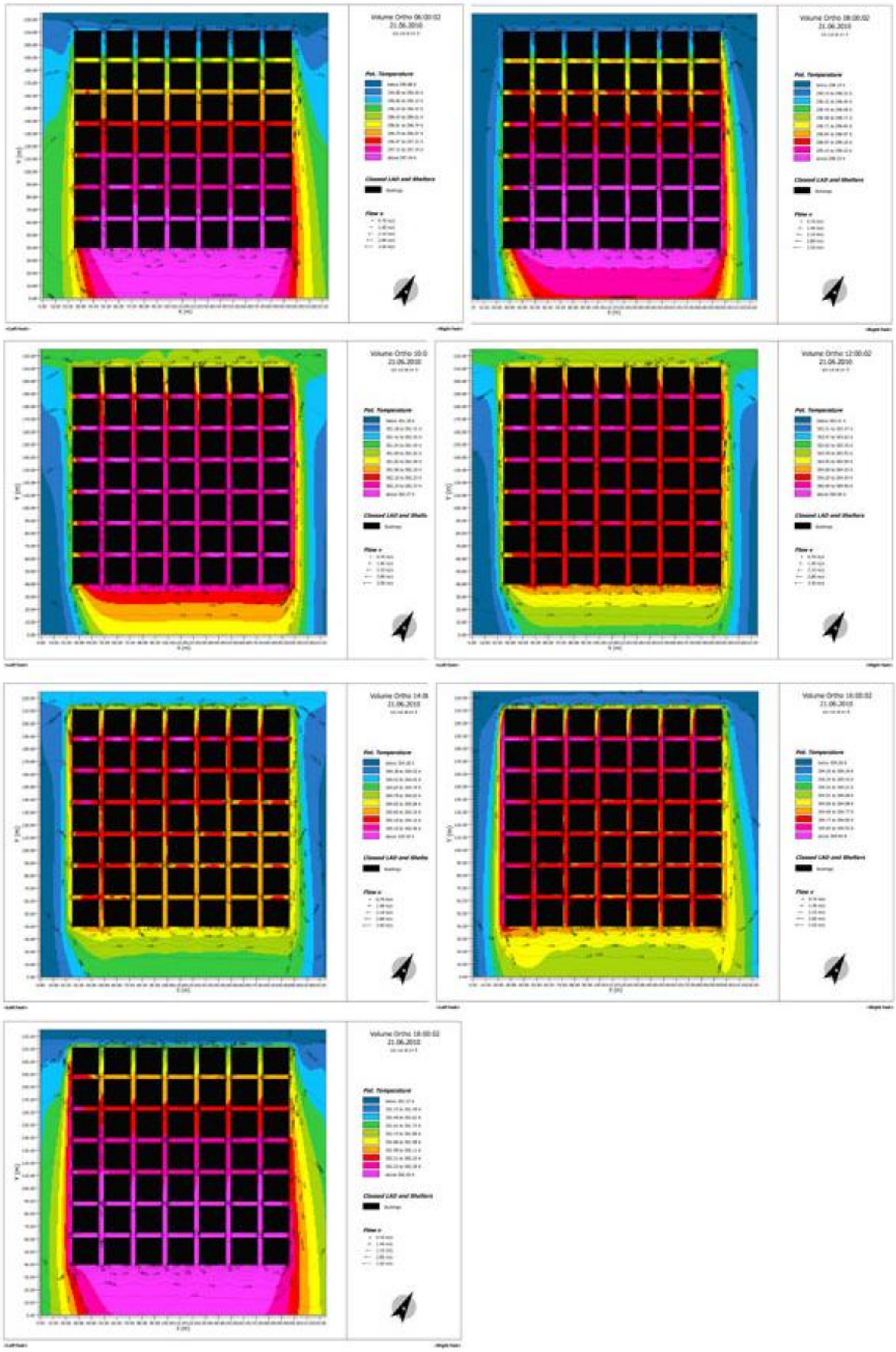

Figure F.7 Temperature gradient for Volume Ortho in June and initial wind speed 3.6m/s

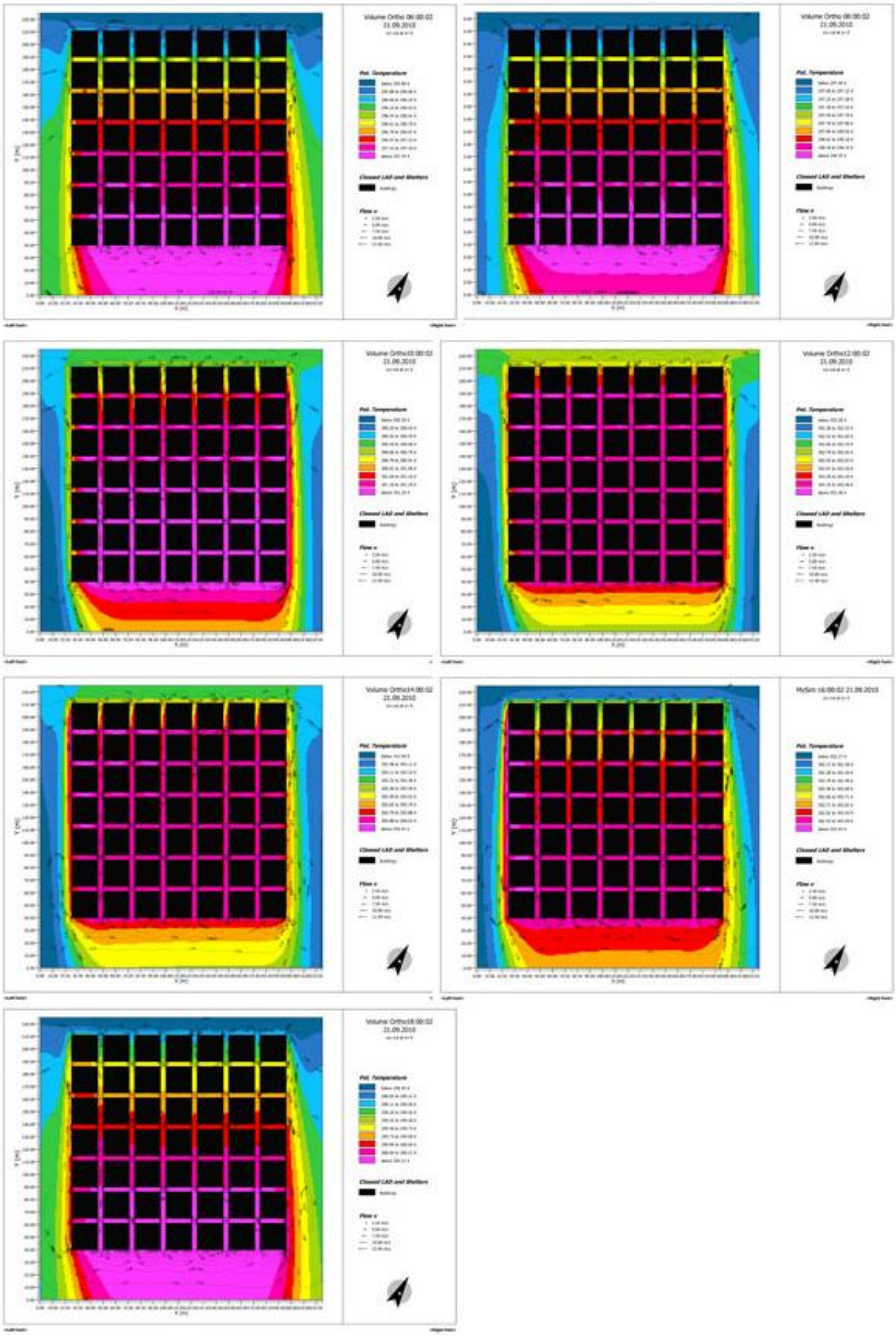

Figure F.8 Temperature gradient for Volume Ortho in September and initial wind speed 3.6m/s

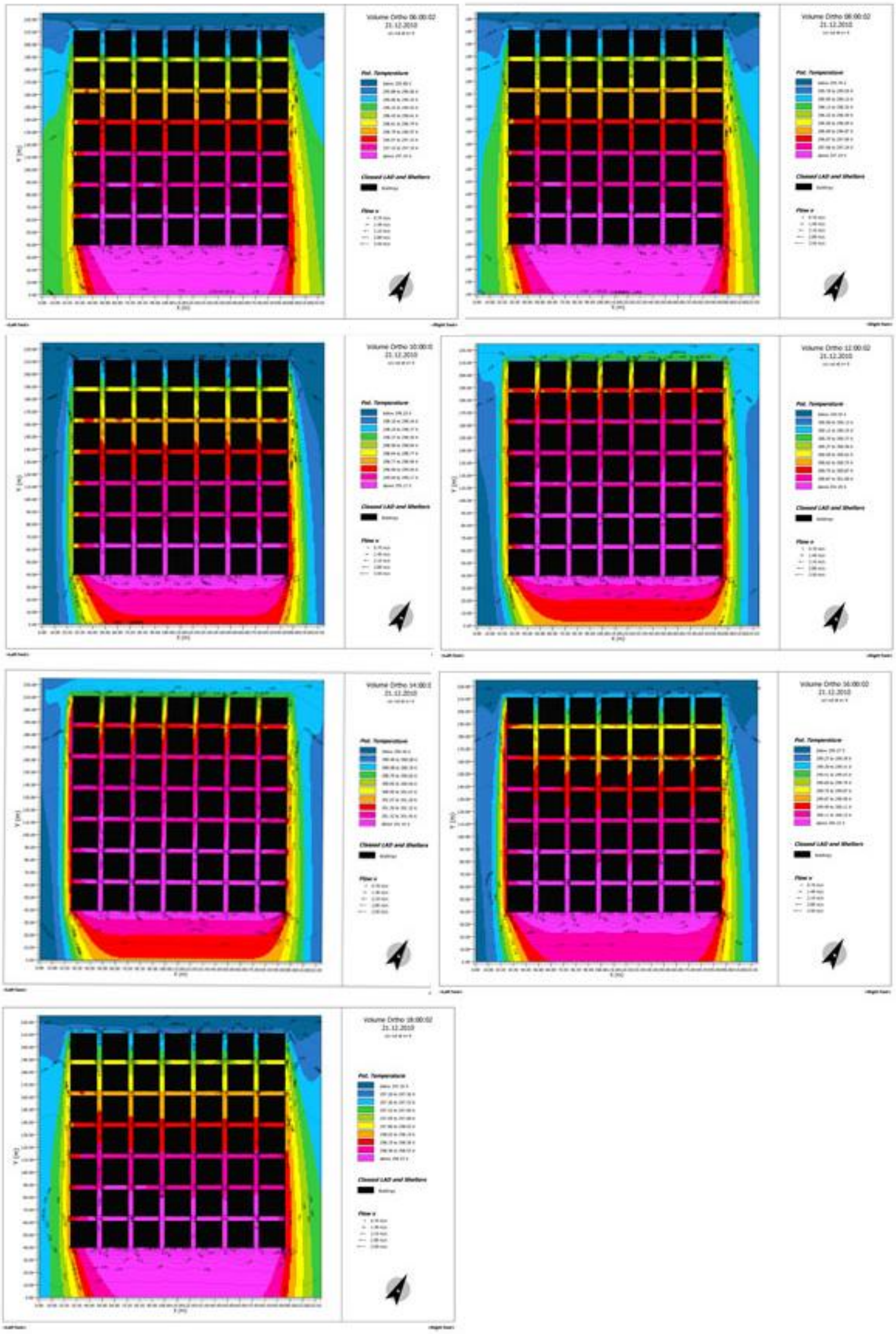

Figure F.9 Temperature gradient for Volume Ortho in December and initial wind speed 3.6m/s

Appendix G

ENVI-met simulation snapshots of Bastakiyah, Orthogonal, and Volume Ortho configurations with initial wind speed of 0.1 m/s.

Note: Snapshots shown in 2 hour intervals from 6:00-18:00 – remaining files are included in soft copy

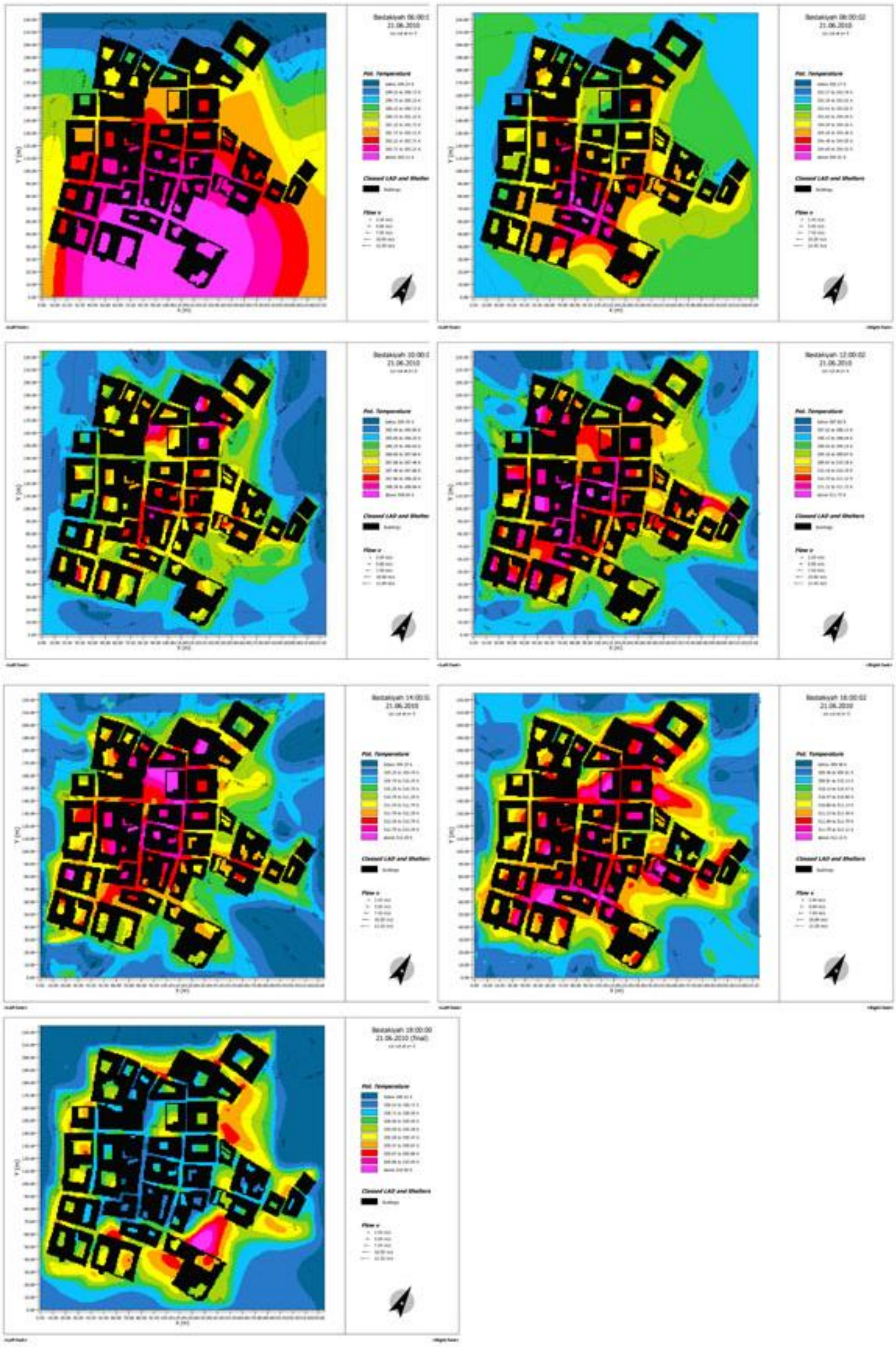

Figure G.1 Temperature gradient for Bastakiyah in June and initial wind speed 0.1m/s

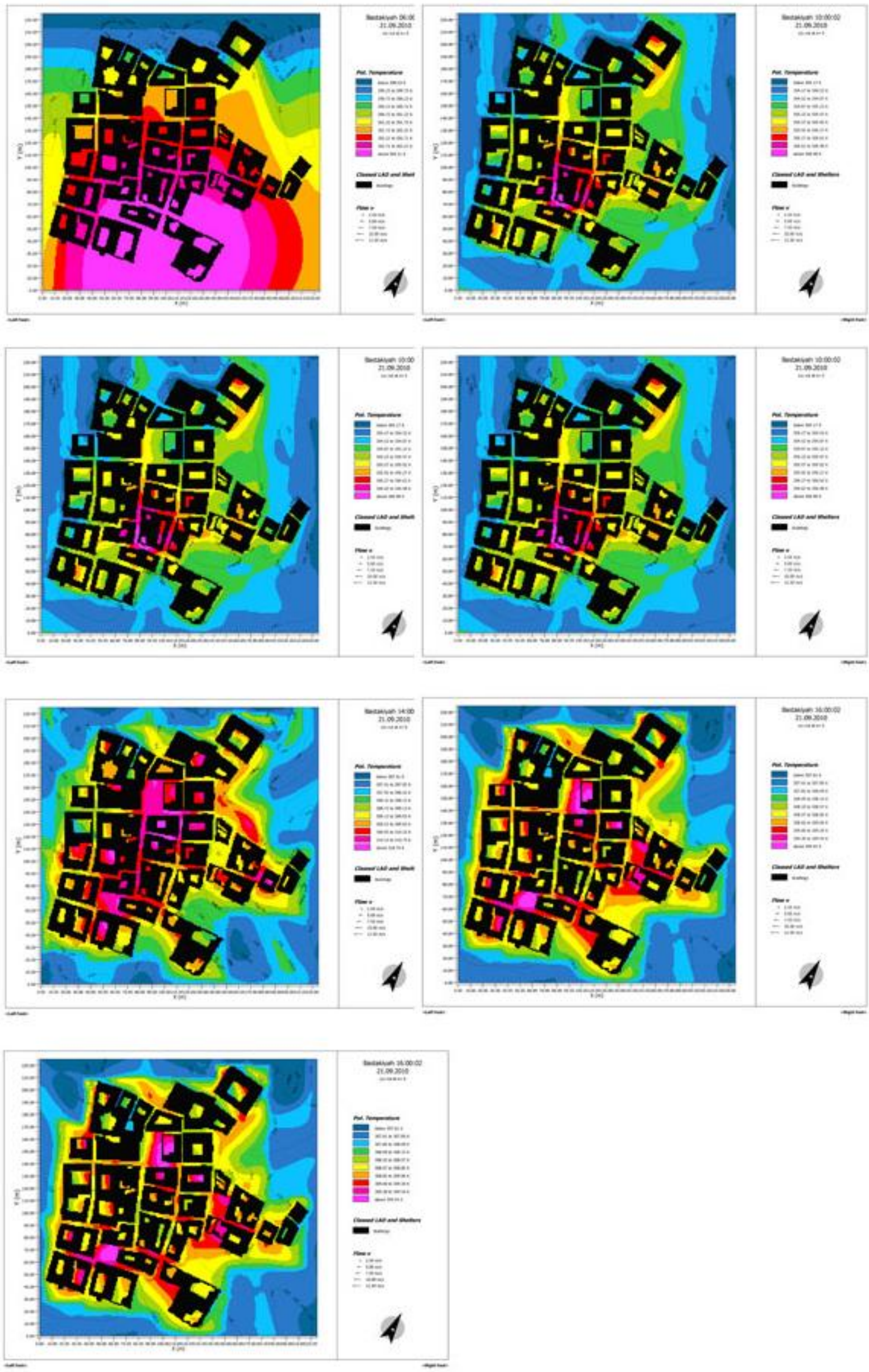

Figure G.2 Temperature gradient for Bastakiyah in September and initial wind speed 0.1m/s

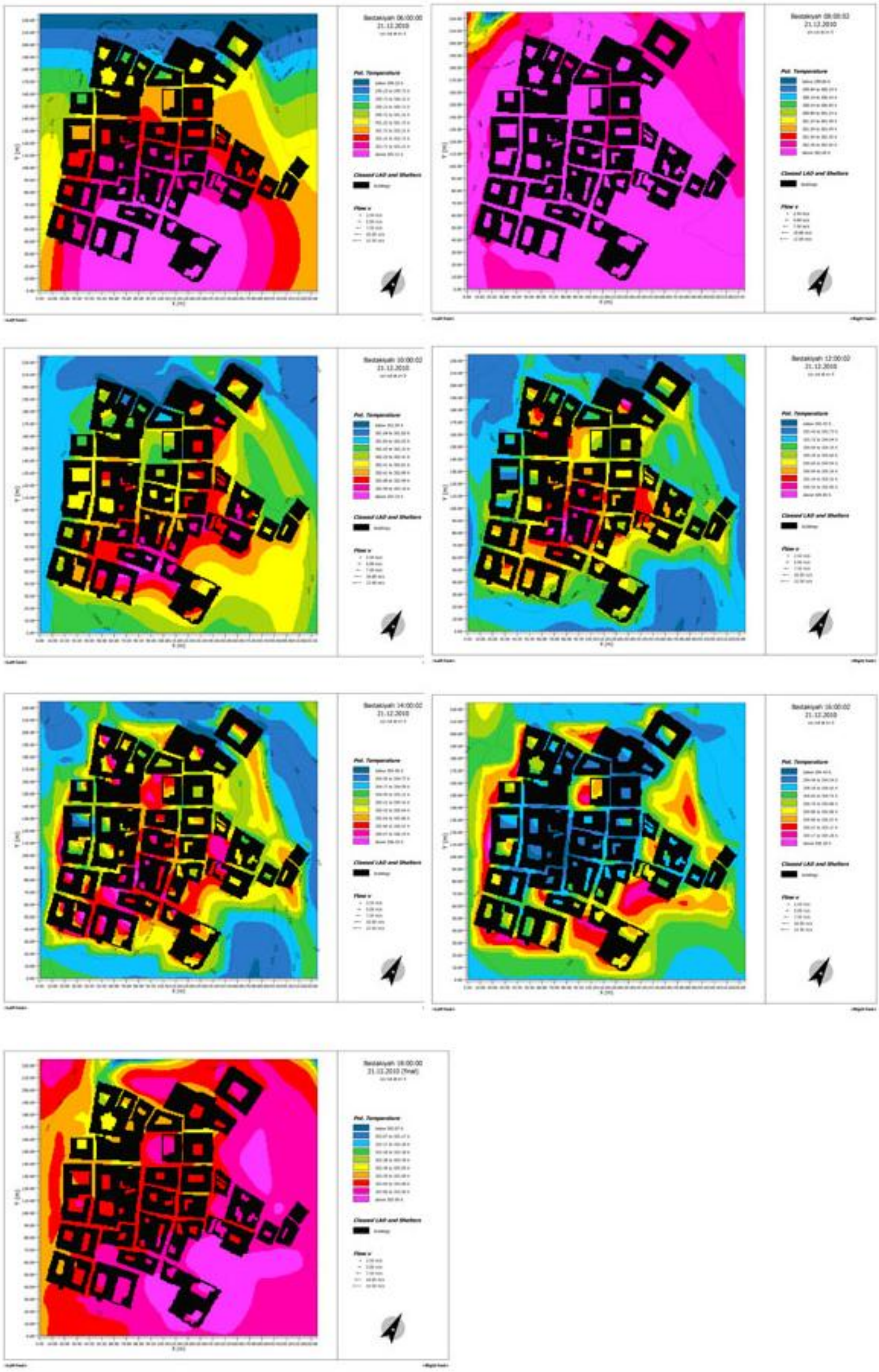

Figure G.3 Temperature gradient for Bastakiyah in December and initial wind speed 0.1m/s

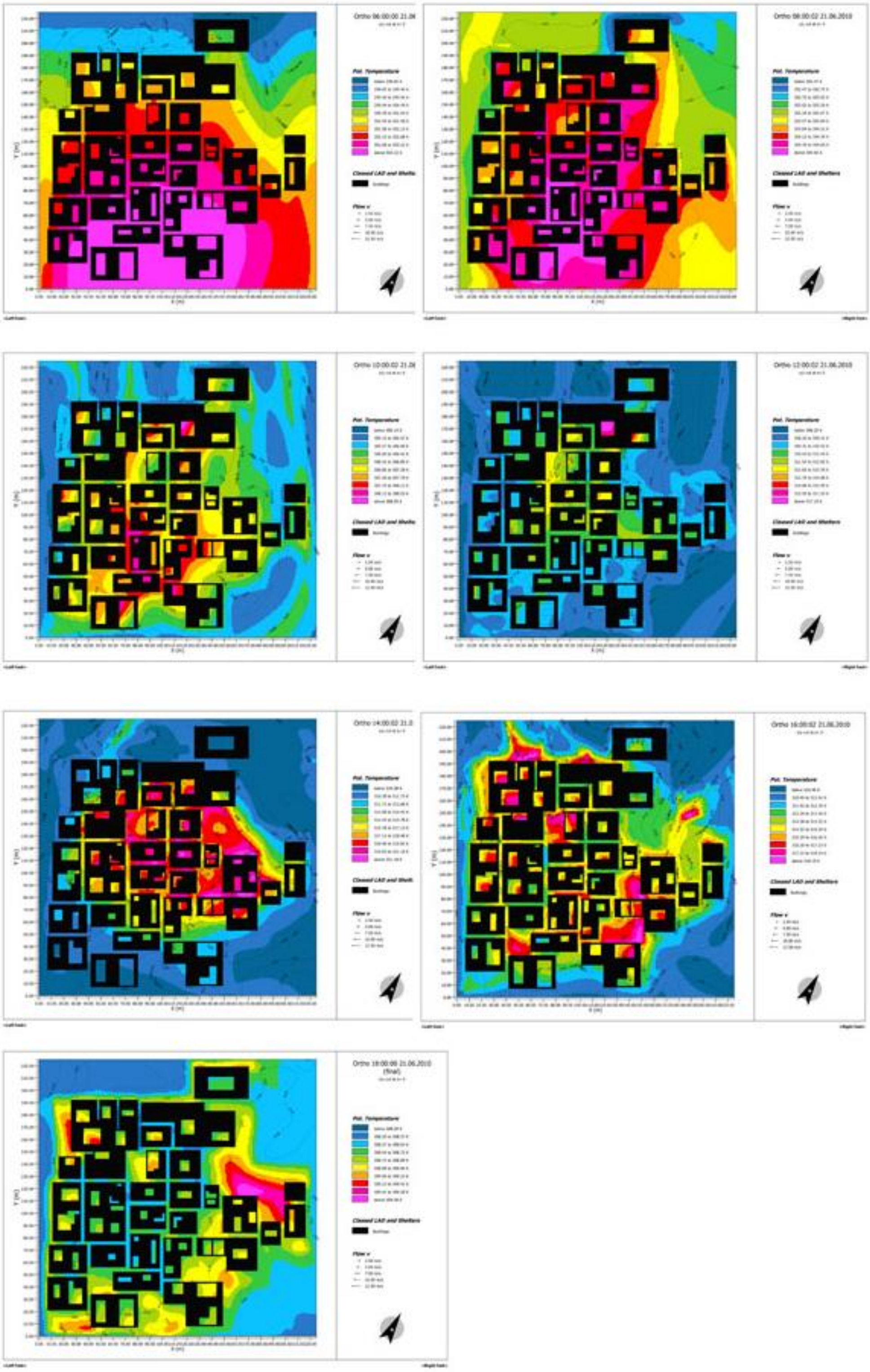

Figure G.4 Temperature gradient for Orthogonal in June and initial wind speed 0.1m/s

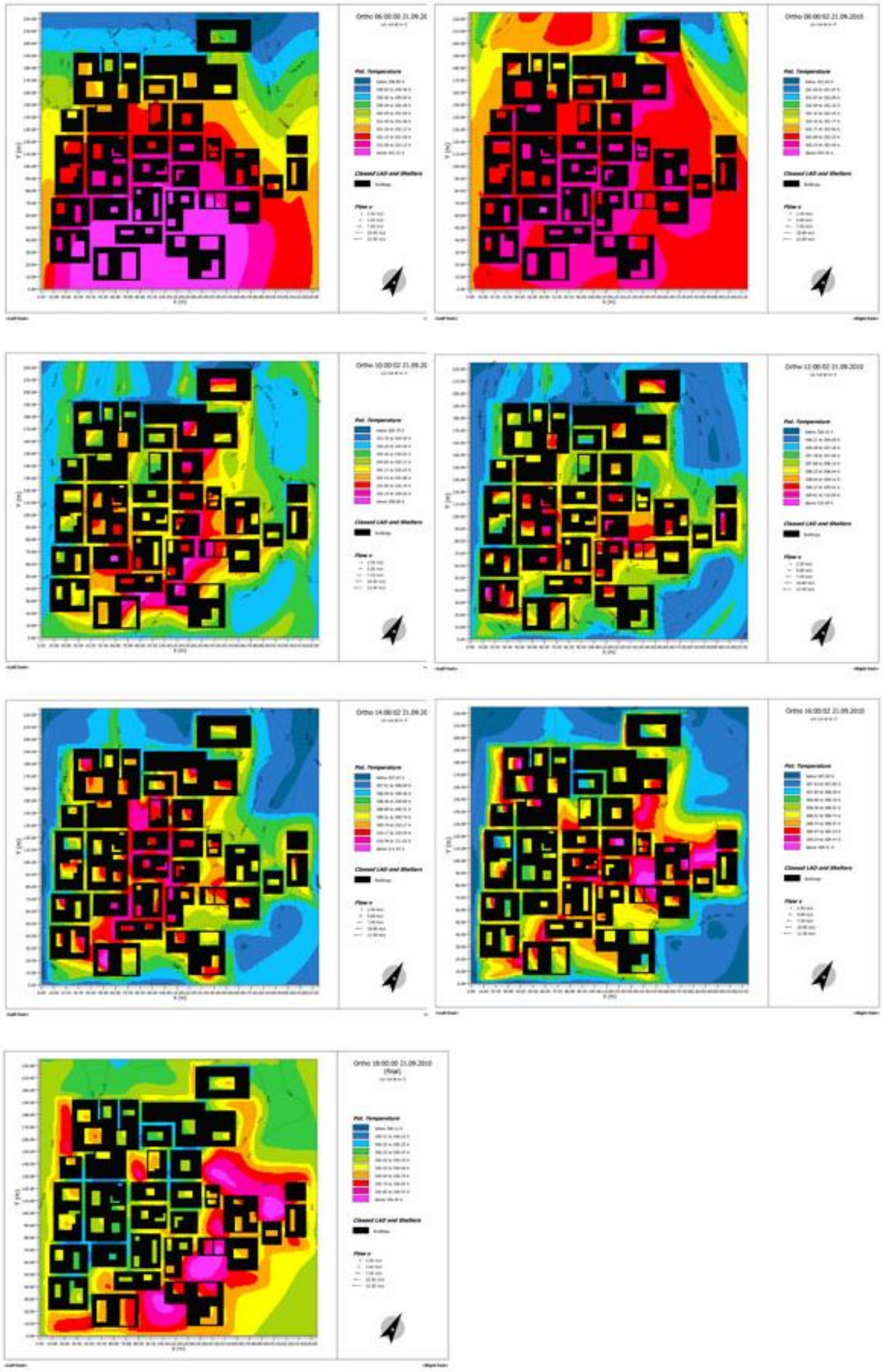

Figure G.5 Temperature gradient for Orthogonal in September and initial wind speed 0.1m/s

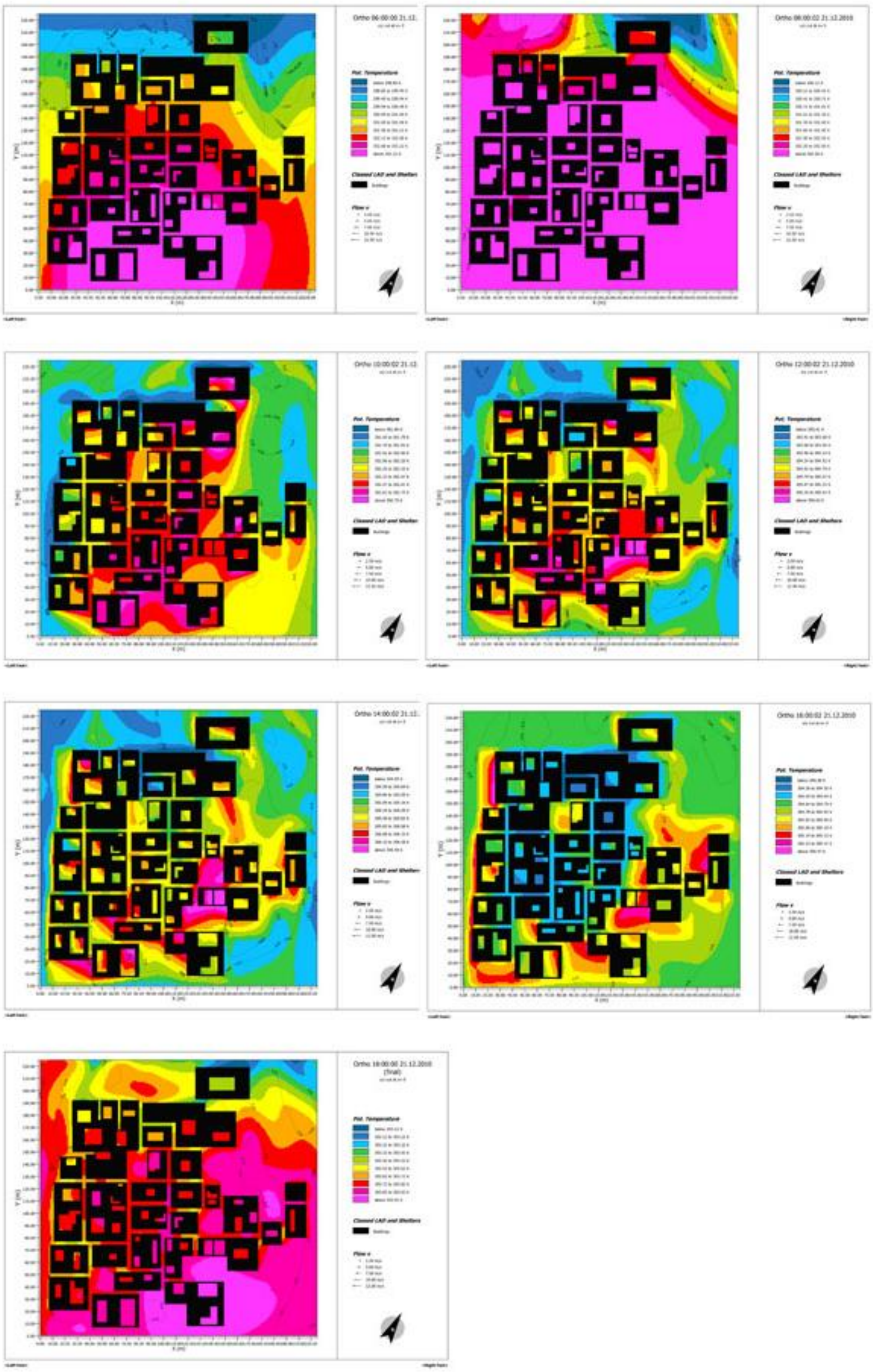

Figure G.6 Temperature gradient for Orthogonal in December and initial wind speed 0.1m/s

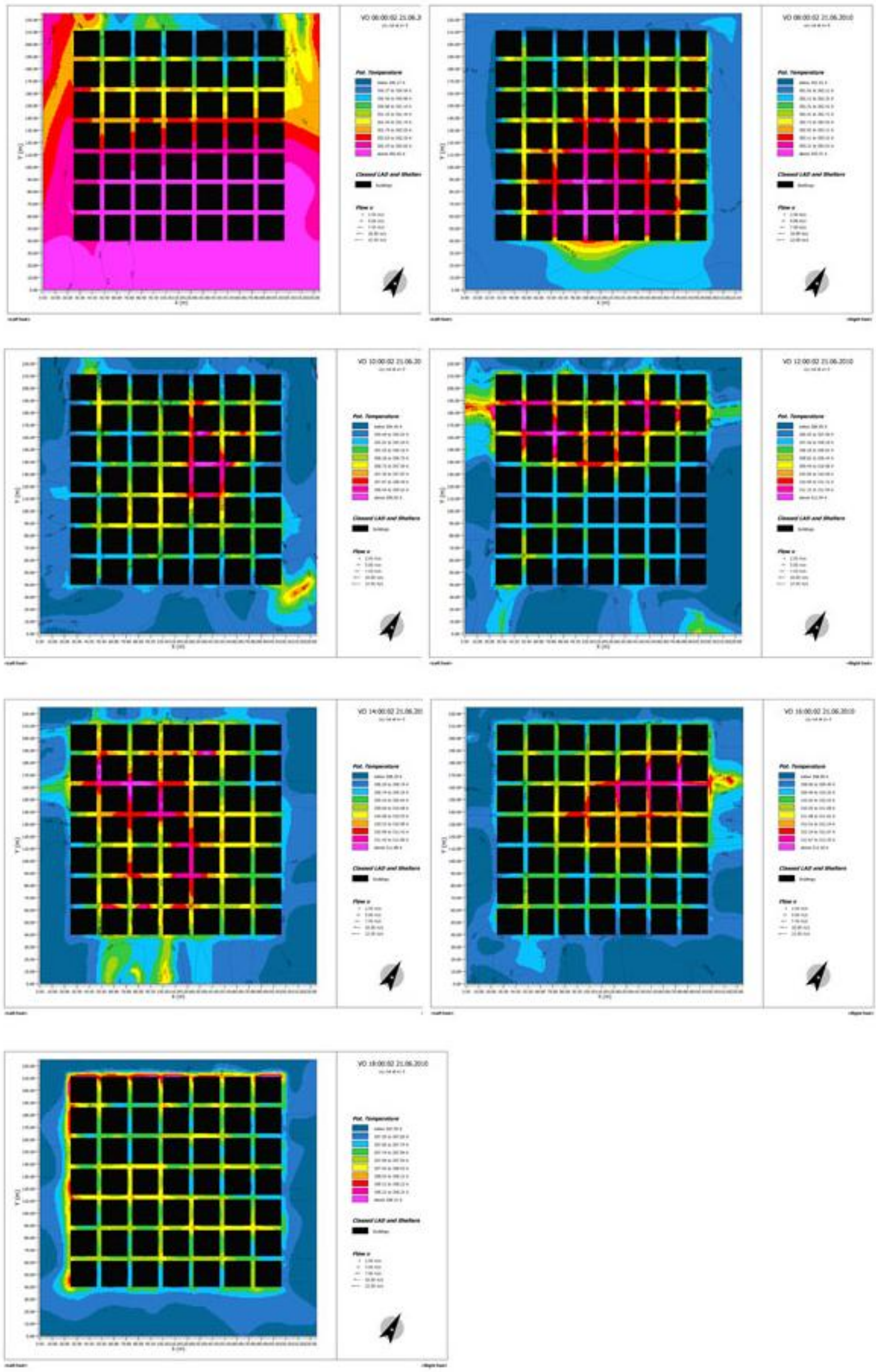

Figure G.7 Temperature gradient for Volume Ortho in June and initial wind speed 0.1m/s

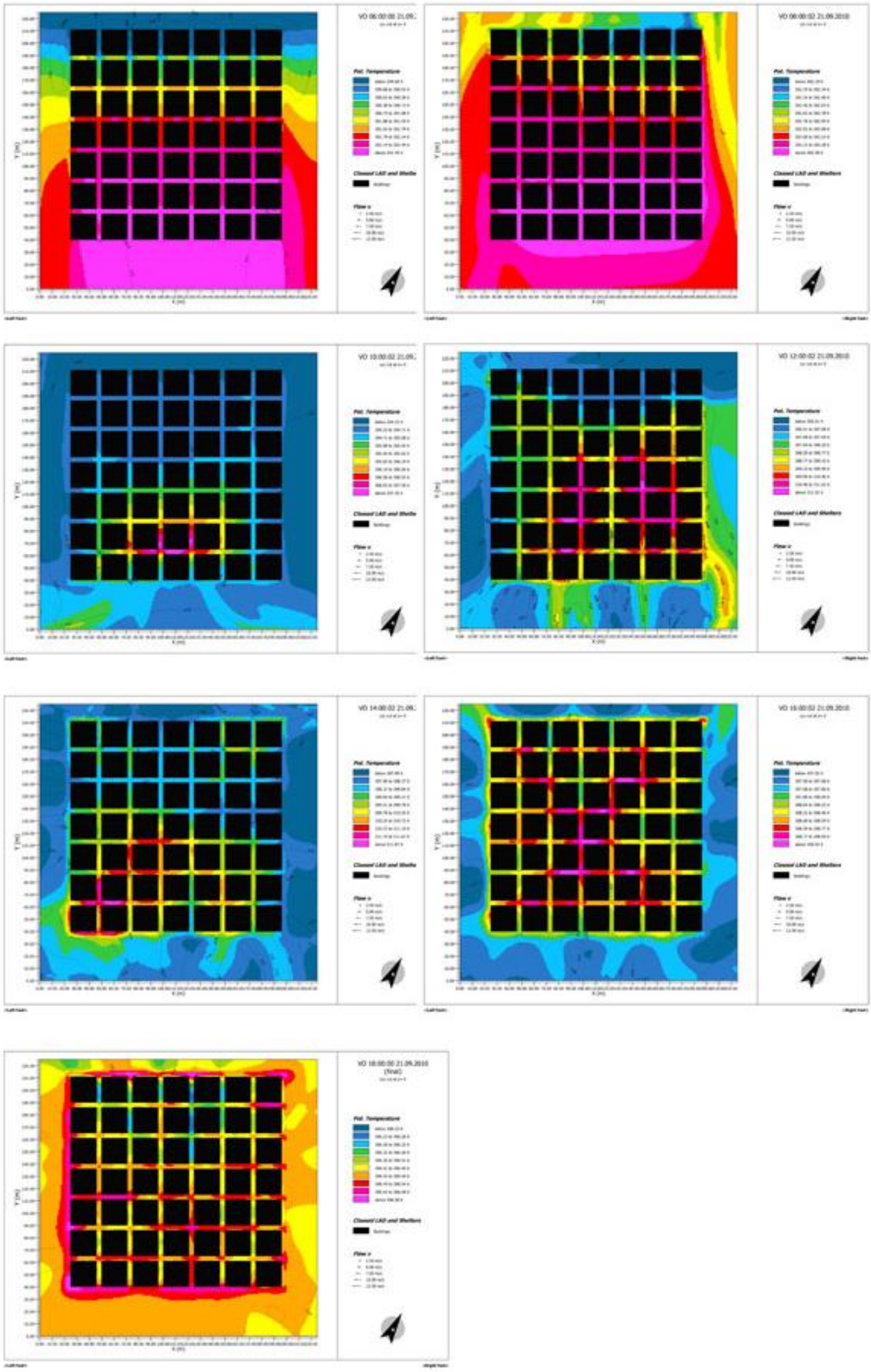

Figure G.8 Temperature gradient for Volume Ortho in September and initial wind speed 0.1m/s

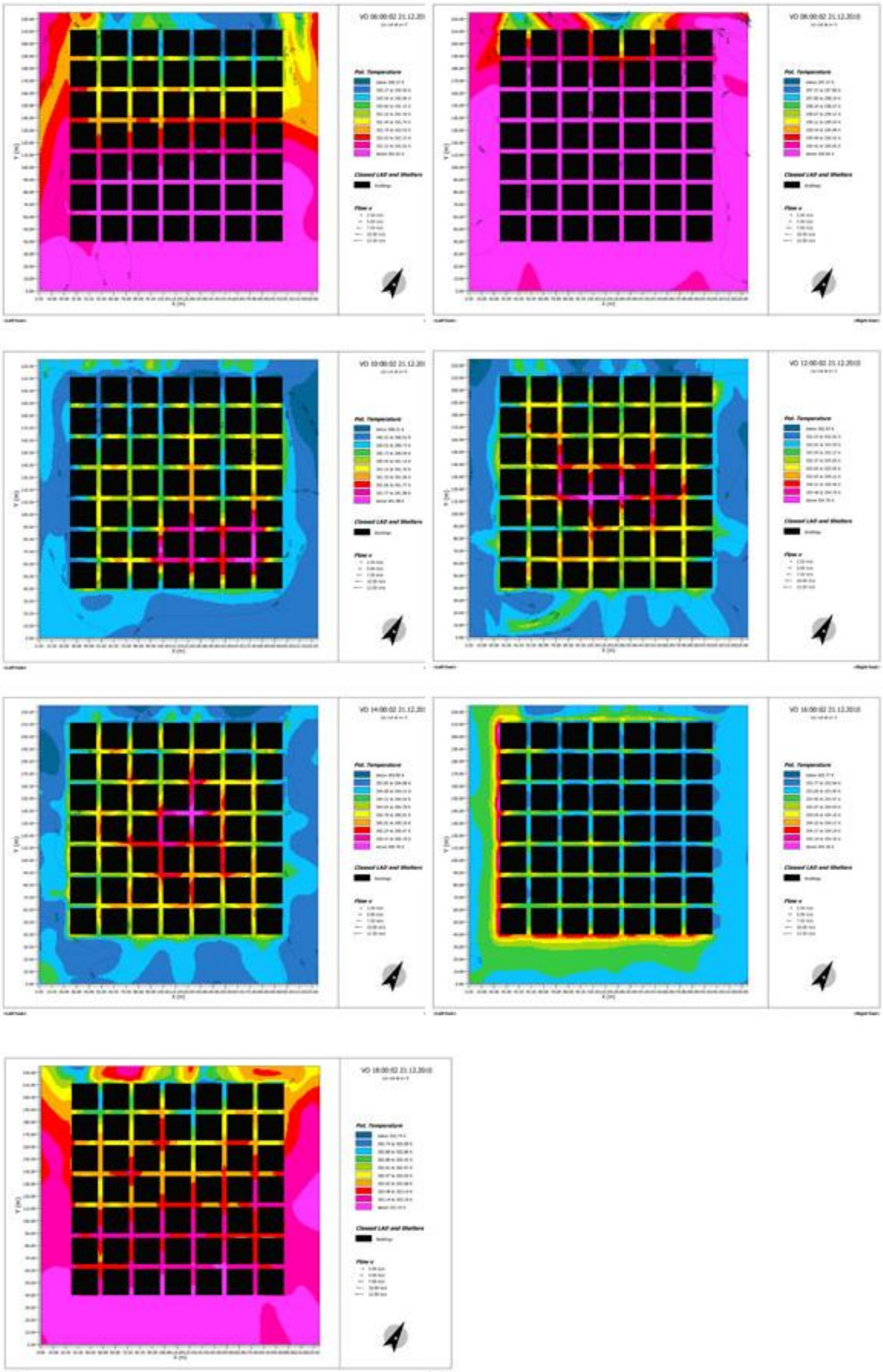

Figure G.9 Temperature gradient for Volume Ortho in December and initial wind speed 0.1m/s

Appendix H

ENVI-met simulation snap shots of Bastakiyah, Orthogonal, and Volume Ortho configurations with initial wind speed of 7.0 m/s in June at two hour intervals (10:00=16:00)

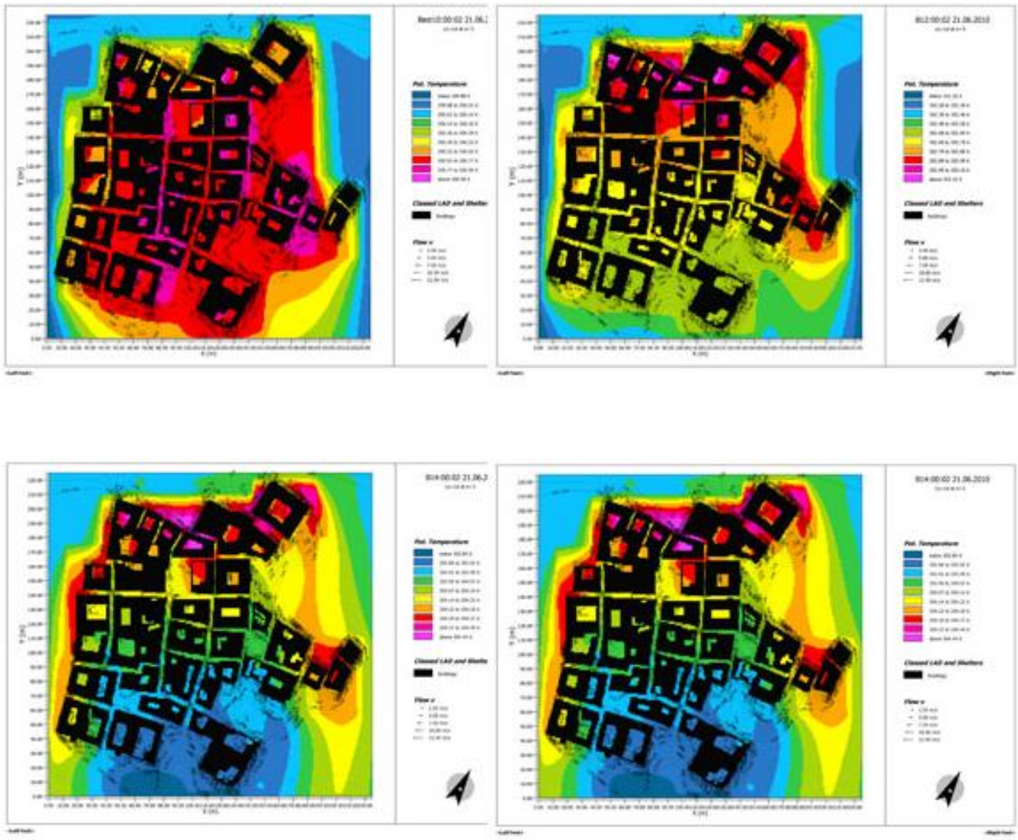

Figure H.1 Temperature gradient for Bastakiyah in June and initial wind speed 7.0m/s

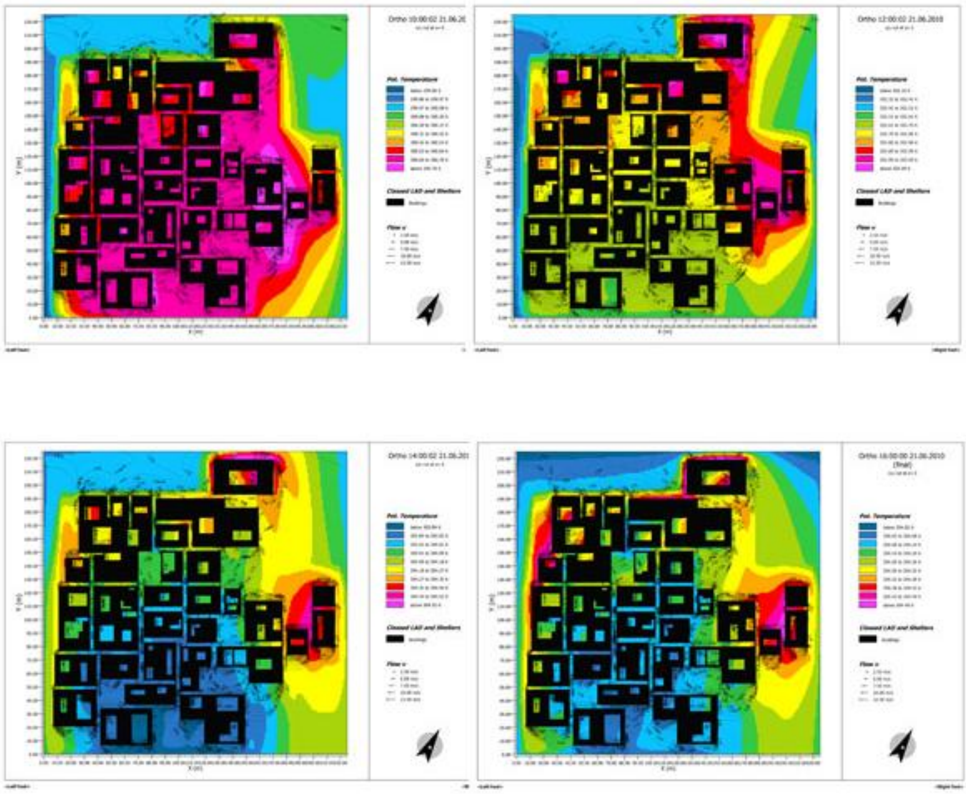

Figure H.2 Temperature gradient for Orthogonal in June and initial wind speed 7.0m/s

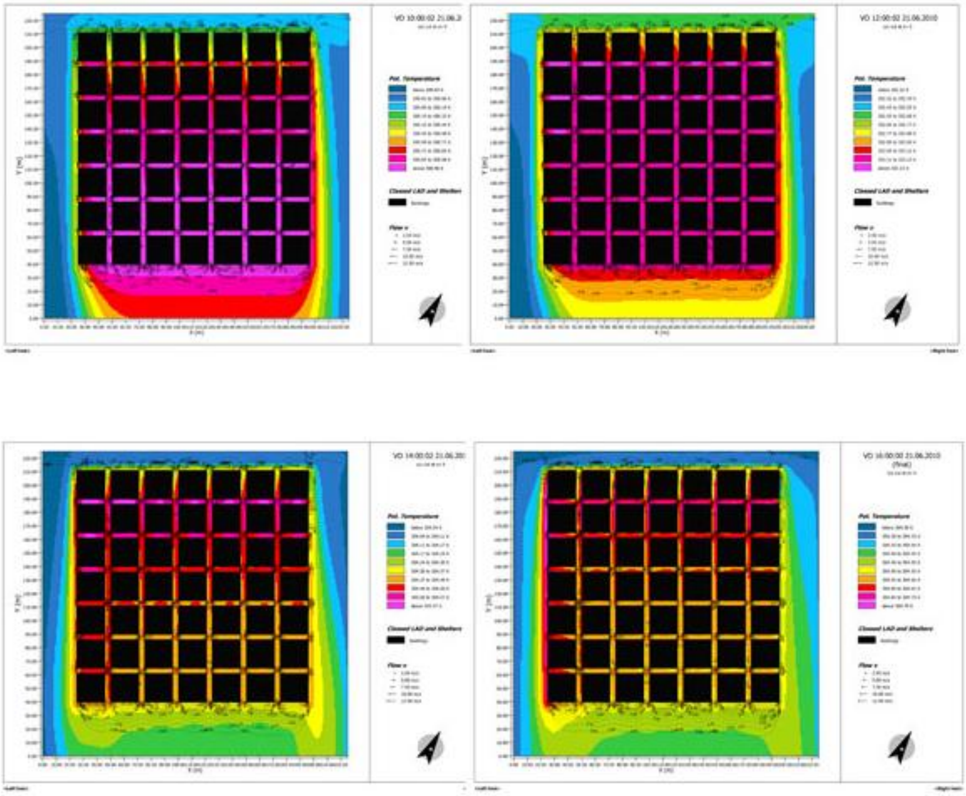

Figure H.3 Temperature gradient for Volume Ortho in June and initial wind speed 7.0m/s